Deformable bodies in viscous fluids: supplementary "tutorial"

Saverio Spagnolie
University of Wisconsin-Madison
Department of Mathematics
June 28, 2016

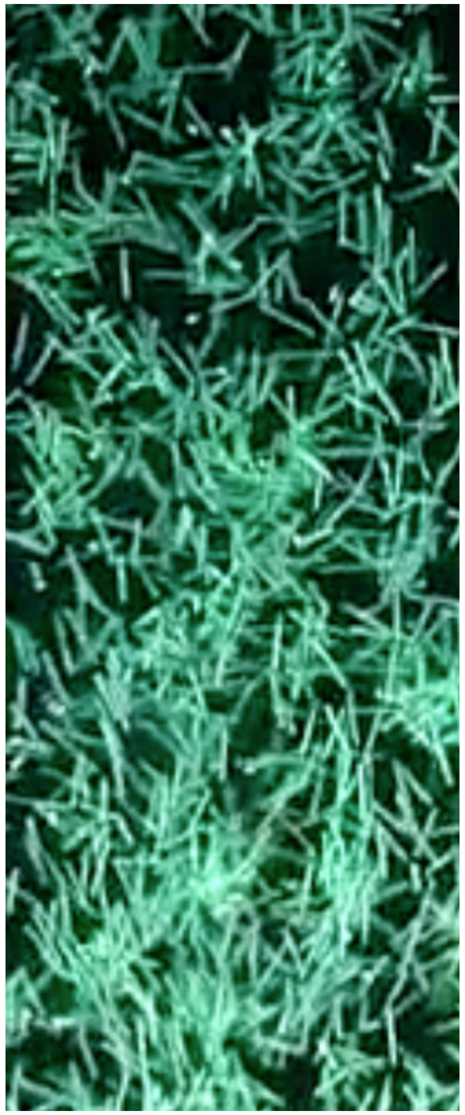

Guazzelli Lab

On the menu

0. Lecture motivation: Alben & Shelley (2008)

1. Continuum mechanics, abridged

2. Euler-Bernoulli beam theory

3. Entertainment

Flapping States of a Flag in an Inviscid Fluid: Bistability and the Transition to Chaos

Silas Alben*
School of Mathematics, Georgia Institute of Technology, Atlanta, Georgia 30332-0160, USA

Michael J. Shelley
Applied Math Laboratory, Courant Institute, New York University, New York, New York 10012, USA

(Received 26 October 2007; published 21 February 2008)

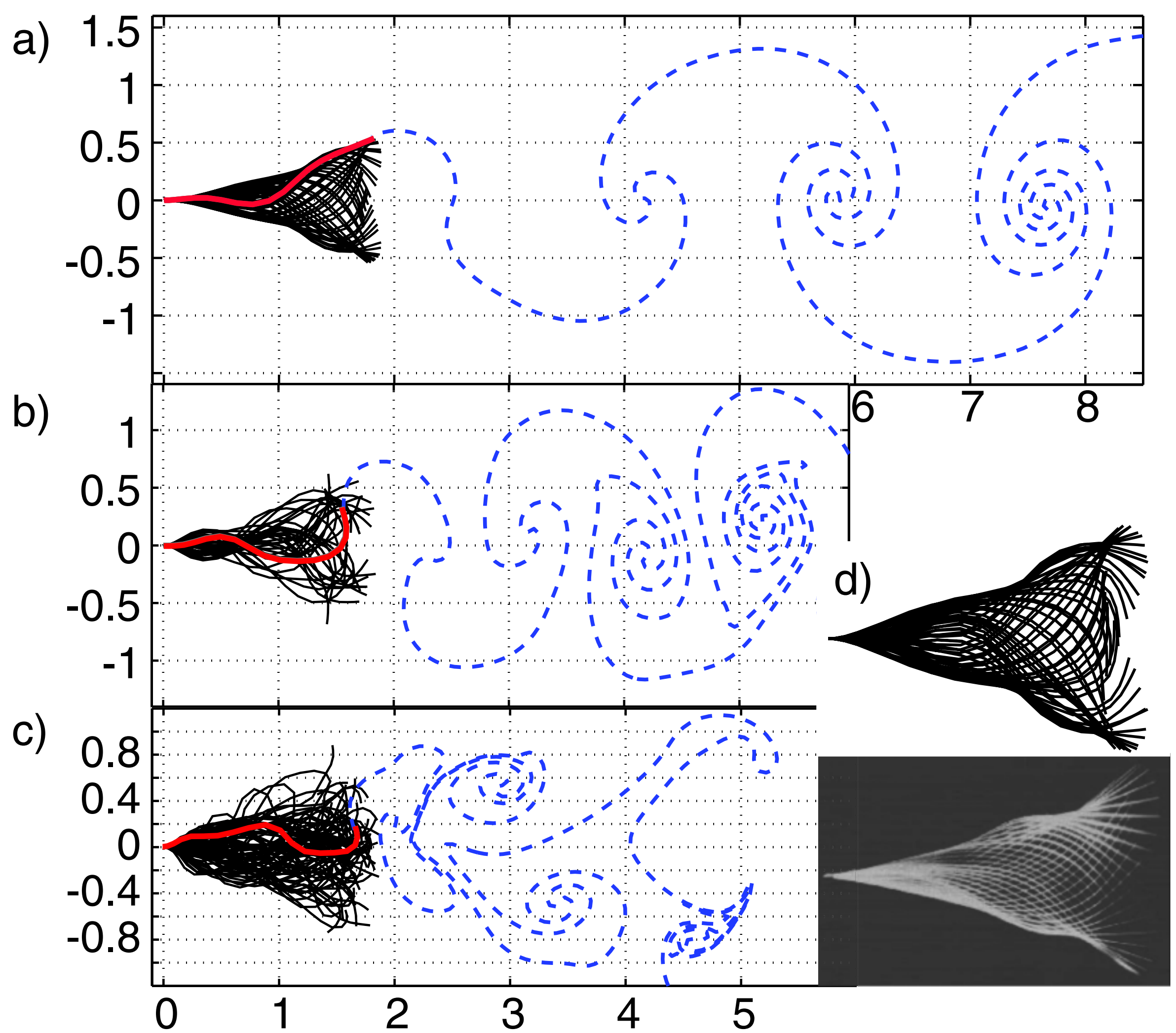

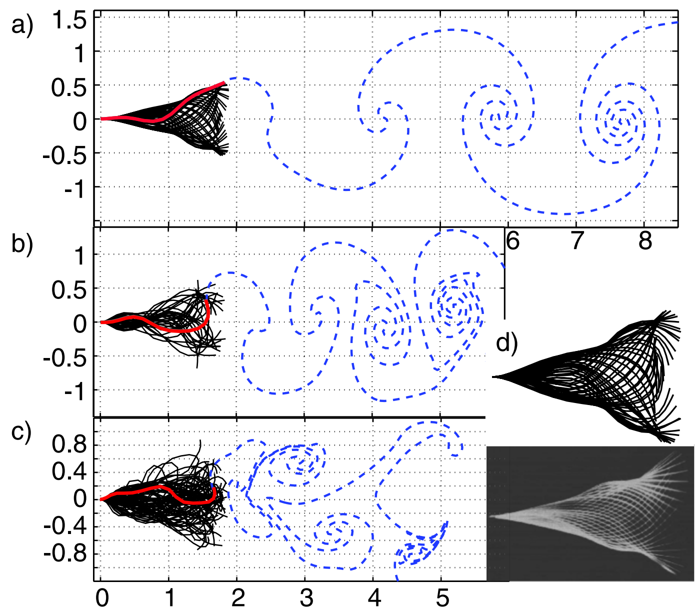

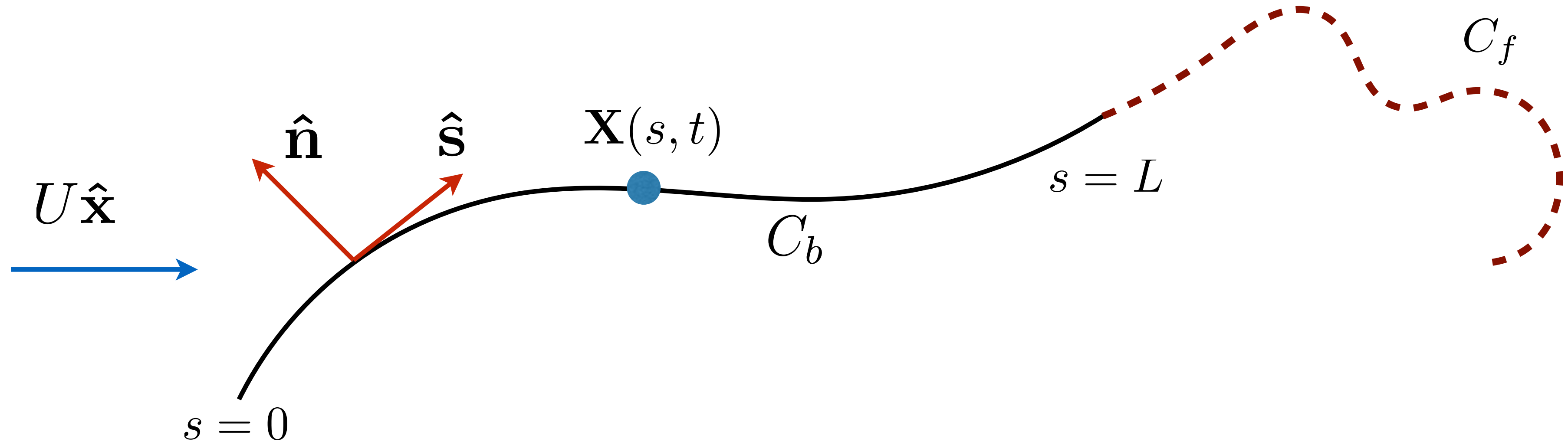

$$\rho_s \mathbf{X}_{tt} = \partial_s(T\hat{\mathbf{s}}) - B\partial_{ss}\left(\kappa\hat{\mathbf{n}}\right) - [p]\hat{\mathbf{n}}$$

Continuum mechanics, abridged.

“Reference configuration”

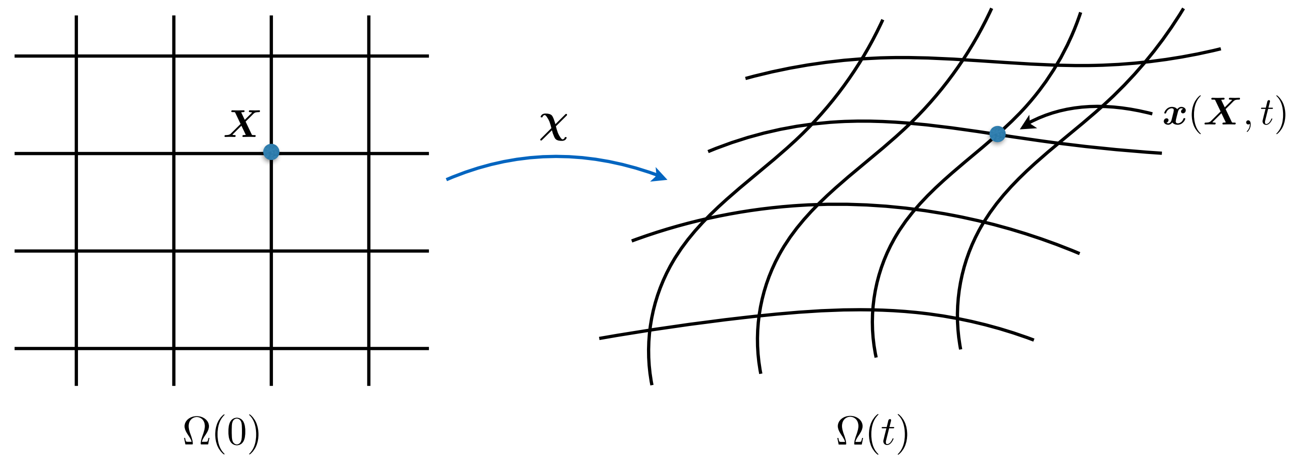

“Current configuration”

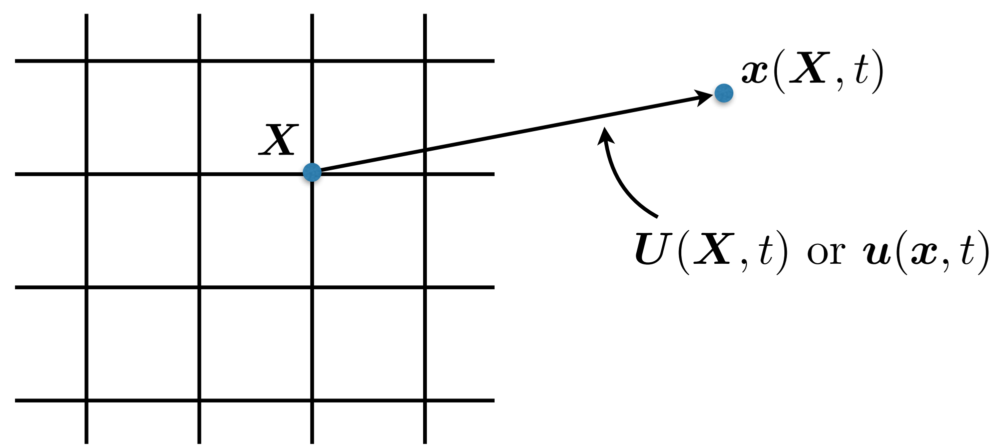

displacement field

- Material description: $\boldsymbol{U}(\boldsymbol{X}, t) = \boldsymbol{x}(\boldsymbol{X}, t) - \boldsymbol{X}$
- Spatial description: $\boldsymbol{u}(\boldsymbol{x}, t) = \boldsymbol{x} - \mathbf{X}(\mathbf{x}, t)$

Continuum mechanics, abridged.

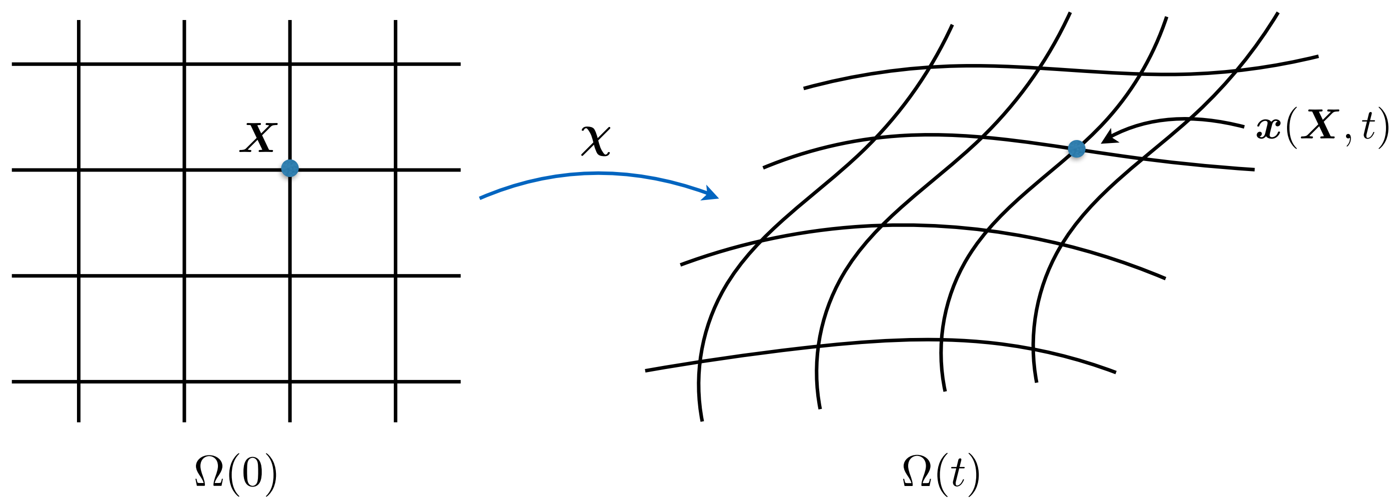

Deformation Gradient Tensor (the Jacobian matrix of the map)

$$\mathbf{F}(\mathbf{X}, t) = \frac{\partial x_i}{\partial X_j}\mathbf{e}_i\mathbf{e}_j = \left(\frac{\partial \mathbf{x}}{\partial \mathbf{X}}\right)^T$$

How does a line element transform?

$$dx_i = \sum_j \frac{\partial x_i}{\partial X_j} dX_j = \frac{\partial x_i}{\partial X_j} dX_j = F_{ij} dX_j$$

(Einstein summation notation:
repeated index —> implied sum)

So: $\boldsymbol{dx} = \mathbf{F} \cdot \boldsymbol{dX}$

Continuum mechanics, abridged.

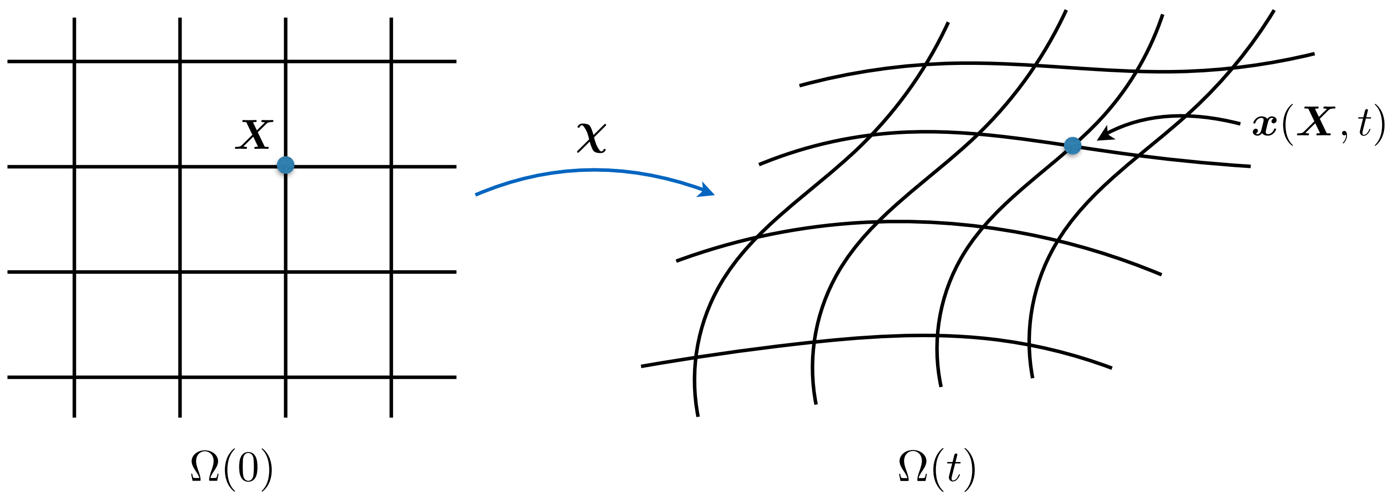

$$\mathbf{F}(\mathbf{X}, t) = \frac{\partial x_i}{\partial X_j}\mathbf{e}_i, \mathbf{e}_j = \left(\frac{\partial \mathbf{x}}{\partial \mathbf{X}}\right)^T$$

$$\boldsymbol{dx} = \mathbf{F} \cdot \boldsymbol{dX}$$

What about the length of a line element?

$$|\boldsymbol{dx}| = \sqrt{\boldsymbol{dx} \cdot \boldsymbol{dx}} = \sqrt{(\mathbf{F} \cdot \boldsymbol{dX}) \cdot (\mathbf{F} \cdot \boldsymbol{dX})} = (\boldsymbol{dX} \cdot \mathbf{F}^T \cdot \mathbf{F} \cdot \boldsymbol{dX})^{1/2}$$

$$= (\boldsymbol{dX} \cdot \mathbf{C} \cdot \boldsymbol{dX})^{1/2}$$

- Right Cauchy-Green tensor: $\mathbf{C}(\boldsymbol{X}, t) = \mathbf{F}^T \cdot \mathbf{F}$

Standard measure of "strain":

- Green-Lagrange Strain tensor $\mathbf{E} = \frac{1}{2}(\mathbf{C} - \mathbf{I}) = \frac{1}{2}(\mathbf{F}^T \cdot \mathbf{F} - \mathbf{I})$

(HW): Show $\boldsymbol{dX} \cdot \mathbf{E} \cdot \boldsymbol{dX} = \frac{1}{2}(|\boldsymbol{dx}|^2 - |\boldsymbol{dX}|^2)$

(Where else do we see "stretch-squared?")

Intuitively, the strain should depend on the displacement *gradient*,

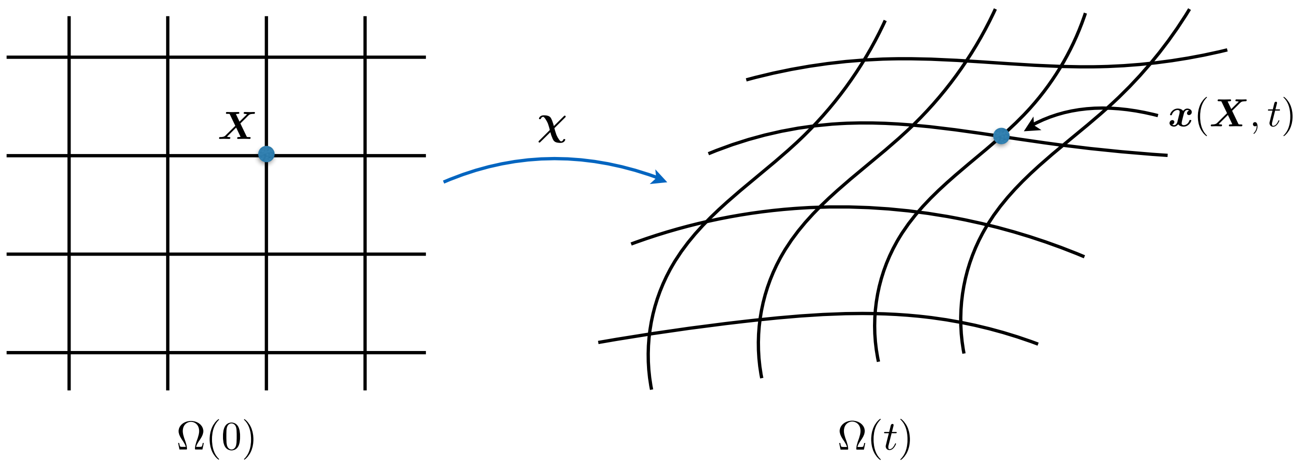

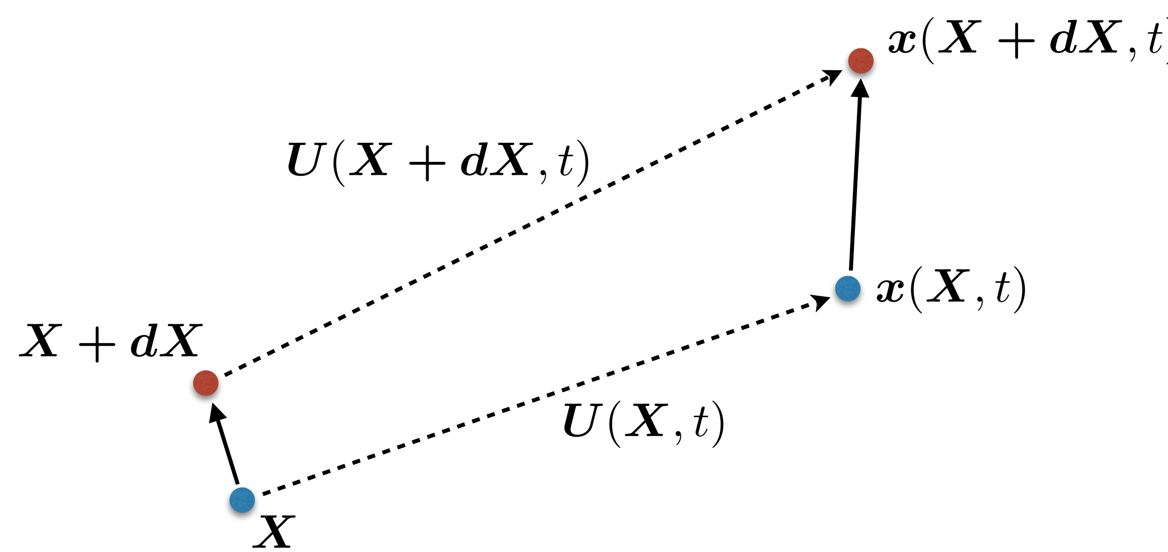

$$\boldsymbol{U}(\boldsymbol{X},t) = \boldsymbol{x}(\boldsymbol{X},t) - \boldsymbol{X}$$

$$\frac{\partial U_j}{\partial X_i} = \frac{\partial x_j}{\partial X_i} - \delta_{ji} \Rightarrow$$

$$\nabla \boldsymbol{U} = \nabla \boldsymbol{x} - \mathbf{I} = \mathbf{F}^T(\boldsymbol{X},t) - \mathbf{I}, \qquad [\nabla \boldsymbol{U}]_{ij} = \frac{\partial U_j}{\partial X_i}.$$

Or, in the current configuration,

$$\nabla_x \boldsymbol{u} = \frac{\partial \boldsymbol{u}}{\partial \boldsymbol{x}} = \mathbf{I} - \frac{\partial \boldsymbol{X}}{\partial \boldsymbol{x}} = \mathbf{I} - \mathbf{F}^{-T}(\boldsymbol{x},t)$$

Therefore, we can write the Strain Tensor $\mathbf{E}$ in terms of $\nabla \boldsymbol{U}$:

$$\mathbf{E} = \tfrac{1}{2}\left[(\mathbf{I} + \nabla \boldsymbol{U}) \cdot (\mathbf{I} + \nabla \boldsymbol{U})^T - \mathbf{I}\right] = \tfrac{1}{2}\left[(\nabla \boldsymbol{U} + \nabla \boldsymbol{U}^T) + \nabla \boldsymbol{U} \cdot \nabla \boldsymbol{U}^T\right],$$

or, in index notation,

$$E_{ij} = \frac{1}{2}\left(\frac{\partial U_i}{\partial X_j} + \frac{\partial U_j}{\partial X_i}\right) + \frac{1}{2}\left(\frac{\partial U_k}{\partial X_i}\frac{\partial U_k}{\partial X_j}\right), \qquad \text{(symmetric)}.$$

- Derive similar tensors in the spatial coordinates:

$$\text{e.g.} \qquad |\boldsymbol{dx}|^2 - |\boldsymbol{dX}|^2 = 2\boldsymbol{dx} \cdot \mathbf{e} \cdot \boldsymbol{dx}\,, \qquad \mathbf{e} = \tfrac{1}{2}\left(\mathbf{I} - \underbrace{\mathbf{F}^{-T} \cdot \mathbf{F}^{-1}}_{\text{(Finger tensor)}}\right)$$

$$\mathrm{e}_{ij} = \frac{1}{2}\left(\frac{\partial u_i}{\partial x_j} + \frac{\partial u_j}{\partial x_i}\right) - \frac{1}{2}\left(\frac{\partial u_k}{\partial x_i}\frac{\partial u_k}{\partial x_j}\right) \qquad \text{(Euler − Almansi strain tensor)}$$

Note: $\mathbf{E} = 0$ does not imply $\mathbf{U} = 0$! However, we do have that $\mathbf{E} = 0 \Rightarrow \mathbf{C} = \mathbf{I} \Rightarrow |\boldsymbol{dx}| = |\boldsymbol{dX}|$

(Rigid body motion)

Linear (Hookean) constitutive law

Assume small deformation everywhere, $\boldsymbol{x}(\boldsymbol{X}, t) \approx \boldsymbol{X}$

Then $\dfrac{\partial}{\partial X_i} \approx \dfrac{\partial}{\partial x_i} \quad \Rightarrow \quad \dfrac{\partial U_j}{\partial X_i} \approx \dfrac{\partial u_j}{\partial x_i},$

And $\mathbf{E} \approx \dfrac{1}{2}(\nabla \mathbf{u} + \nabla \mathbf{u}^{\mathbf{T}}) = \mathbf{e}$

Hooke's Law is an observation of a linear relationship between the stress $\boldsymbol{\sigma}$ and the strain $\mathbf{e}$.

$$\sigma_{ij} = C_{ijkl} e_{kl},$$

81 constant model…. weeee !
Use symmetries (to 36) and demand isotropy (down to two!) $\quad \boldsymbol{\sigma} = \lambda(\nabla \cdot \boldsymbol{u})\mathbf{I} + 2\mu\mathbf{e}$

Side notes:

F = ma: Navier (or Lamé) equation $\quad \rho_0 \boldsymbol{u}_{tt} = (\lambda + \mu)\nabla(\nabla \cdot \boldsymbol{u}) + \mu\Delta\boldsymbol{u}$

Stored elastic energy: $\quad W(\mathbf{e}) = \dfrac{1}{2}\lambda(e_{kk})^2 + \mu(e_{ij}e_{ij})$

On the menu

0. Lecture motivation: Alben & Shelley (2008)

1. Continuum mechanics, abridged

2. Euler-Bernoulli beam theory

3. Entertainment

Euler-Bernoulli beam theory:
mechanically linear, geometrically nonlinear

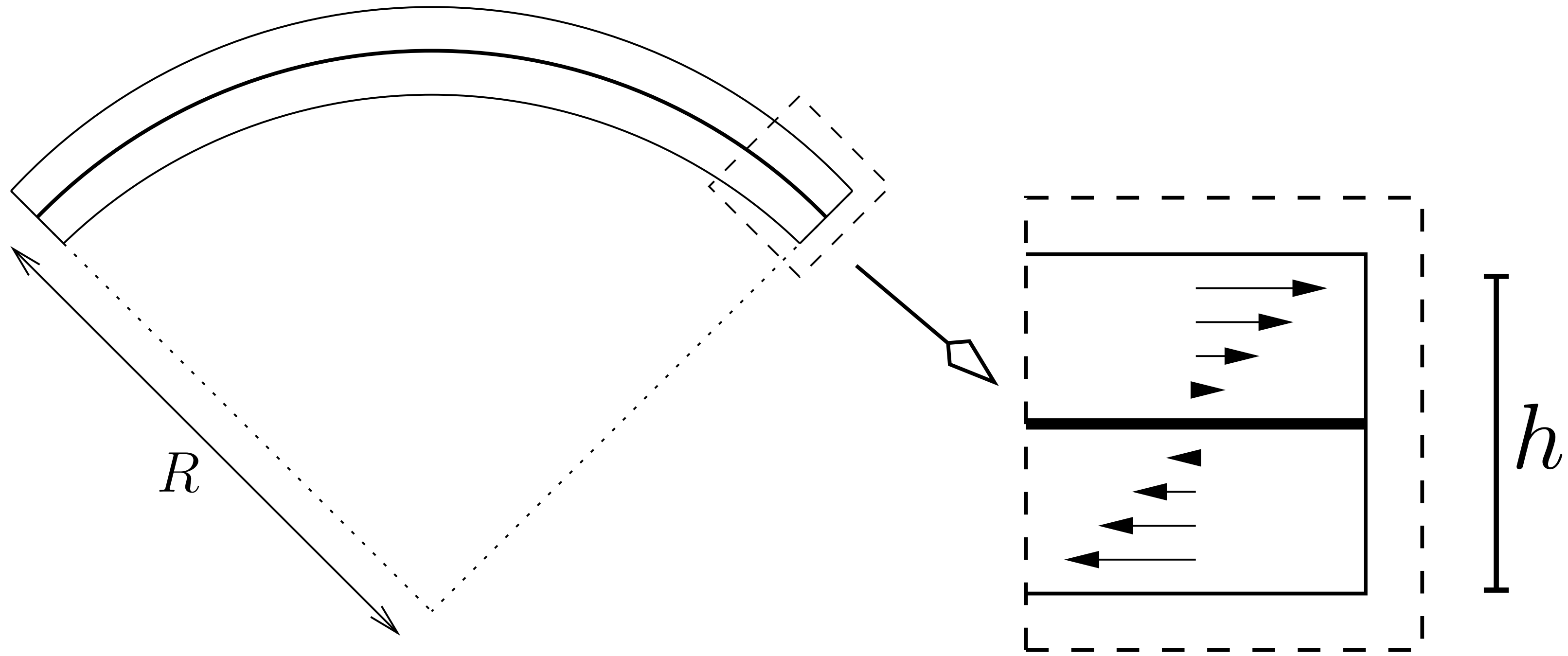

If $h/R \ll 1$

The displacements $\mathbf{U}(\mathbf{X},t)$ might be huge (so $\mathbf{U} \not\approx \mathbf{u}$)

But the gradients $\nabla\mathbf{U}(\mathbf{X},t)$ are order h/R << 1.

In this theory it is still assumed that the Hookean constitutive law applies,
even though large deformations are permissible.

Historical aside:

1638: Galileo Galilei, Fracture of rods and cylinders.

1678: Hooke's Law, F=-kx *Ut tensio sic vis*

1705: Jacob Bernoulli, Elastic line or *Elastica*

Resistance to bending is proportional to curvature

1744: Daniel Bernoulli suggests to Euler:
minimize the integral of the square curvature

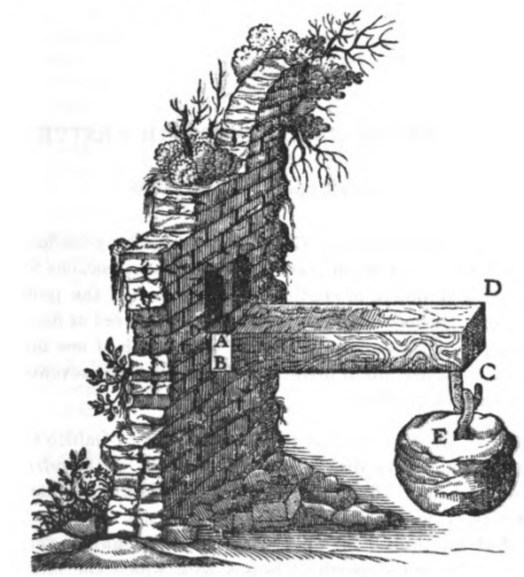

(From the *Discorsi*, Leiden 1638.)

"Galileo's Problem"

Euler-Bernoulli beam theory

The complete approach is an asymptotic calculation based on the small number $\varepsilon = h/R$ where R is the inverse of the largest curvature in the problem.

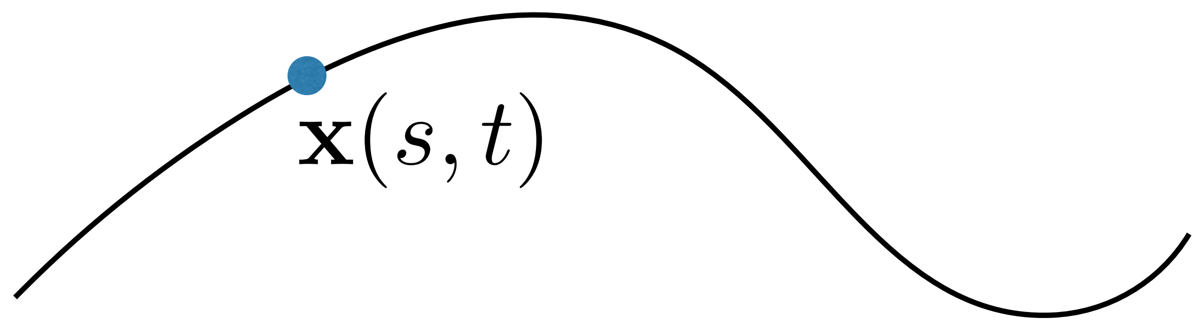

Arc-length s is the reference configuration label $\mathbf{X}$!

In the asymptotic calculation (or ask Bernoulli) it is shown that the elastic energy is given by

$$\mathcal{E} = \frac{B}{2}\int_0^L \kappa^2\, ds \qquad \kappa = |\mathbf{x}_{ss}|$$

If we wish to study an inextensible rod/sheet, we need a Lagrange multiplier:

$$\mathcal{E} = \frac{B}{2}\int_0^L |\mathbf{x}_{ss}|^2\, ds + \int_0^L \frac{T(s)}{2}(|\mathbf{x}_s| - 1)^2\, ds$$

Why all this talk about inextensibility?

$$\text{Stretching energy} \propto h$$

$$\text{Bending energy} \propto h^3$$

Euler-Bernoulli beam theory

$$\mathcal{E} = \frac{B}{2}\int_0^L |\mathbf{x}_{ss}|^2\, ds + \int_0^L \frac{T(s)}{2}(|\mathbf{x}_s| - 1)^2\, ds$$

Principle of virtual work: at equilibrium,

$$\mathbf{g}\cdot\frac{\delta\mathcal{E}}{\delta\mathbf{x}} = \lim_{\varepsilon\to 0}\frac{\mathcal{E}[\mathbf{x}+\varepsilon\mathbf{g}] - \mathcal{E}[\mathbf{x}]}{\varepsilon} = 0\ \forall\mathbf{g}$$

$$\mathcal{E}[\mathbf{x}+\varepsilon\mathbf{g}] = \frac{B}{2}\int_0^L |\mathbf{x}_{ss}+\varepsilon\mathbf{g}_{ss}|^2\, ds + \int_0^L \frac{T(s)}{2}(|\mathbf{x}_s+\varepsilon\mathbf{g}_s| - 1)^2\, ds$$

Integrate by parts…

$$\int_0^L (-B\mathbf{x}_{ssss} + (T(s)\mathbf{x}_s)_s)\cdot\mathbf{g}\, ds = 0\ \forall\mathbf{g}$$

Since true for all **g:** $-B\mathbf{x}_{ssss} + (T(s)\mathbf{x}_s)_s = 0$

Euler-Bernoulli beam theory

Had we included kinetic energy in the calculation, we would have found F=ma:

$$\rho \mathbf{x}_{tt} = -B\mathbf{x}_{ssss} + (T(s)\mathbf{x}_s)_s$$

"Euler-Bernoulli beam"

While integrating by parts we find "solvability" conditions from the boundary terms:

$$(B\boldsymbol{x}_{ss})(0) = 0, \quad (B\boldsymbol{x}_{ss})(L) = 0$$

$$(T\boldsymbol{x}_s)(0) = (B\boldsymbol{x}_{ss})_s(0), \quad (T\boldsymbol{x}_s)(L) = (B\boldsymbol{x}_{ss})_s(L).$$

Euler-Bernoulli beam theory

Even better!

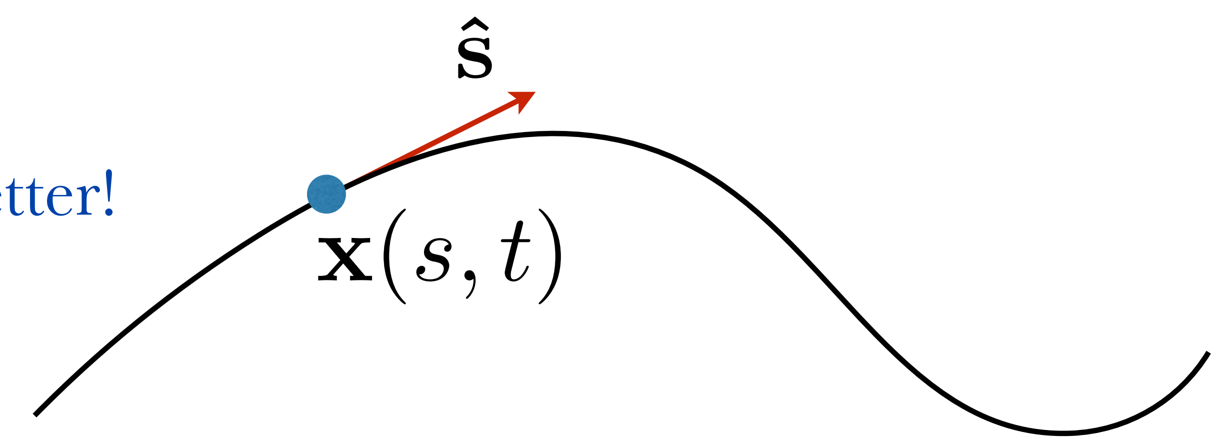

Let $\hat{\mathbf{s}} = \mathbf{x}_s = (\cos\theta(s), \sin\theta(s))$

Then $\kappa(s) = \theta_s(s)$ (so choose arc-length and tangent angle whenever possible!)

$$\mathbf{f} = -B\left(\kappa_{ss} + \frac{1}{2}\kappa^3\right)\hat{\mathbf{n}} = -B\left(\theta_{sss} + \frac{1}{2}\theta_s^3\right)\hat{\mathbf{n}}$$

(Flag model!)

Small amplitude?

$$(s, y(s)) \approx (x, y(x))$$

$$\theta \approx y_x$$

$$\mathbf{f} \approx -By_{xxxx}\hat{\mathbf{y}}$$

Euler-Bernoulli beam theory

An equation for the tension: use the constraint! $\partial_t(|\mathbf{x}_s|^2) = 0 \Rightarrow \mathbf{x}_s \cdot \mathbf{x}_{st} = 0$

(stay tuned)

On the menu

0. Lecture motivation: Alben & Shelley (2008)
1. Continuum mechanics, abridged
2. Euler-Bernoulli beam theory
3. Entertainment

WAVE PROPAGATION ALONG FLAGELLA

By K. E. MACHIN
Department of Zoology, University of Cambridge

(*Received* 13 *May* 1958) J. Exp. Biol.

Biophysical Journal Volume 74 February 1998 1043–1060 1043

Trapping and Wiggling: Elastohydrodynamics of Driven Microfilaments

Chris H. Wiggins,* D. Riveline,# A. Ott,# and Raymond E. Goldstein§
*Department of Physics, Princeton University, Princeton, New Jersey 08544 USA; #Institut Curie, Section de Physique et Chimie, 75231 Paris Cedex 05, France; and §Department of Physics and Program in Applied Mathematics, University of Arizona, Tucson, Arizona 85721 USA

Active elastohydrodynamics

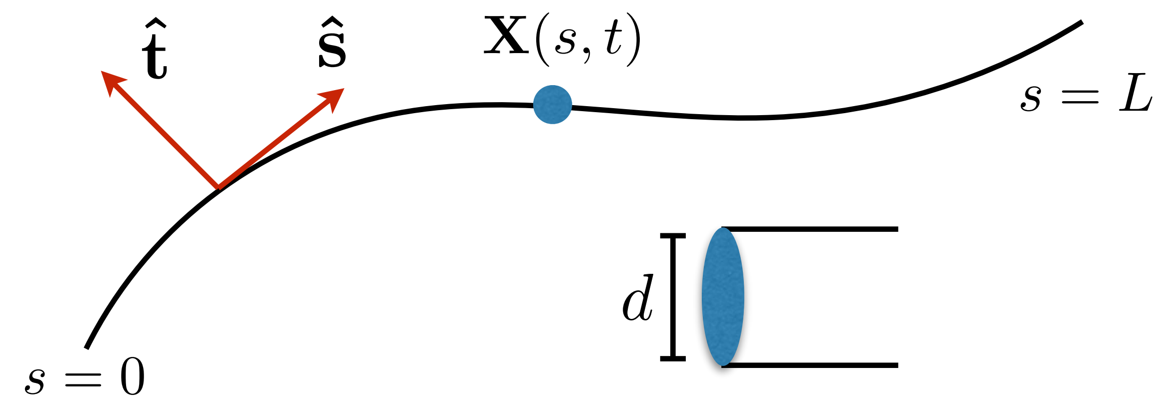

Force balance: $-\zeta\left[\hat{\mathbf{n}}\hat{\mathbf{n}} + \beta\hat{\mathbf{t}}\hat{\mathbf{t}}\right] \cdot \mathbf{x}_t = B\left(\kappa_{ss} + \frac{1}{2}\kappa^3\right)\hat{\mathbf{n}}$ $\quad \zeta = \dfrac{4\pi\mu}{\ln(L/d) - 1/2} \quad \beta = \dfrac{1}{2}$

Small amplitude approximation: $\zeta y_t = -B y_{xxxx}$

Nondimensionalize: $x = L\tilde{x}, \quad y = L\tilde{y}, \quad t = \tilde{t}/\omega,$

$$\tilde{y}_{\tilde{t}} = -\alpha\, \tilde{y}_{\tilde{x}\tilde{x}\tilde{x}\tilde{x}}$$

A hyperdiffusion equation

$$\alpha = \frac{B}{\zeta\omega L^4} = \left(\frac{\ell(\omega)}{L}\right)^4$$

$$\ell(\omega) = (B/\zeta\omega)^{1/4}$$

Penetration length

Or: $\mathrm{Sp} = L/\ell(\omega)$ (Sperm number)

Biophysical Journal Volume 74 February 1998 1043–1060

Trapping and Wiggling: Elastohydrodynamics of Driven Microfilaments

Chris H. Wiggins,* D. Riveline,# A. Ott,# and Raymond E. Goldstein§
*Department of Physics, Princeton University, Princeton, New Jersey 08544 USA; #Institut Curie, Section de Physique et Chimie, 75231 Paris Cedex 05, France; and §Department of Physics and Program in Applied Mathematics, University of Arizona, Tucson, Arizona 85721 USA

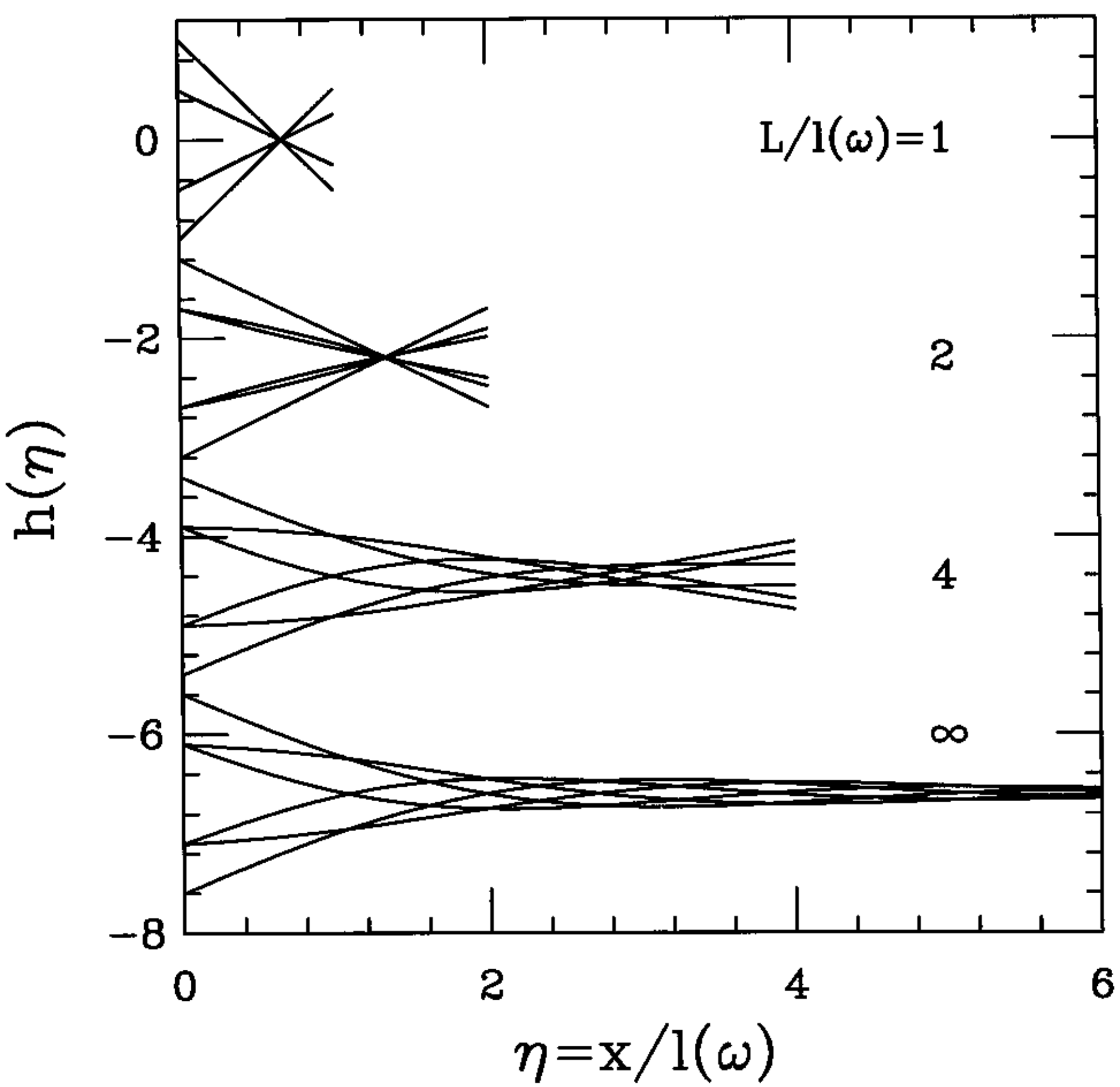

FIGURE 6 Solutions to EHD problem II for filaments of various rescaled lengths $\mathcal{L}$.

Propulsive Force

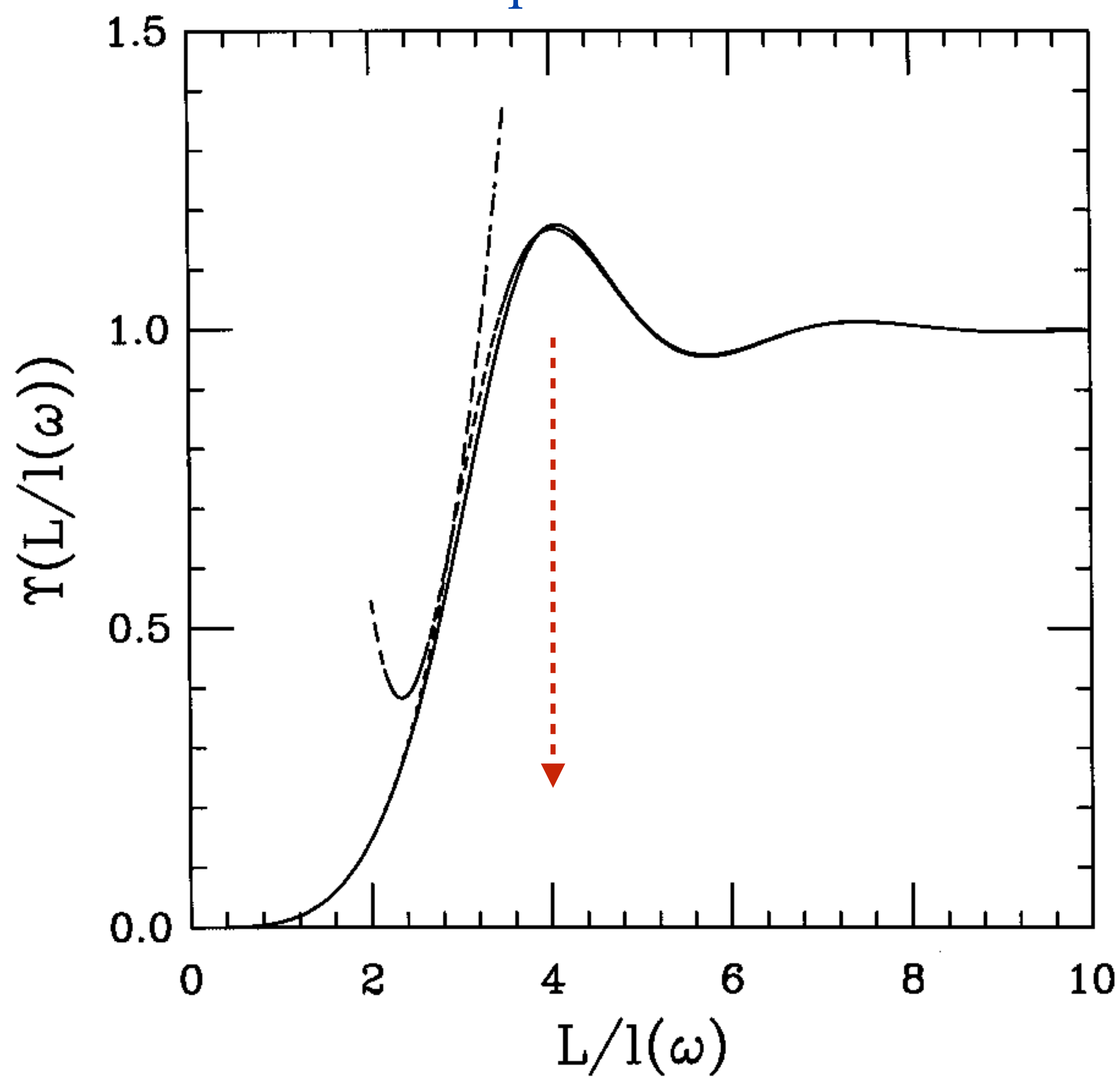

FIGURE 7 Scaling function Υ for propulsive force. The large $\mathcal{L}$ expansion is plotted for $\mathcal{L} > 2$, and the small-$\mathcal{L}$ solution is plotted for $\mathcal{L} < 3.5$.

WAVE PROPAGATION ALONG FLAGELLA

BY K. E. MACHIN

Department of Zoology, University of Cambridge

(*Received* 13 *May* 1958) J. Exp. Biol.

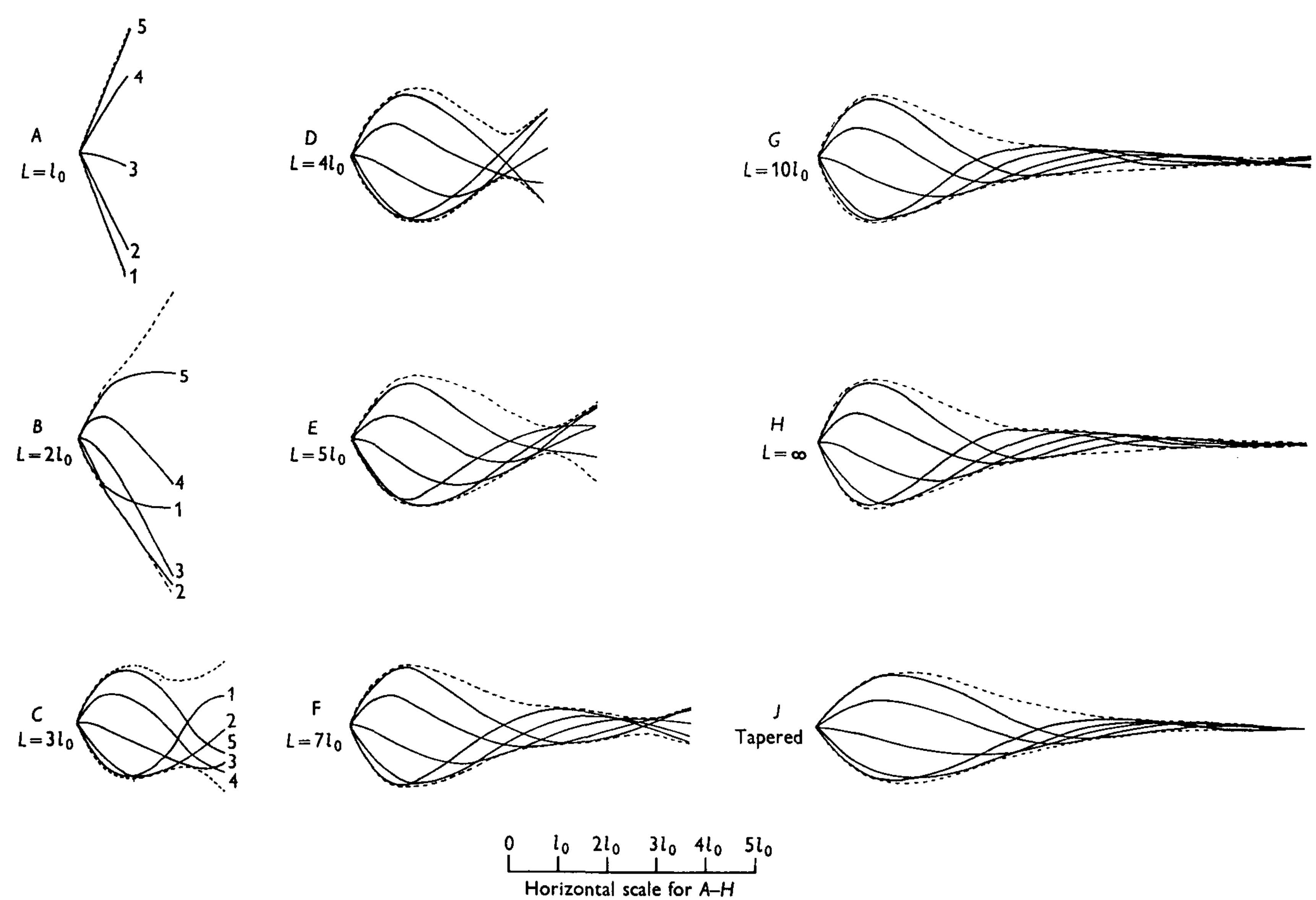

Fig. 3. Calculated wave-patterns on a flagellum. Vertical amplitudes have been exaggerated for clarity.

WAVE PROPAGATION ALONG FLAGELLA

By K. E. MACHIN
Department of Zoology, University of Cambridge

(*Received* 13 *May* 1958)

However, it is clear from Fig. 3 that a passive elastic flagellum of uniform cross-section driven from one end cannot exhibit more than $1\frac{1}{2}$ wavelengths along its length. Further, the amplitude of the wave decreases exponentially. If a flagellum exhibits more than $1\frac{1}{2}$ wavelengths, or has a sustained amplitude along its length, the propagation of the waves cannot be due to a passive mechanism. This conclusion is unaffected by the nature of the drive at the proximal end, since the secondary wave becomes negligible beyond $3l_0$.

$L \approx 50\,\mu m$

$d \approx 500\,nm$

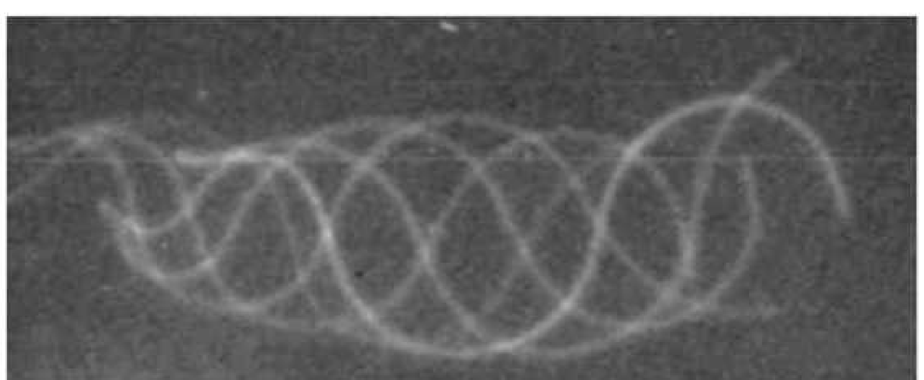

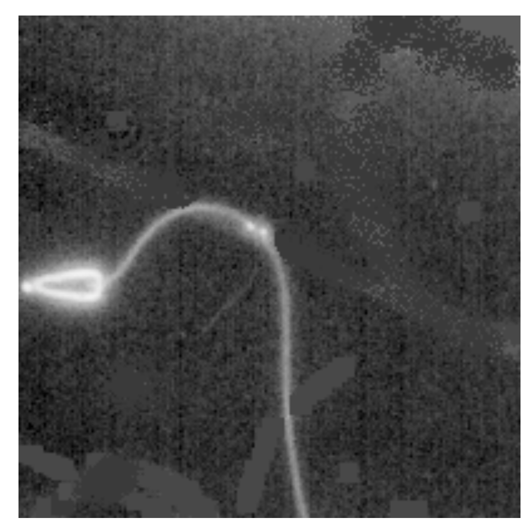

Spermatozoa of *Lytechinus* and *Ciona* (sea urchin)
Brokaw, J. Exp. Biol. (1965).

New Journal of Physics
An Institute of Physics and Deutsche Physikalische Gesellschaft Journal

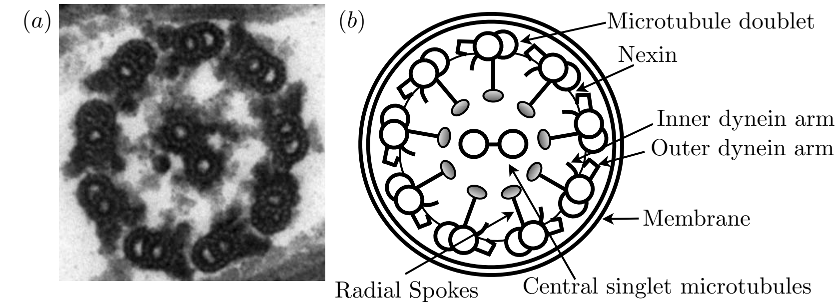

Generic aspects of axonemal beating

Sébastien Camalet and Frank Jülicher
PhysicoChimie Curie, UMR CNRS/IC 168, 26 rue d'Ulm, 75248 Paris Cedex 05, France
E-mail: `scamalet@curie.fr` and `julicher@curie.fr`

New Journal of Physics **2** (2000) 24.1–24.23 (http://www.njp.org/)
Received 7 June 2000; online 4 October 2000

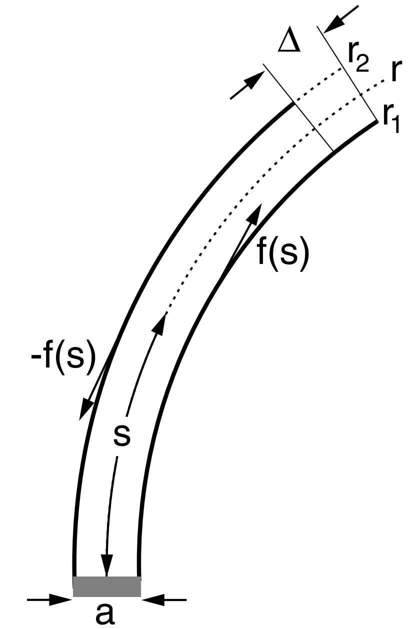

$$G \equiv \int_0^L \left[\frac{B}{2}C^2 + f\Delta + \frac{\Lambda}{2}\dot{\boldsymbol{r}}^2\right] \mathrm{d}s. \quad (C = \kappa)$$

$$\Delta = a\int_0^s \mathrm{d}s'\, C$$

$$\frac{\delta G}{\delta \boldsymbol{r}} = \partial_s[(B\dot{C} - af)\boldsymbol{n} - \tau \boldsymbol{t}]$$

$$\partial_t \boldsymbol{r} = -\left(\frac{1}{\xi_\perp}\boldsymbol{n}\boldsymbol{n} + \frac{1}{\xi_\parallel}\boldsymbol{t}\boldsymbol{t}\right)\cdot\frac{\delta G}{\delta \boldsymbol{r}}$$

$$\boldsymbol{t} = (\cos\psi, \sin\psi)$$
$$C = \dot{\psi}.$$

$$\partial_t \psi = \frac{1}{\xi_\perp}(-B\ddddot{\psi} + a\ddot{f} + \dot{\psi}\dot{\tau} + \tau\ddot{\psi}) + \frac{1}{\xi_\parallel}\dot{\psi}(B\dot{\psi}\ddot{\psi} - af\dot{\psi} + \dot{\tau})$$

$$\ddot{\tau} - \frac{\xi_\parallel}{\xi_\perp}\dot{\psi}^2\tau = a\partial_s(\dot{\psi}f) - B\partial_s(\dot{\psi}\ddot{\psi}) + \frac{\xi_\parallel}{\xi_\perp}\dot{\psi}(a\dot{f} - B\dddot{\psi})$$

$$\boldsymbol{r}(s,t) = \boldsymbol{r}(0,t) + \int_0^s (\cos\psi, \sin\psi)\,\mathrm{d}s'$$

Small amplitude: $\psi = \epsilon\psi_1 + \epsilon^2\psi_2 + \mathrm{O}(\epsilon^3)$

$$\tau = \tau_0 + \epsilon\tau_1 + \epsilon^2\tau_2 + \mathrm{O}(\epsilon^3)$$

$\tau_0 = \sigma$ is a constant,

$$\xi_\perp \partial_t \psi_1 = -B\ddddot{\psi}_1 + \sigma\ddot{\psi}_1 + a\ddot{f}_1$$

Self-organized beating

$$f(t) = \sum_n f_n \, \mathrm{e}^{\mathrm{i}n\omega t}$$

$$\Delta(t) = \sum_n \Delta_n \, \mathrm{e}^{\mathrm{i}n\omega t}$$

Two-state model for molecular motors $f_n = \chi(\Omega, \omega)\Delta_n$

$$\chi(\Omega, \omega) = \; K + \mathrm{i}\lambda\omega - \rho\, k\Omega \frac{\mathrm{i}\omega/\alpha + (\omega/\alpha)^2}{1 + (\omega/\alpha)^2}$$

which is the linear response function obtained for a two-state model, see appendix C. Here, K is an elastic modulus per motor, λ an internal friction coefficient per motor, k is the cross-bridge elasticity of a motor and Ω, with $0 < \Omega < \pi^2$, plays the role of a control parameter, α is a characteristic ATP cycling rate. Higher-order terms $F^{(2n+1)}$ have to be taken into account if the third or higher order in ϵ is considered.

For $\Omega < \Omega_c$, the system is passive and not moving, for $\Omega > \Omega_c$ it exhibits spontaneous oscillations

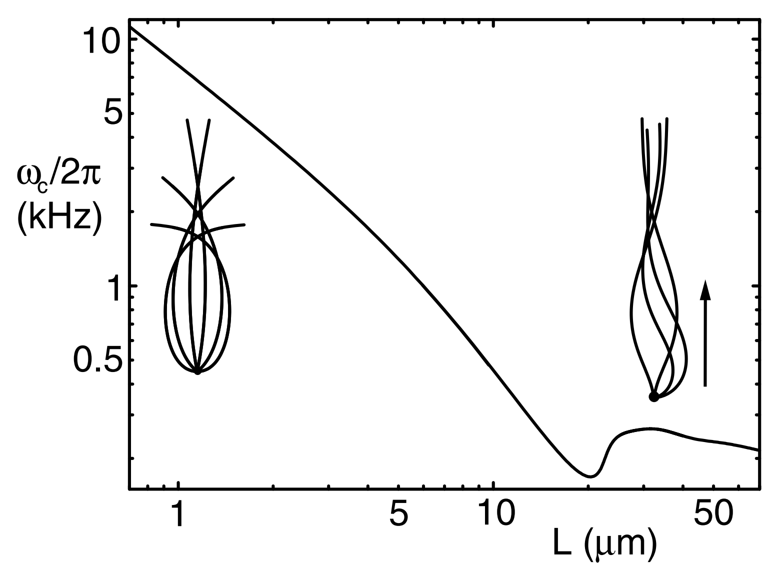

Figure 8. Oscillation frequency $\omega_c/2\pi$ at the bifurcation point

Question: What is the 'optimal' geometry for *planar*, slender body (headless) locomotion?

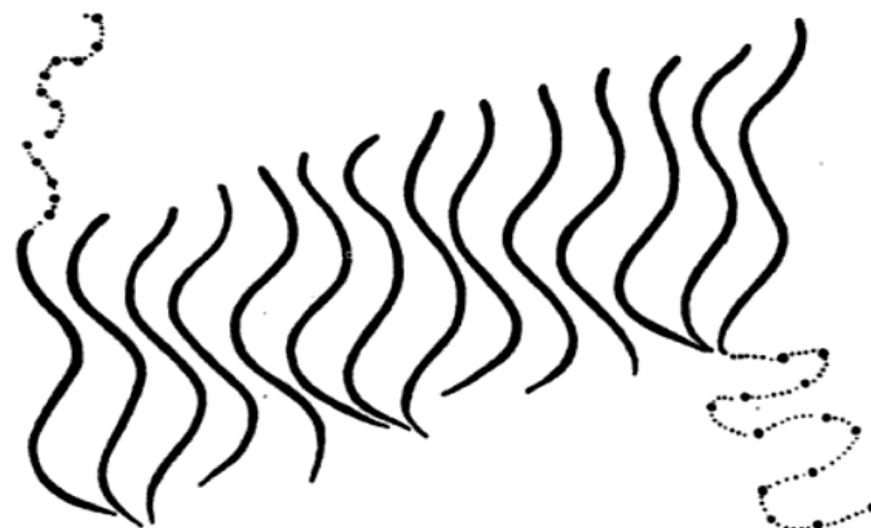

Partial answer:

Periodic waves (Pironneau & Katz, JFM (1974), Tam [PhD Thesis, MIT] (2008)).

Infinite length

optimality condition: $|\psi| \approx 40^\circ$ Lighthill, SIAM Rev. (1976)

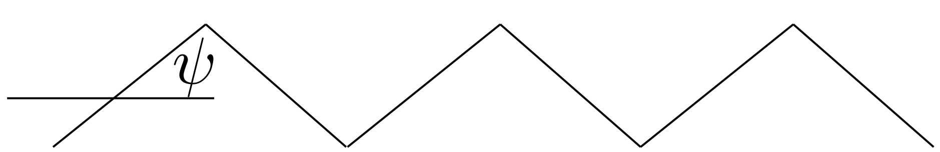

(Helical motions avoid this complication)

But what if there are other energetic costs?

What is the shape of the optimal elastic flagellum?

PHYSICS OF FLUIDS **22**, 031901 (2010)

The optimal elastic flagellum

Saverio E. Spagnolie[a] and Eric Lauga[b]
Department of Mechanical and Aerospace Engineering, University of California, San Diego, 9500 Gilman Drive, La Jolla, California 92093-0411, USA

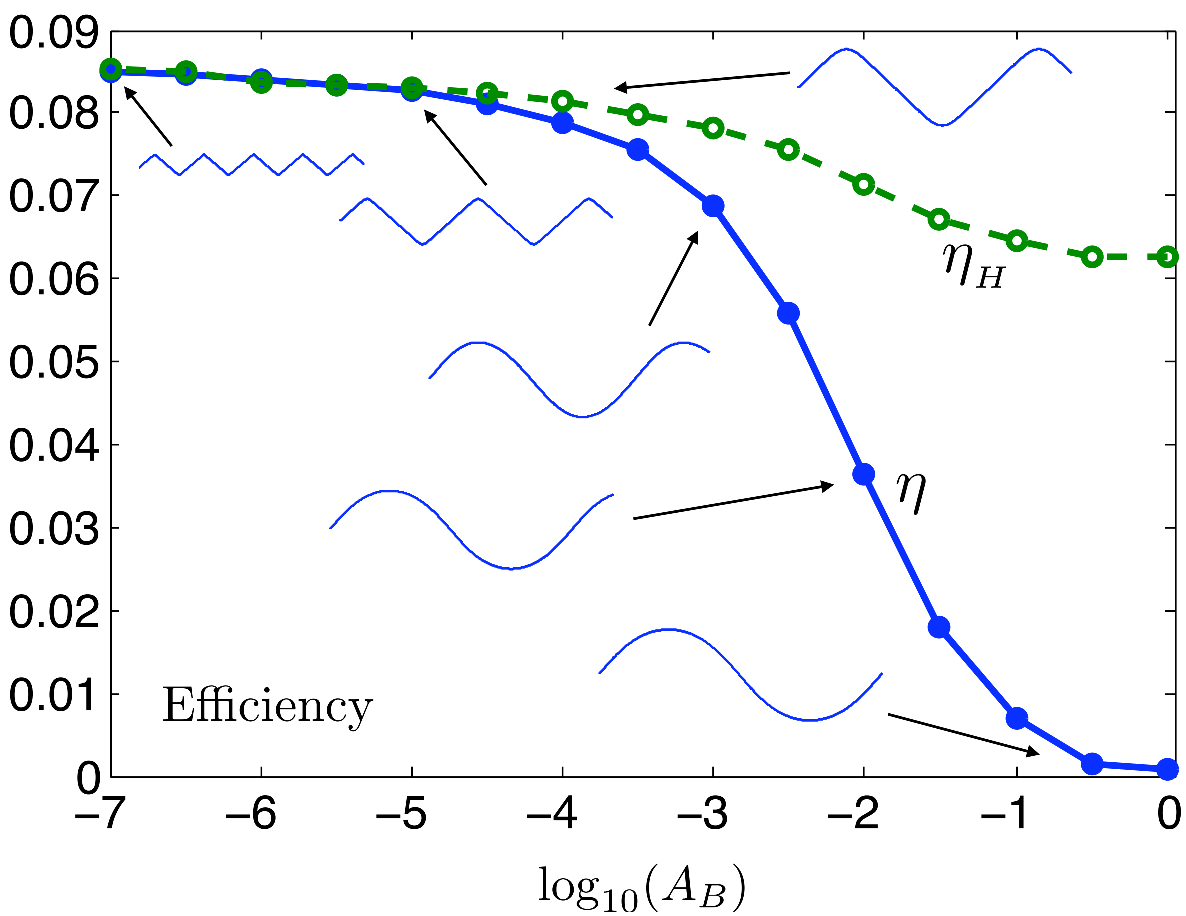

FIG. 11. (Color online) Swimming efficiencies for the optimal flagellum of finite length as a function of the bending cost A_B: total (η, solid line) and hydrodynamic (η_H, dashed line) efficiencies.

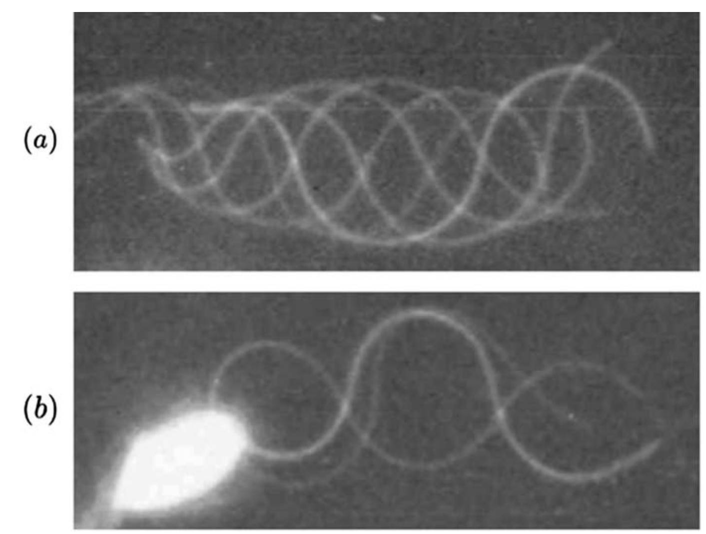

FIG. 15. Spermatozoa of two marine invertebrates. (a) Superimposed images of the headless spermatozoon of *Lytechinus*. (b) Spermatozoon of *Chaetopterus* exhibits nonintegral spatial wave numbers. [Reproduced with permission from C. J. Brokaw, J. Exp. Biol. **43**, 455 (1965). Copyright © 1965, The Company of Biologists.]

And much more…

IOP Publishing — Reports on Progress in Physics

Rep. Prog. Phys. **72** (2009) 096601 (36pp) doi:10.1088/0034-4885/72/9/096601

The hydrodynamics of swimming microorganisms

Eric Lauga[1] **and Thomas R Powers**[2]

[1] Department of Mechanical and Aerospace Engineering, University of California, San Diego, La Jolla, CA 92093-0411, USA
[2] Division of Engineering, Brown University, Providence, RI 02912-9104, USA

E-mail: elauga@ucsd.edu and Thomas_Powers@brown.edu

Available online at www.sciencedirect.com
SCIENCE DIRECT®
Journal of Computational Physics 196 (2004) 8–40
JOURNAL OF COMPUTATIONAL PHYSICS
www.elsevier.com/locate/jcp

Simulating the dynamics and interactions of flexible fibers in Stokes flows

Anna-Karin Tornberg *, Michael J. Shelley

Courant Institute of Mathematical Sciences, New York University, 251 Mercer Street, NY 10012, USA

Received 11 June 2003; received in revised form 10 October 2003; accepted 20 October 2003

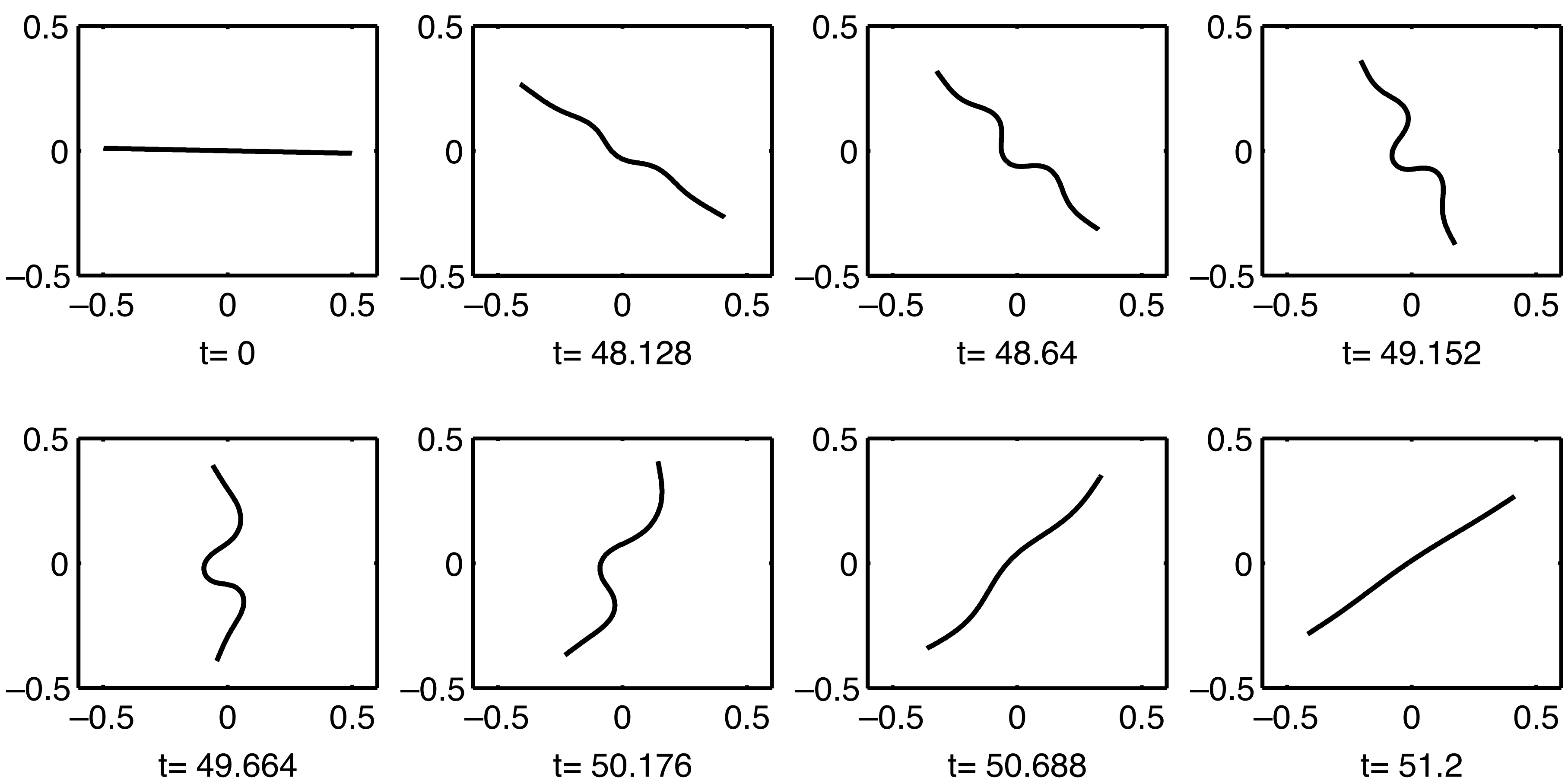

Fig. 3. Pronounced buckling occurs for $\bar{\mu} = 3 \times 10^5$.

Soft Matter

RSC Publishing

PAPER

Elastocapillary self-folding: buckling, wrinkling, and collapse of floating filaments

Cite this: *Soft Matter*, 2013, **9**, 1711

Arthur A. Evans,*[a] Saverio E. Spagnolie,*[b] Denis Bartolo[cd] and Eric Lauga[e]

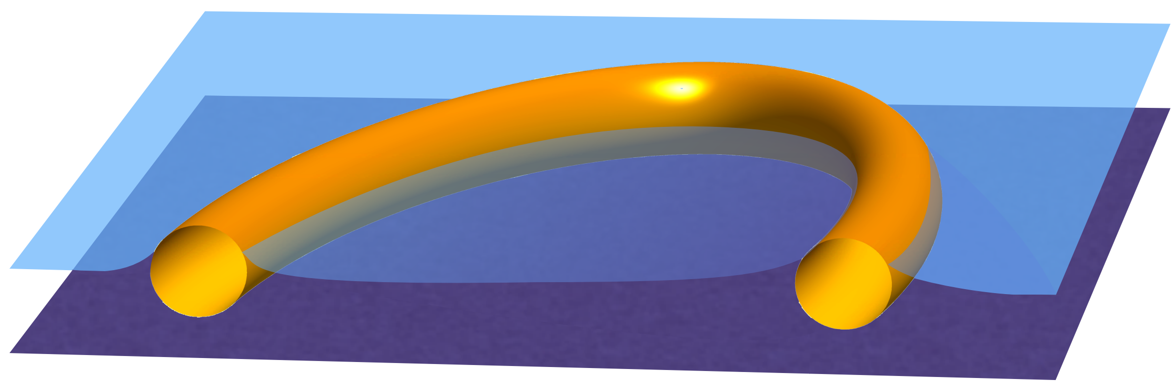

$$E = \int_0^1 \left\{ \frac{1}{2} |\mathbf{x}_{ss}|^2 + T(s)[|\mathbf{x}_s|^2 - 1] + \frac{\Omega}{2} \int' \ln R(s,s') ds' \right\} ds.$$

$$R(s,s') = |\mathbf{x}(s) - \mathbf{x}(s')|$$

(Non-dimensionalized on L, B/L)

$$\boxed{\Omega = \frac{\gamma L^3}{B} \sim \frac{\text{Attraction}}{\text{Bending}}}$$

The Cheerios effect

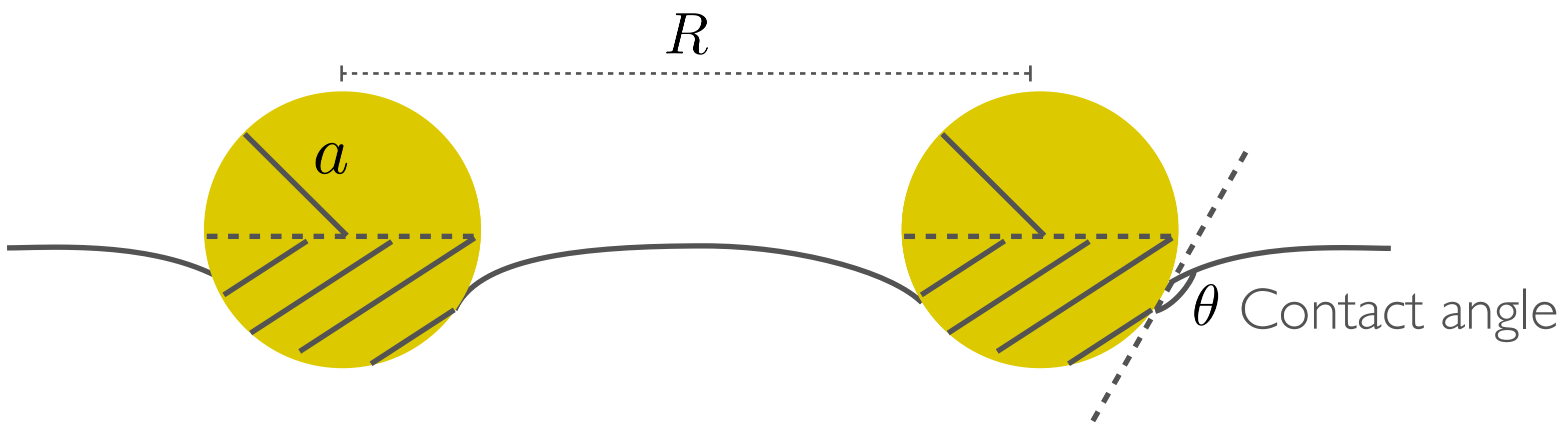

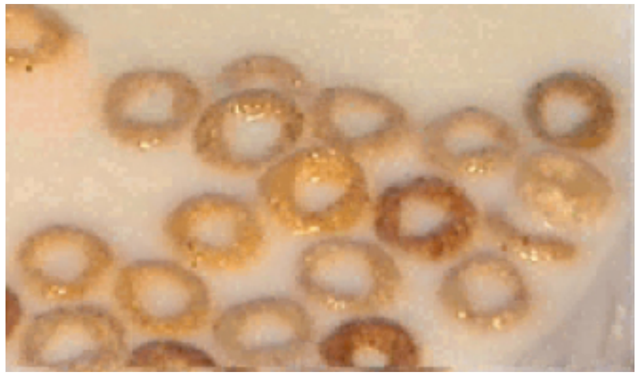

$$E_{\text{int}} = \gamma a^2 \ln(R/\ell_c),$$ "Capillary monopoles"

γ Interaction strength

- Fluid (Surface tension)
- Material (Contact angle, gravity)
- Particle geometry

ℓ_c Capillary length $= \sqrt{\sigma/\Delta\rho g}$

Nicolson, 1948
Keller, 1998
Vella & Mahadevan, 2005

Anurida Maritima springtail (cosmopolitan collembolan)

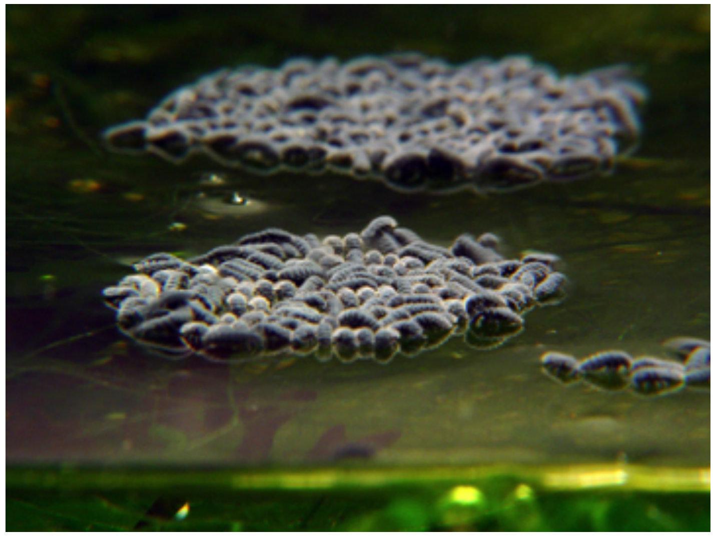

Mendel, Hu & Bush 2005

Linear stability analysis

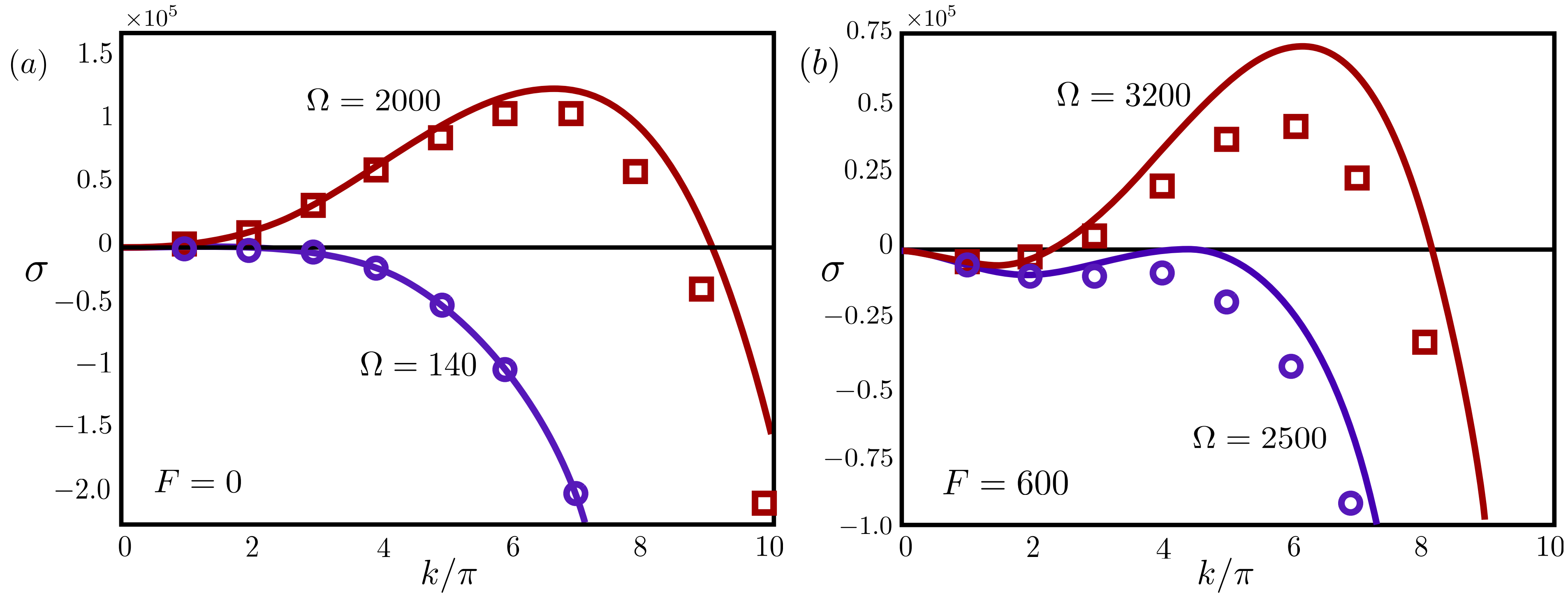

Full simulation:

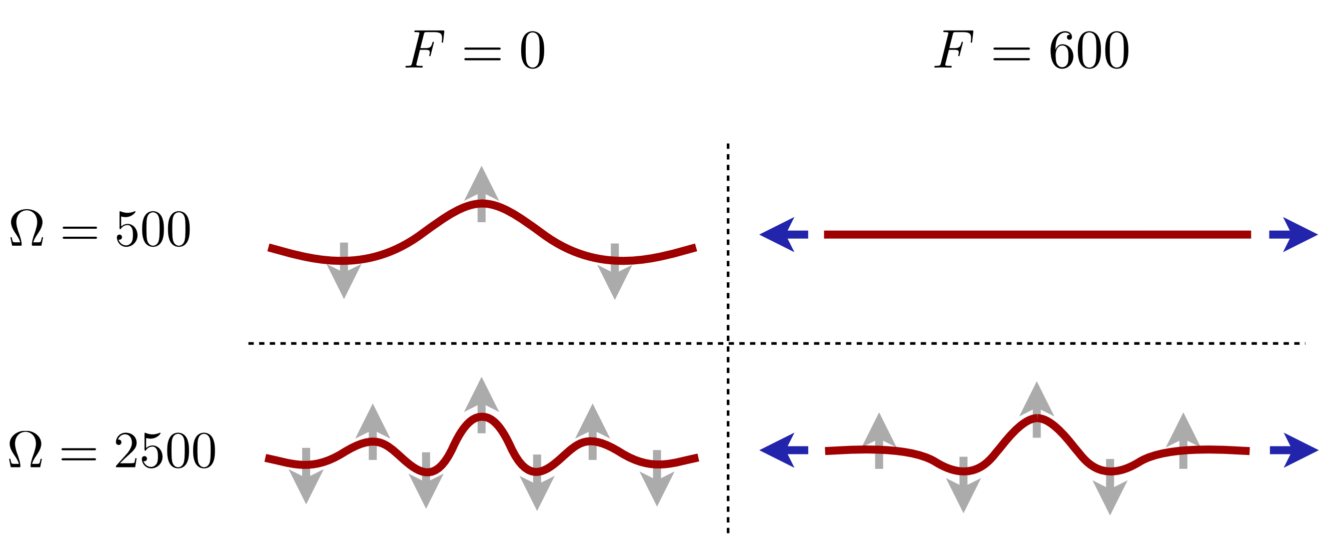

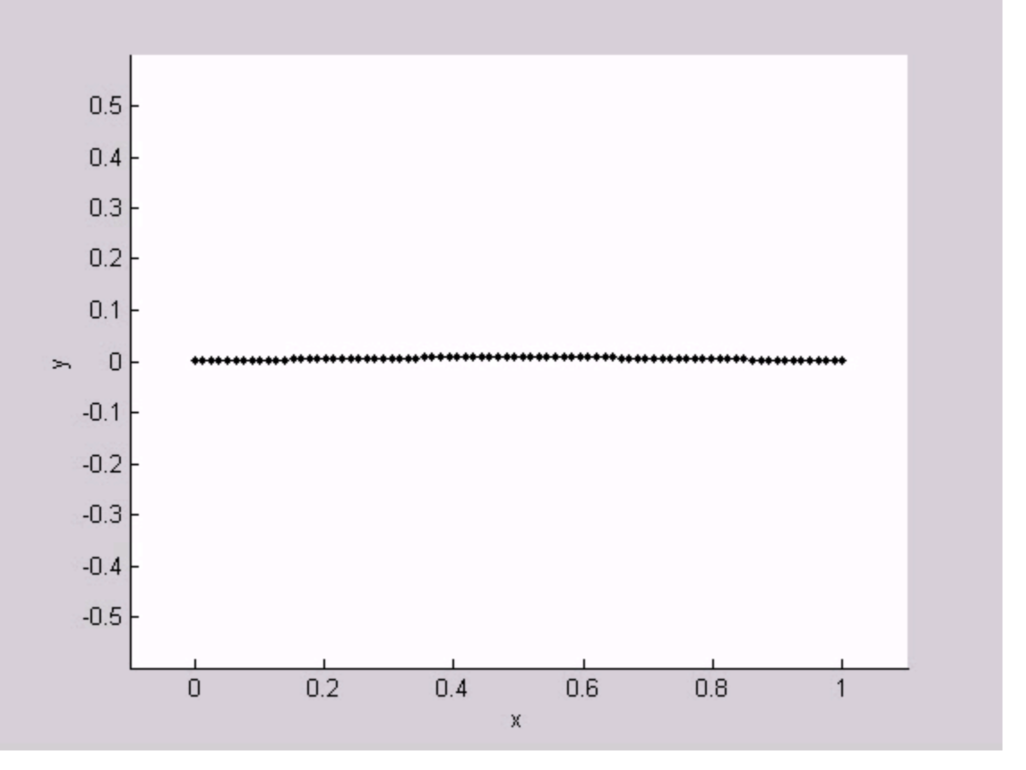

Long-time behavior?

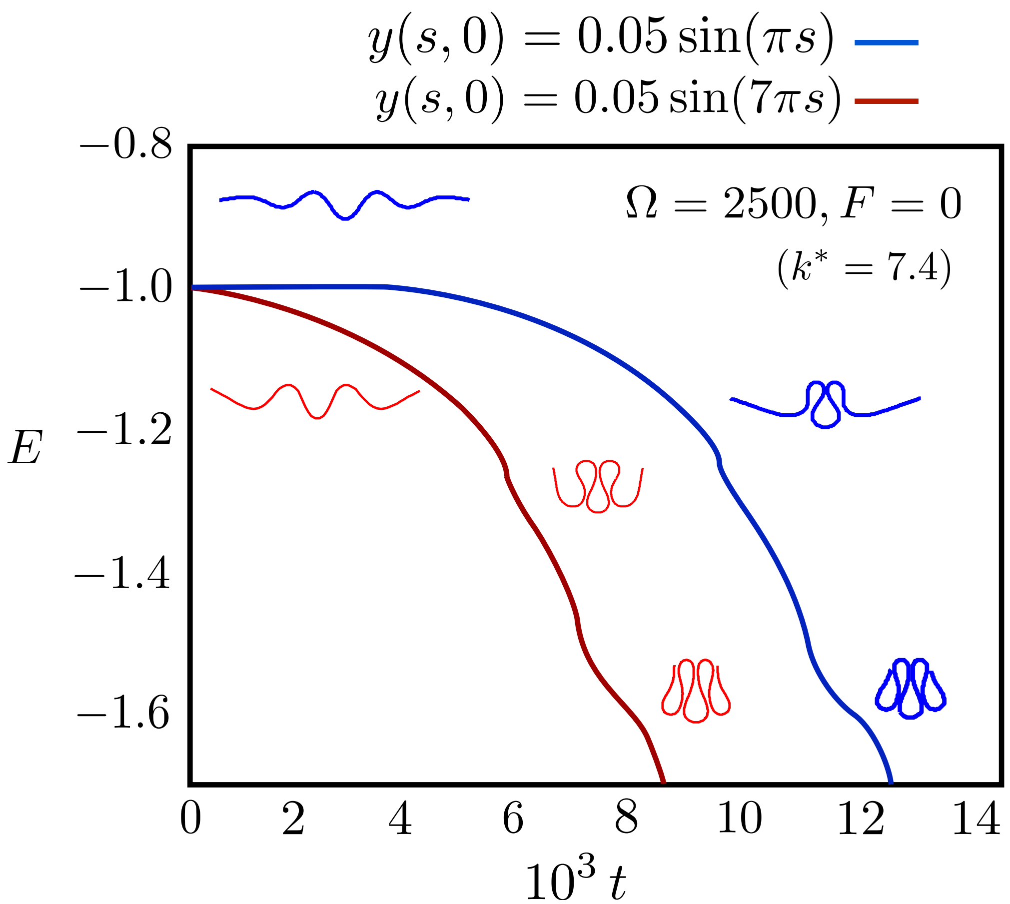

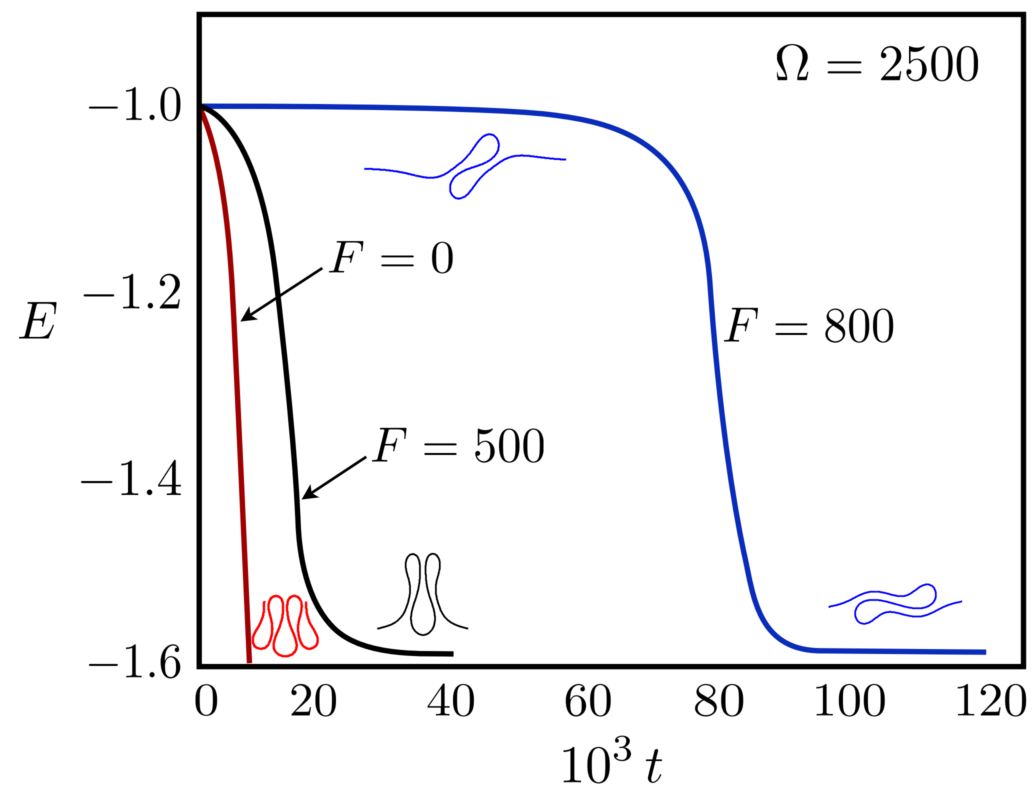

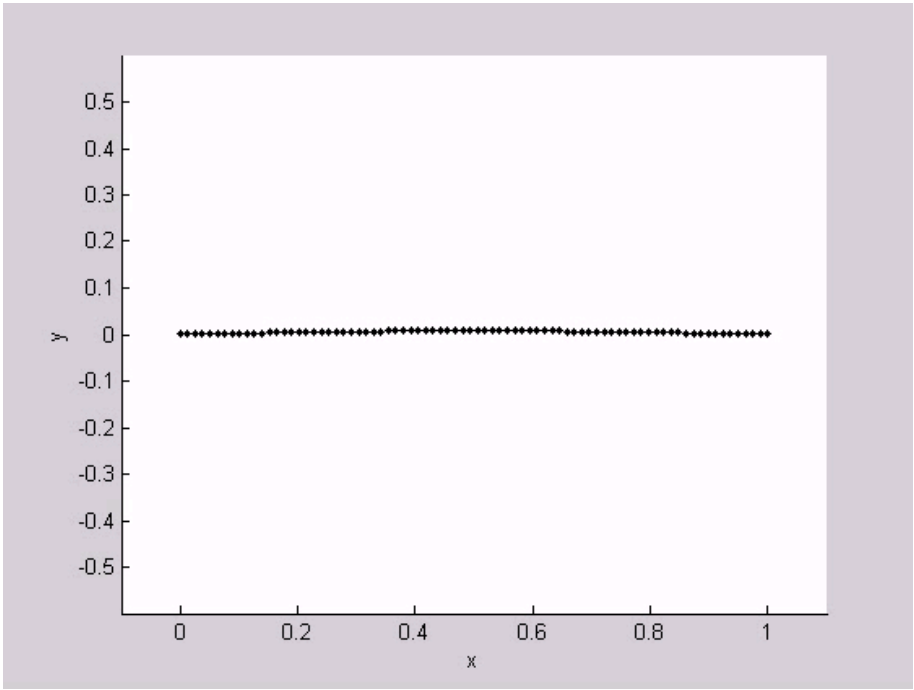

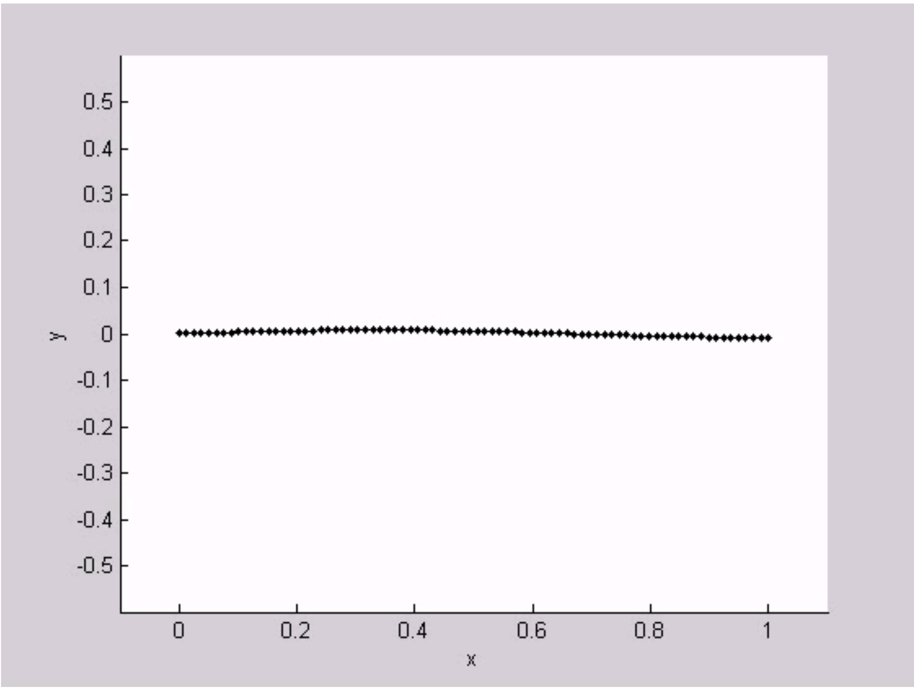

Gross features of ultimate shapes are suggested by linear stability analysis

Highly deformed states

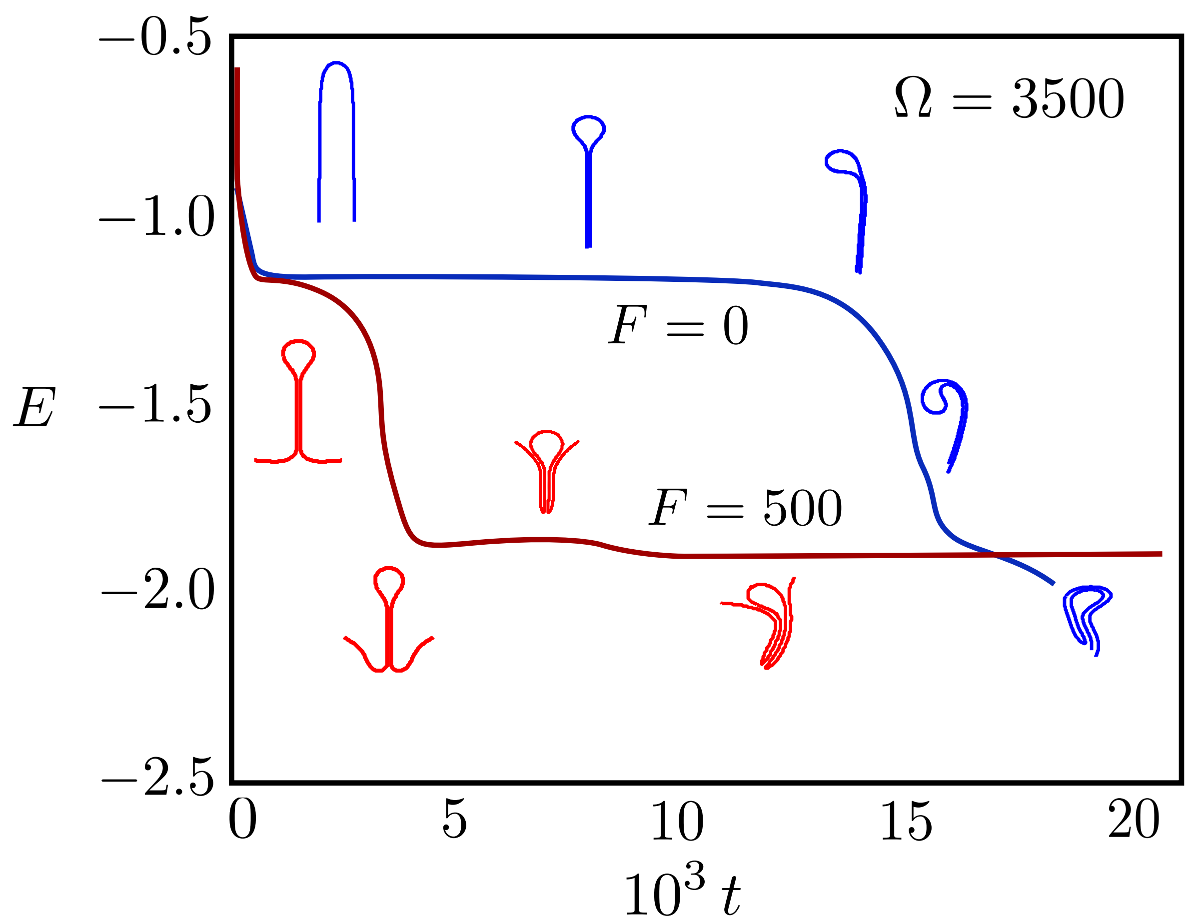

A self-folding cascade

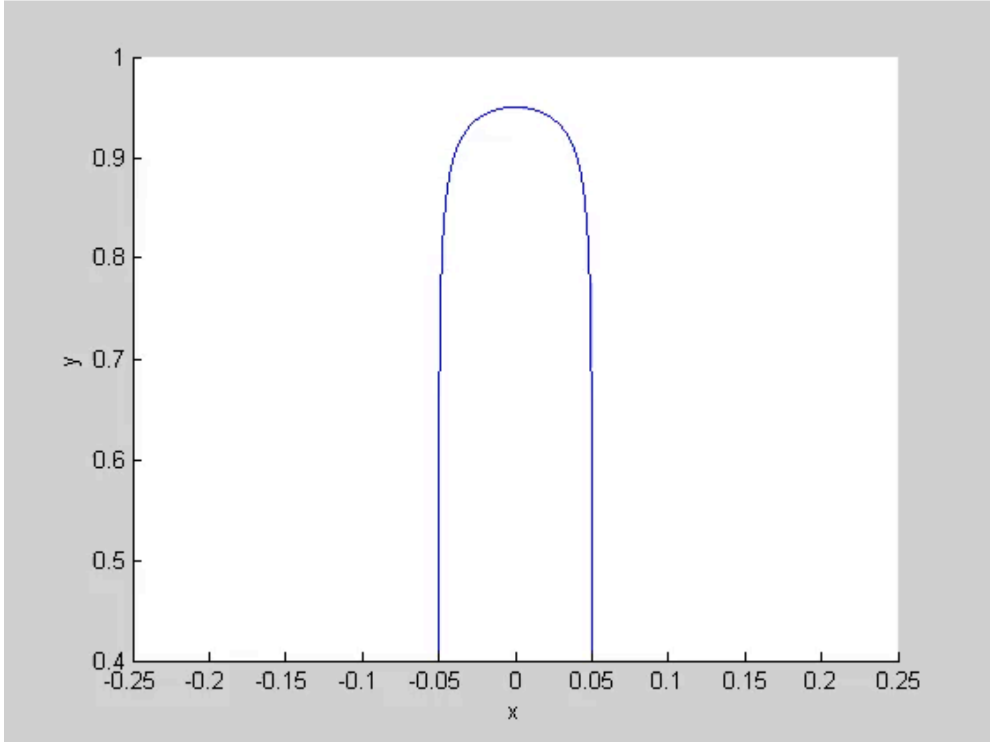

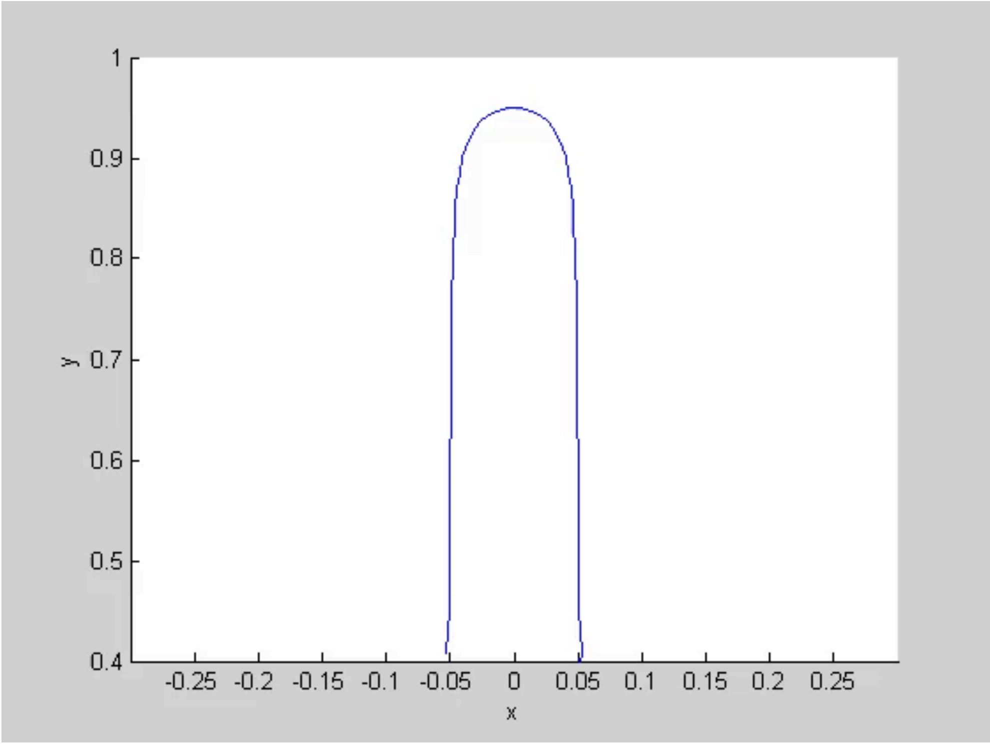

J. Fluid Mech. (2013), *vol.* 735, *pp.* 705–736.
doi:10.1017/jfm.2013.512

The sedimentation of flexible filaments

Lei Li[1], **Harishankar Manikantan**[2], **David Saintillan**[2] **and Saverio E. Spagnolie**[1,†]

$$\mathscr{E} = \frac{1}{2}\int_0^L B(s)|\boldsymbol{x}_{ss}|^2\,\mathrm{d}s + \frac{1}{2}\int_0^L T(s)(|\boldsymbol{x}_s|^2 - 1)\,\mathrm{d}s - \int_0^L \boldsymbol{f}(s)\cdot\boldsymbol{x}(s)\,\mathrm{d}s - \int_0^L \boldsymbol{F}_g(s)\cdot\boldsymbol{x}(s)\,\mathrm{d}s,$$

Sedimenting fiber suspensions are beautiful and complex

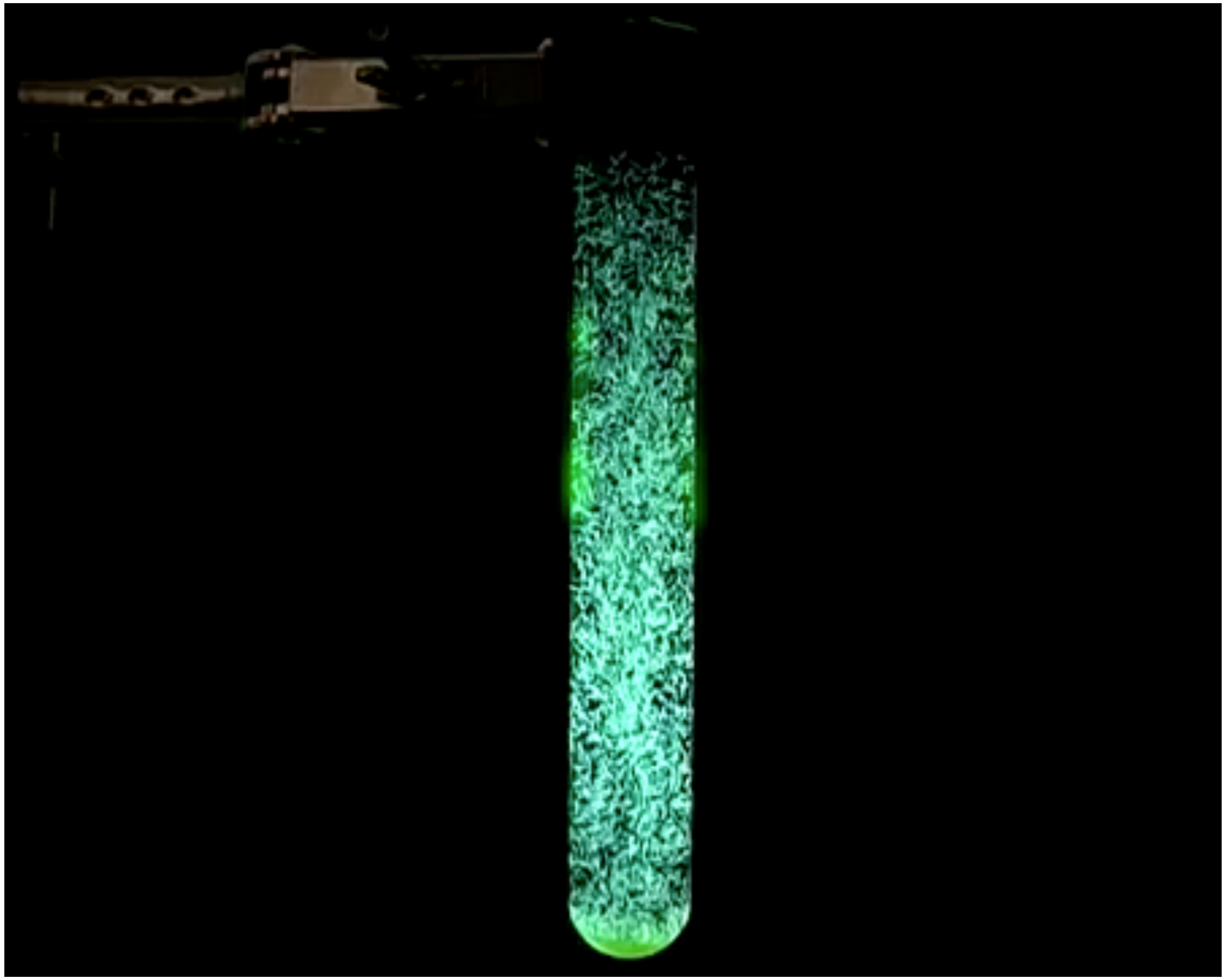

Guazzelli Lab

Q: What is the role of flexibility?

(Start with one fiber!)

Koch & Shaqfeh, (1989),
Metzger, Guazzelli & Butler (2005),
Saintillan et al. (2006),
Tornberg & Gustavvson (2009),
Guazzelli & Hinch (2011).

Hydrodynamic interactions lead to **drag anisotropy** of slender filaments

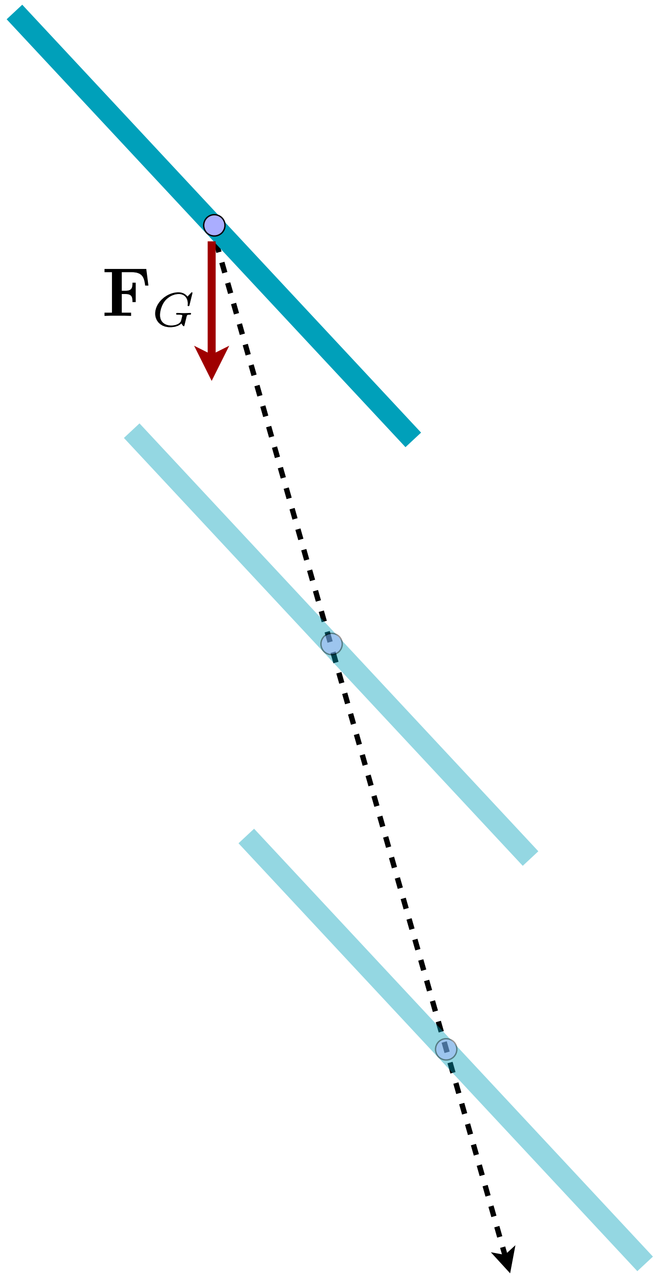

$$\mathbf{U} = [\mu_\perp(\mathbf{I} - \hat{\mathbf{t}}\hat{\mathbf{t}}) + \mu_{||}\hat{\mathbf{t}}\hat{\mathbf{t}}] \cdot \mathbf{F}_G$$

There are two physical mechanisms which may lead to bending

vs.

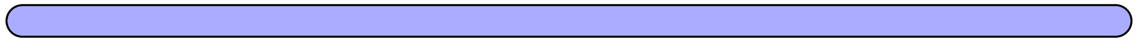

There are two physical mechanisms which may lead to bending

vs.

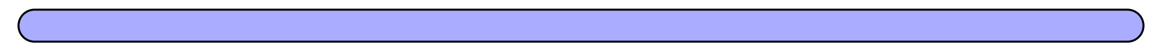

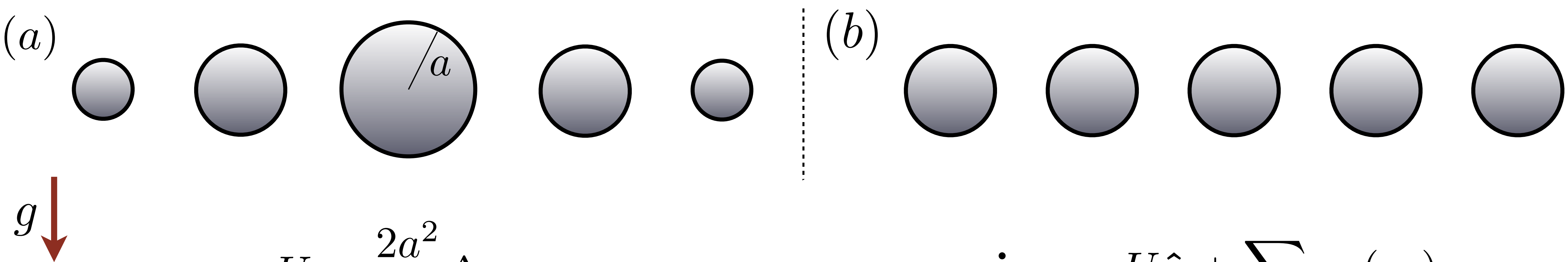

$$U = \frac{2a^2}{9\mu} \Delta \rho g$$

$$\dot{\mathbf{x}}_i = -U\hat{\mathbf{y}} + \sum_{j \neq i} \mathbf{u}_j(\mathbf{x}_i)$$

Two sources of bending:

Spatial variation in gravitational potential

(to be described in this talk)

"Internal" hydrodynamic interactions

The force per unit length on the filament is found by the principal of virtual work

Scaling upon...

$$s = L\,\bar{s} \qquad T = |\mathbf{F}_G|\bar{T}$$

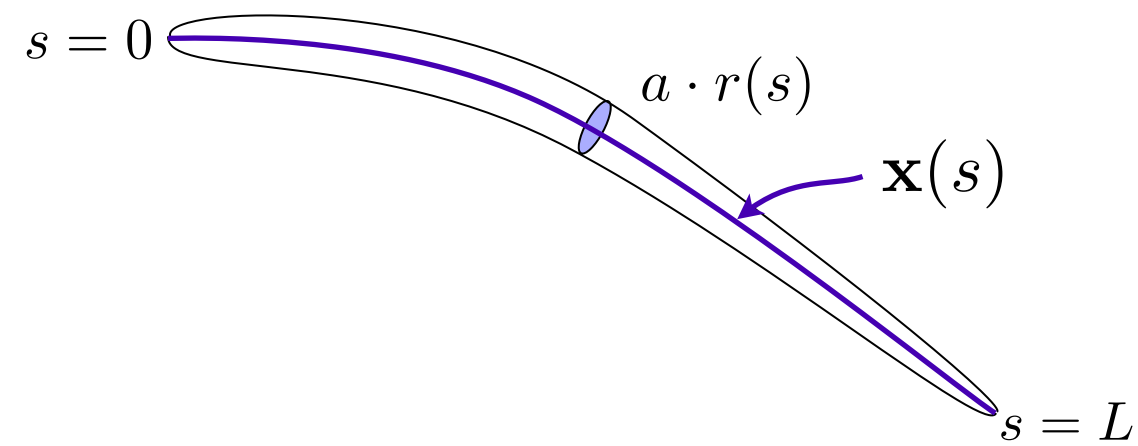

Dimensionless viscous drag:

$$\mathbf{f}(s) = -\mathbf{F}_g(s) - (T(s)\mathbf{x}_s)_s + \beta(B(s)\mathbf{x}_{ss})_{ss}$$

Viscous drag | Gravity | Tension | Elasticity

Elasto-gravitation number: $$\beta = \frac{\pi E a^4}{4|\mathbf{F}_G|L^2}$$

$\beta \gg 1$: Stiff filaments (rods)

$\beta \ll 1$: Floppy filaments

Fluid-body interactions are determined by **slender-body theory** (Johnson, 1980)

$$\epsilon = \frac{a}{L} \ll 1 \longrightarrow$$

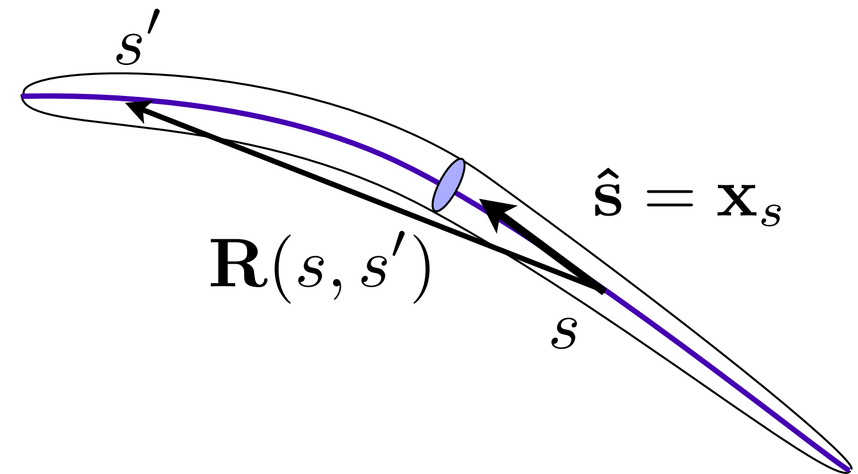

$$\mathbf{x}_t = -\mathbf{\Lambda}[\mathbf{f}] - \mathbf{K}[\mathbf{f}] + (\epsilon^2 \log(\epsilon))$$

Local operator

Nonlocal integral operator

$$\mathbf{f}(s) = -\mathbf{F}_g(s) - (T(s)\mathbf{x}_s)_s + \beta(B(s)\mathbf{x}_{ss})_{ss}$$

An equation for the tension: use the constraint! $\partial_t(|\mathbf{x}_s|^2) = 0 \Rightarrow \mathbf{x}_s \cdot \mathbf{x}_{st} = 0$

$$\begin{aligned} -2(c-1)T_{ss} &+ (c+1)|\boldsymbol{x}_{ss}|^2 T - 2c_s T_s - \boldsymbol{x}_s \cdot \partial_s \boldsymbol{K}[(T\boldsymbol{x}_s)_s] \\ &= (7c-5)\beta B(s)\boldsymbol{x}_{ss} \cdot \boldsymbol{x}_{ssss} + 6(c-1)\beta B(s)|\boldsymbol{x}_{sss}|^2 + 6\beta c_s B(s)\boldsymbol{x}_{ss} \cdot \boldsymbol{x}_{sss} \\ &\quad + \beta(4c_s B_s + (5c-3)B_{ss})|\boldsymbol{x}_{ss}|^2 + 4(4c-3)\beta B_s \boldsymbol{x}_{ss} \cdot \boldsymbol{x}_{sss} - \beta \boldsymbol{x}_s \cdot \partial_s \boldsymbol{K}[(B\boldsymbol{x}_{ss})_{ss}] \\ &\quad + (c-3)\boldsymbol{x}_{ss} \cdot \boldsymbol{F}_g + 2(c-1)\boldsymbol{x}_s \cdot \partial_s \boldsymbol{F}_g + 2c_s \boldsymbol{x}_s \cdot \boldsymbol{F}_g + \boldsymbol{x}_s \cdot \partial_s \boldsymbol{K}[\boldsymbol{F}_g(s)]. \end{aligned} \tag{2.12}$$

Weakly flexible filaments are not rigid rods:
shapes and trajectories slowly vary towards equilibrium

$$\beta = \frac{\pi E a^4}{4|\mathbf{F}_G|L^2} \text{ “} \gg 1\text{”}$$

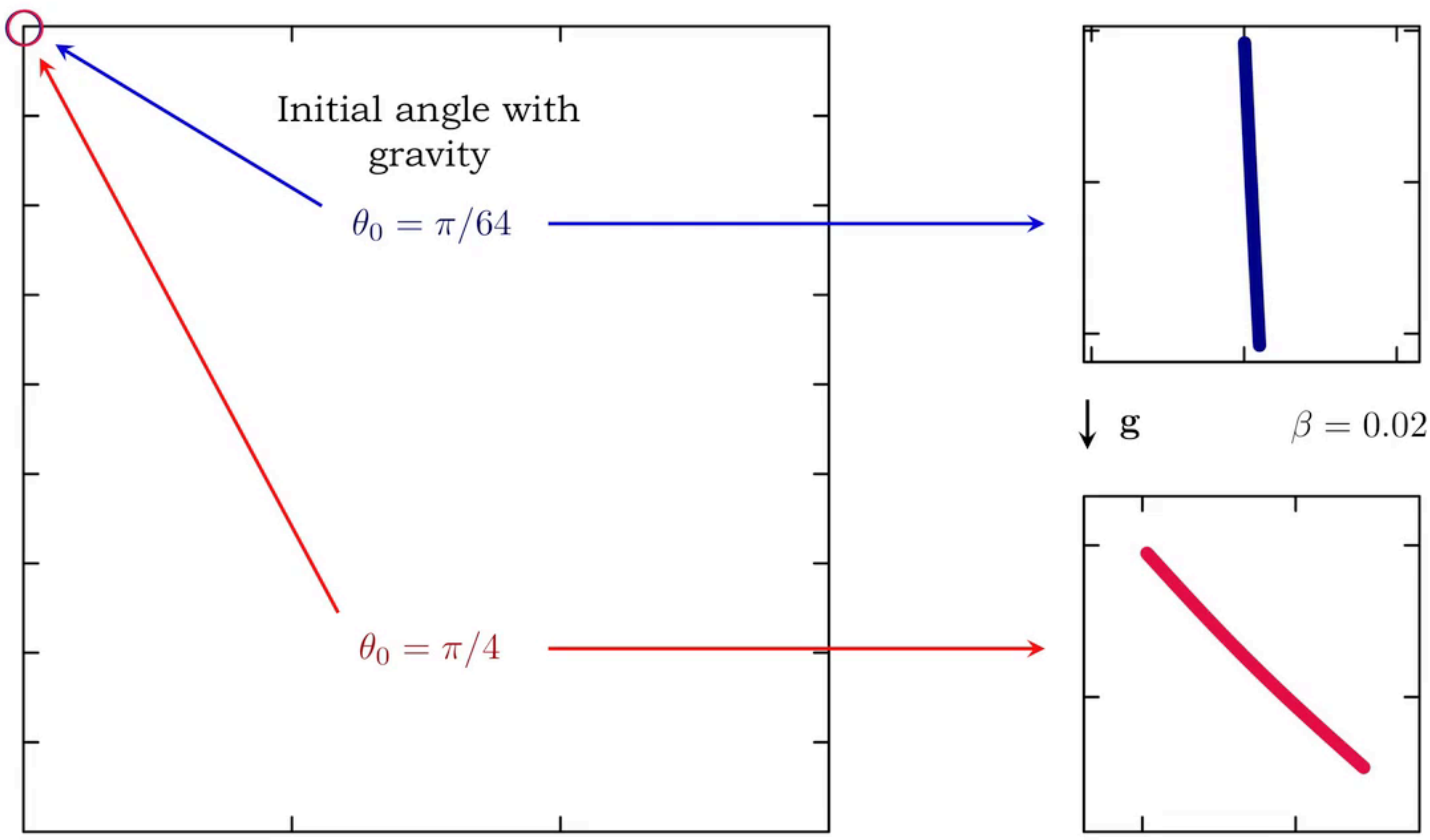

Terminal sedimenting shapes

Rigid rod: $\beta \to \infty$

Xu & Nadim, (1994)

Flexible filament dynamics vary on well separated time-scales $(\beta \gg 1)$

Two (three) time scales:

1. Very fast time scale for relaxation from initial state (ignored)
2. Time scale for sedimenting one body length: $t = O(1)$
3. Time scale for shape changes and reorientation: $\tau = t/\beta = O(1)$

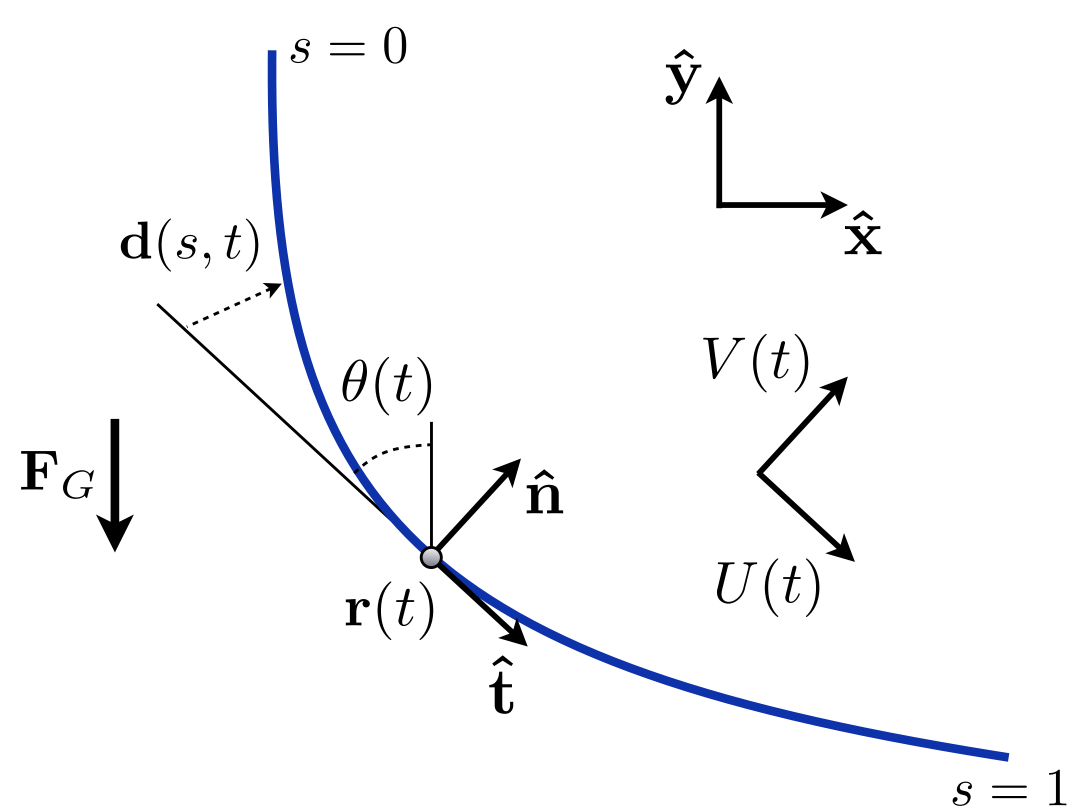

$$\boldsymbol{x}(s,t) = \boldsymbol{r}(t) + (s - 1/2)\hat{\boldsymbol{t}}(\theta(t)) + \boldsymbol{d}(s,t),$$

Confined cloud shapes are predicted in dilute suspensions $(\beta \gg 1)$

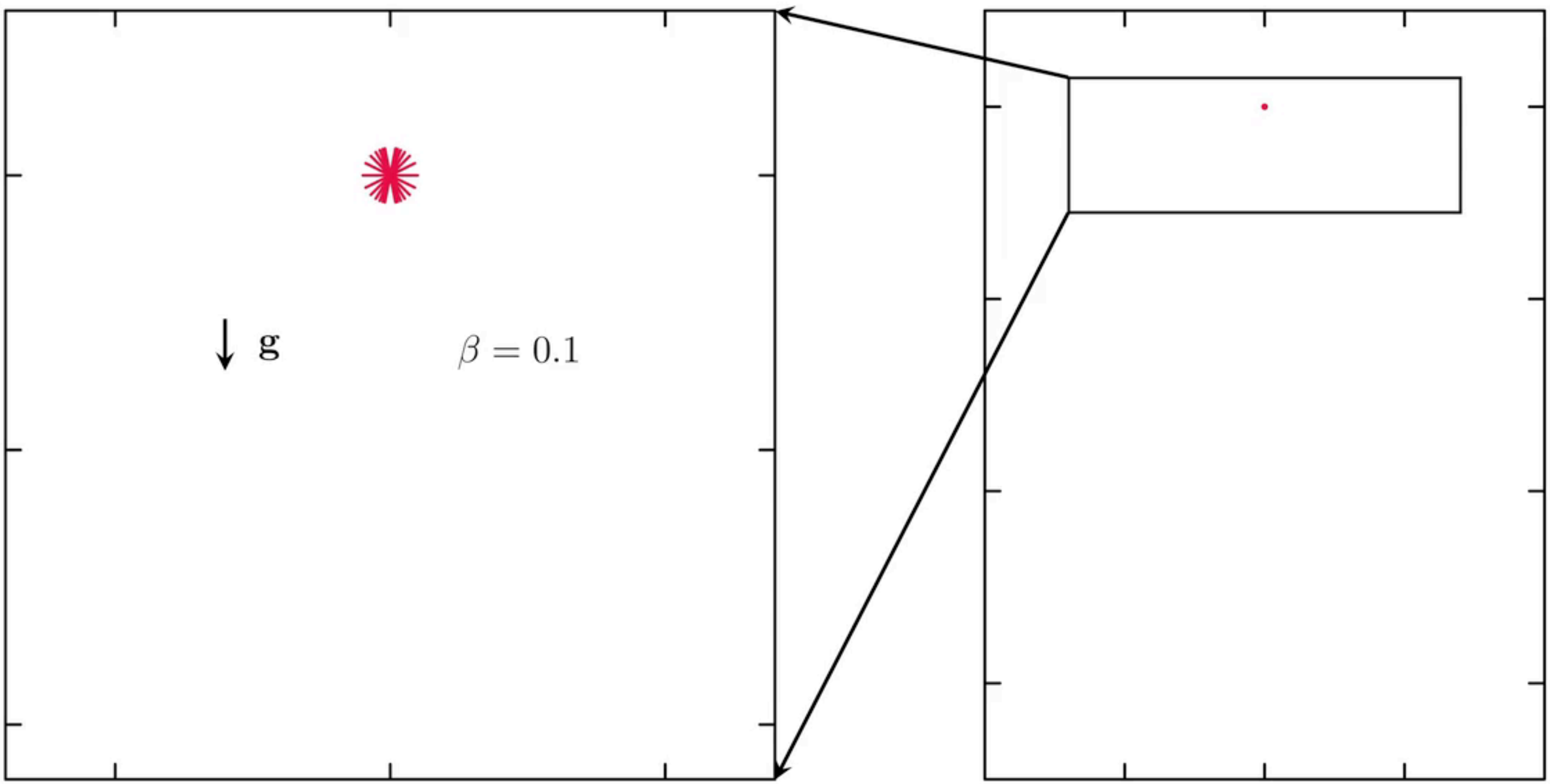

Confined cloud shapes are predicted in dilute suspensions $(\beta \gg 1)$

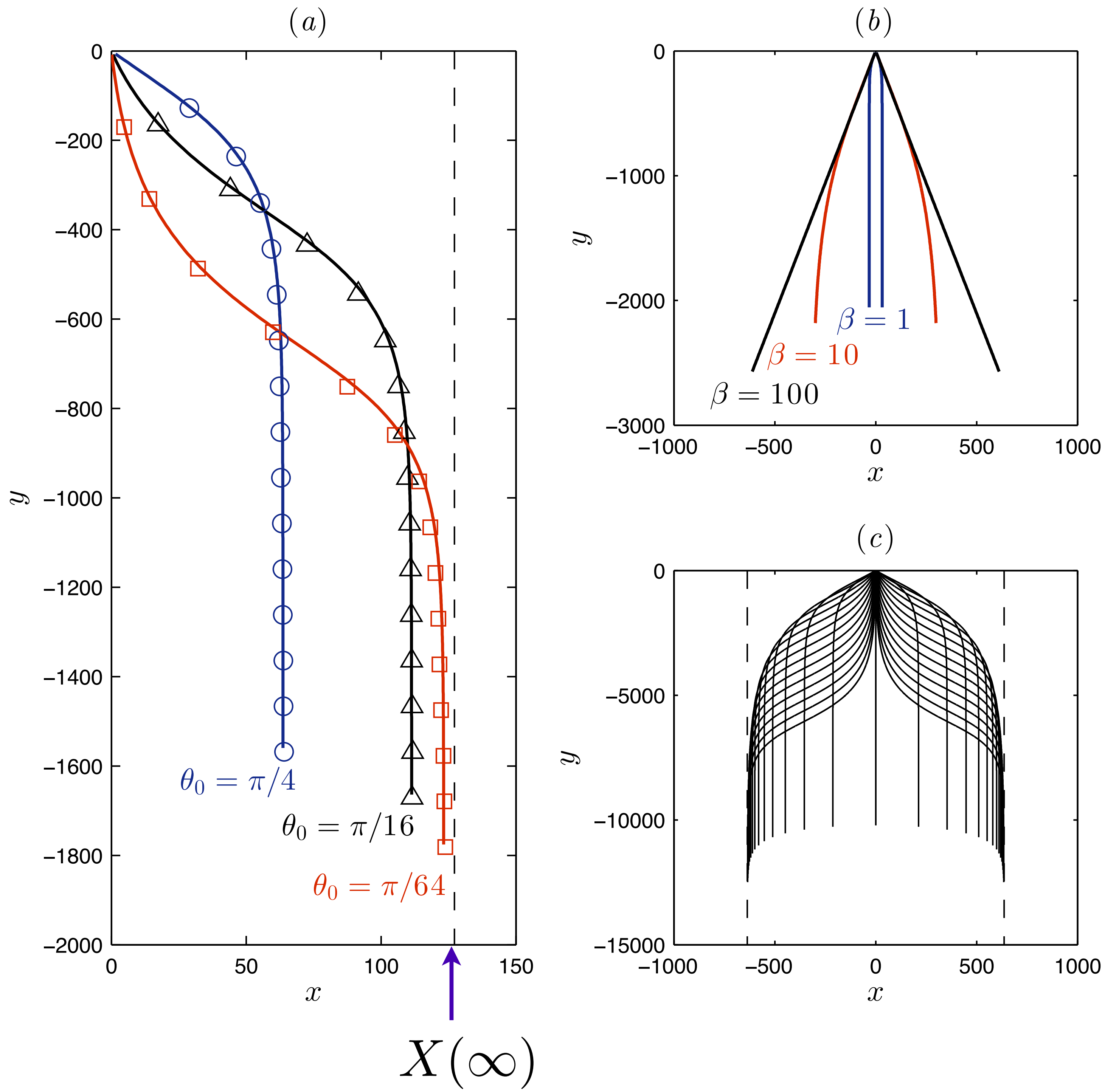

Uniform orientational distribution...

$$A = \frac{3}{80}\left(c - \frac{7}{2}\right)$$

$$\langle X(\infty)\rangle = \left(\frac{\pi}{2} - 1\right)(c-3)\frac{\beta}{A} \propto \beta$$

$$c = \log\left(\frac{1}{\epsilon^2}\right)$$

Sedimentation of flexible filaments in the floppy regime: a surprise? $(\beta \ll 1)$

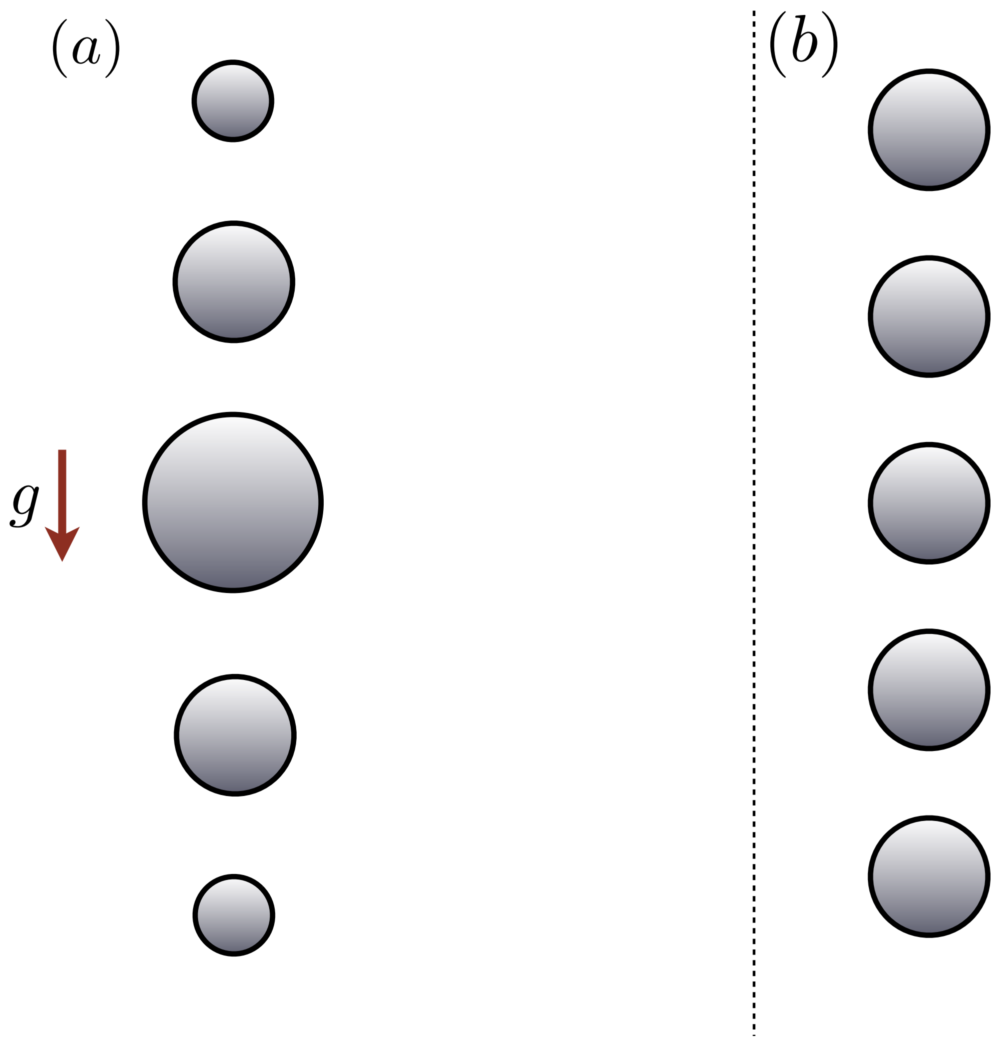

Sedimentation of flexible filaments in the floppy regime: a surprise? $(\beta \ll 1)$

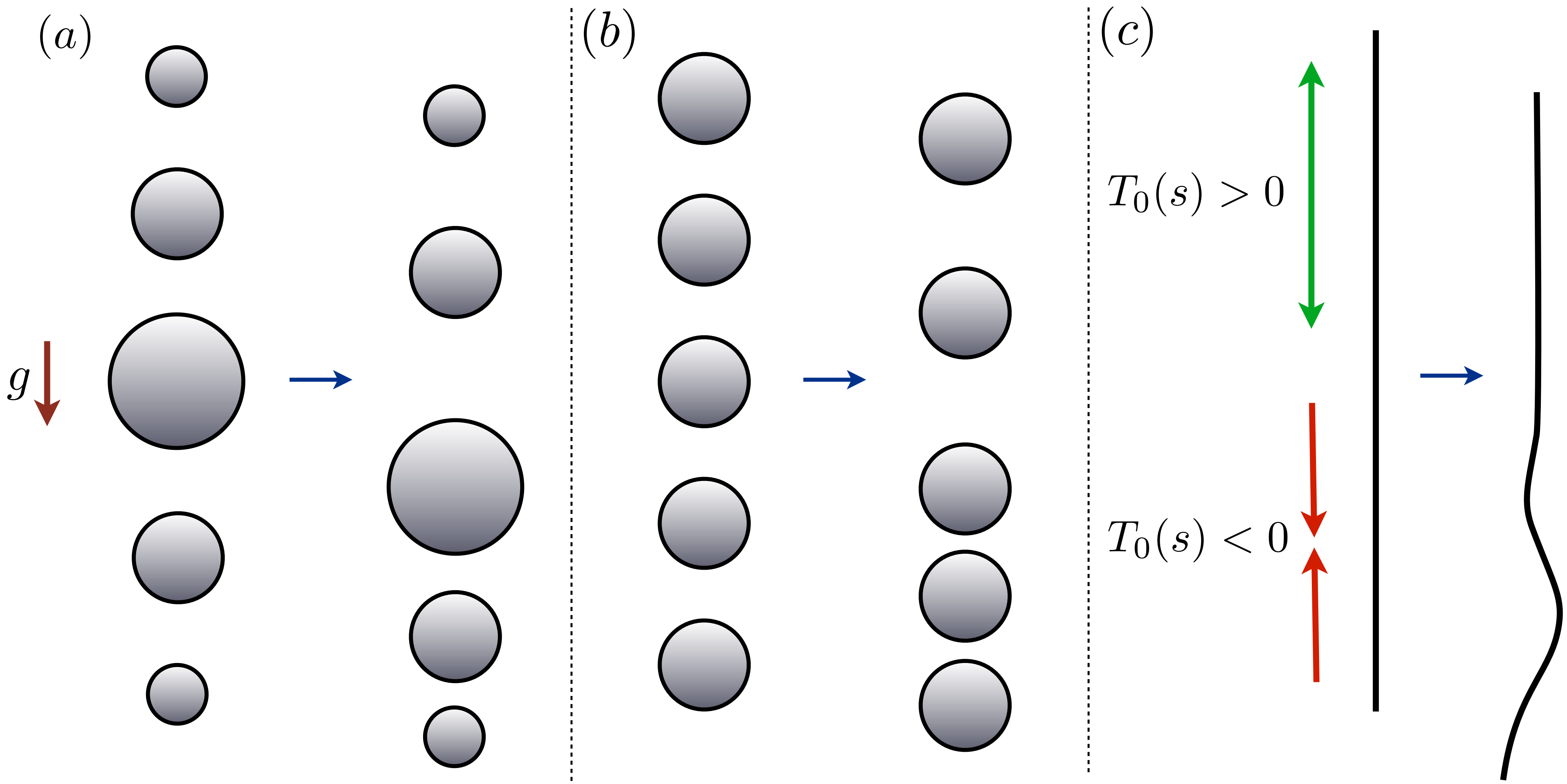

A sedimenting flexible filament should buckle!

Numerical simulations show filament buckling in the floppy regime $(\beta \ll 1)$

$\beta = 5 \times 10^{-4}$

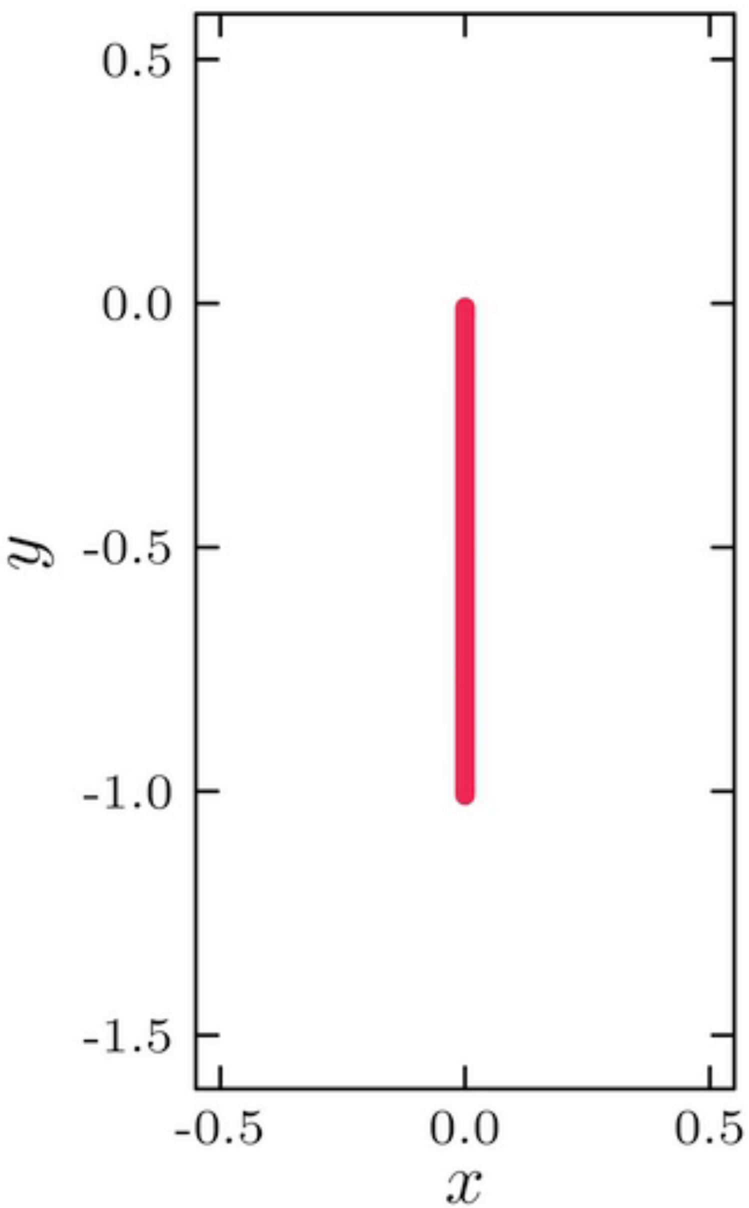

Filament buckling: linear stability analysis

$\forall \beta$

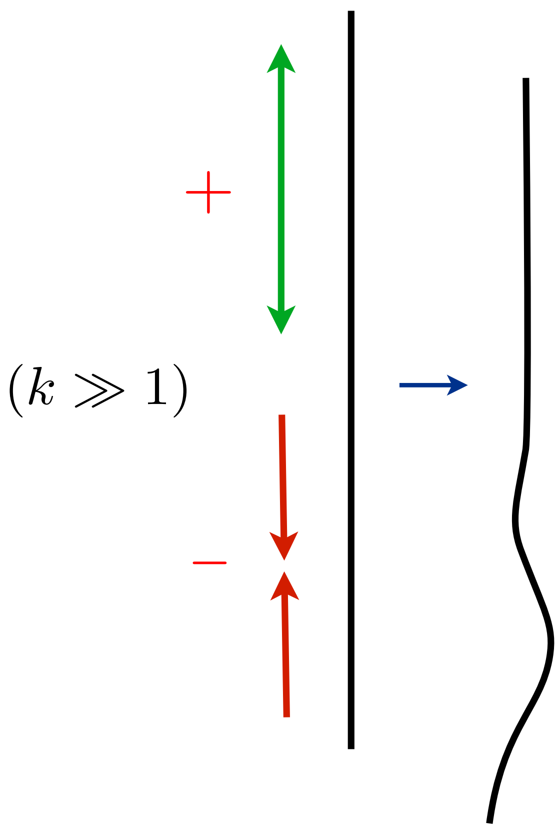

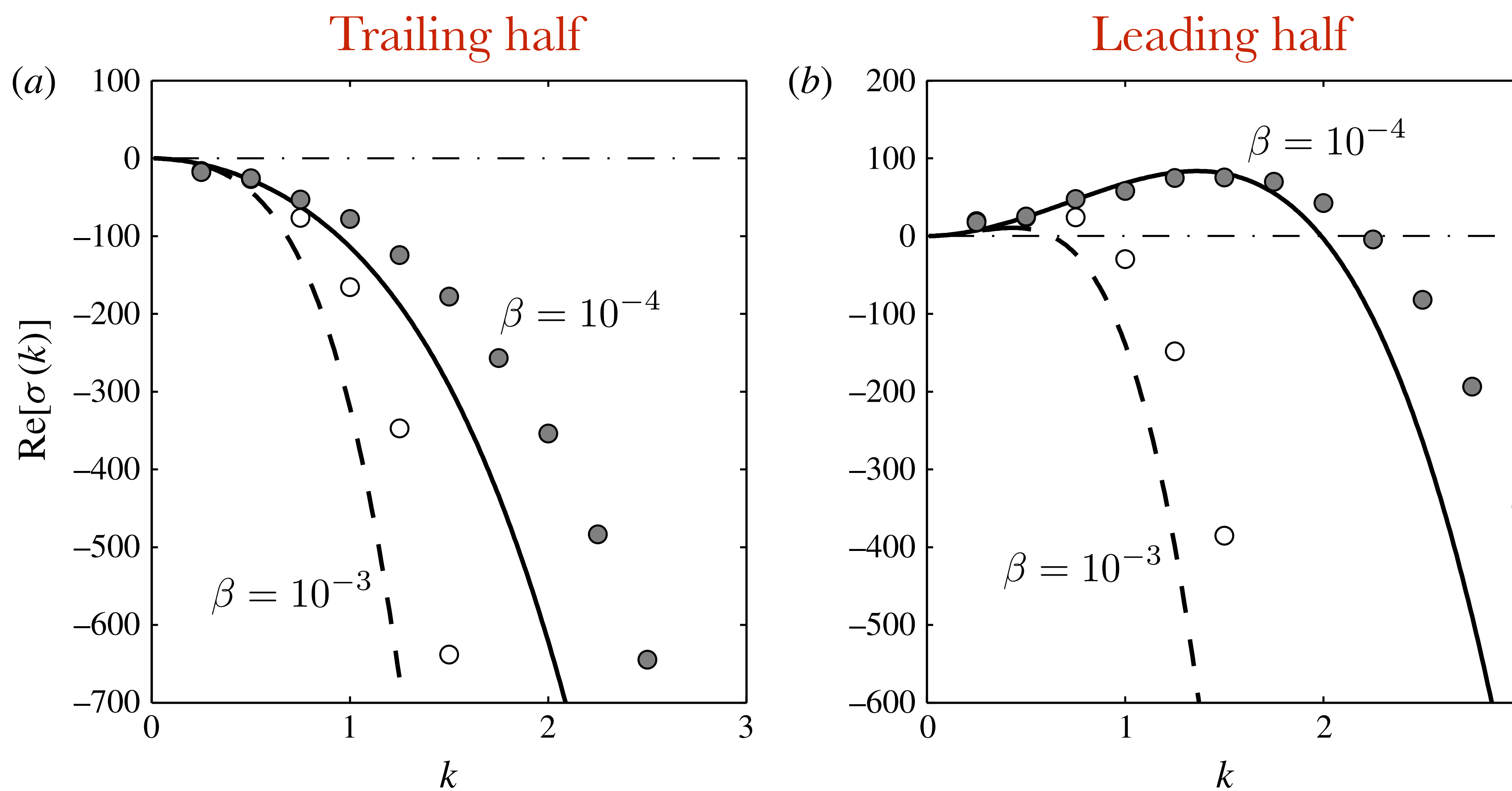

$$\sigma(k) \approx \log\left(\frac{1}{\epsilon^2 k^2}\right)\left(\pm\pi^2 k^2 - \beta(4\pi k)^4 + 4\pi i k\right)$$

tension

elastic restoration

traveling wave

Buckling can occur in the range $0 < k < \dfrac{1}{16\pi\sqrt{\beta}}$ Most unstable mode: $k^* = \dfrac{1}{16\pi\sqrt{2\beta}}$

What about suspensions?

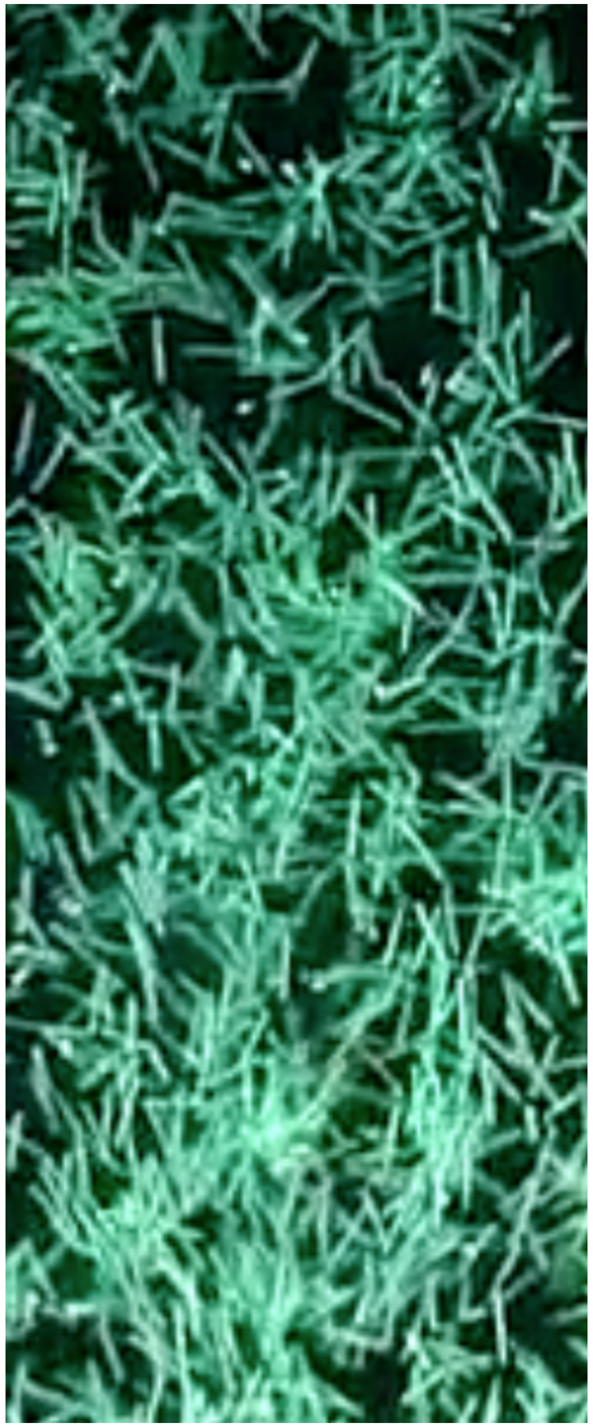

A suspension of spheroids is unstable to density perturbations

Koch & Shaqfeh, (1989)

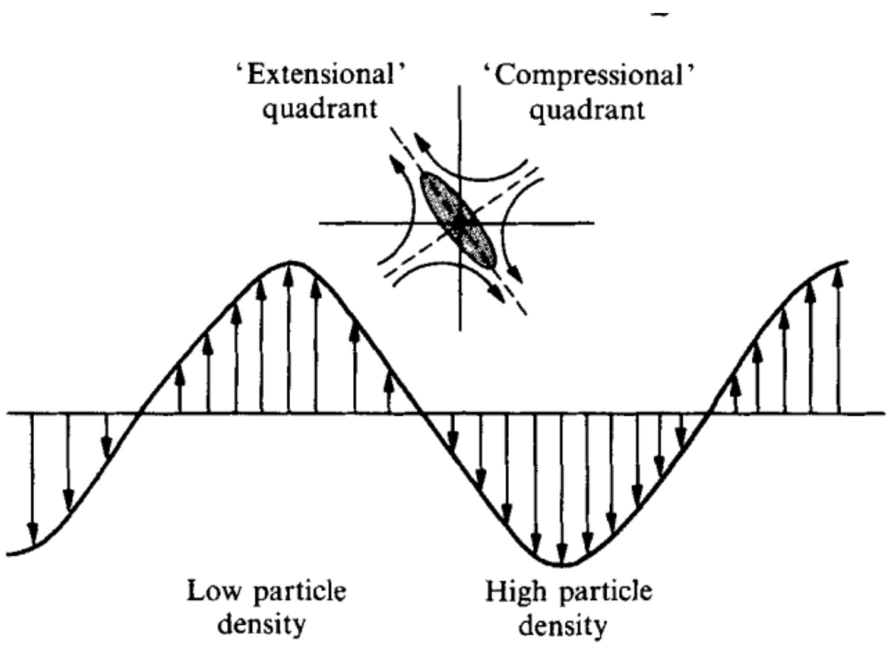

Regions of higher density increase sedimentation speeds and promote particle rotations

Longest wavelengths are most unstable (container size)

A suspension of spheroids is unstable to density perturbations

Koch & Shaqfeh, (1989)

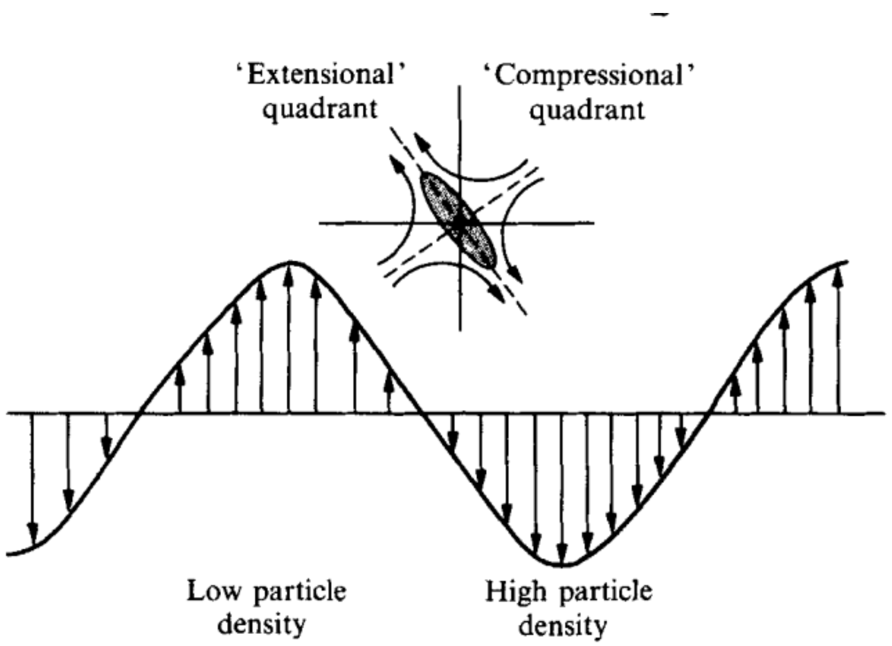

Regions of higher density increase sedimentation speeds and promote particle rotations

Longest wavelengths are most unstable (container size)

Basic kinetic model: $$\frac{1}{V}\int_V\int_\Omega \Psi(\mathbf{x},\mathbf{p},t)\,d\mathbf{x}\,d\mathbf{p} = n$$

Ψ : probability distribution

Conservation of particles: $$\frac{\partial\Psi}{\partial t} + \nabla_{\mathbf{x}}\cdot(\dot{\mathbf{x}}\Psi) + \nabla_{\mathbf{p}}\cdot(\dot{\mathbf{p}}\Psi) = 0$$

$$\dot{\mathbf{x}} = \mathbf{u}_s + \mathbf{u}_d - \mathbf{D}\cdot\nabla_{\mathbf{x}}\ln\Psi$$

$$\dot{\mathbf{p}} = \dot{\mathbf{p}}_s + \dot{\mathbf{p}}_d - \mathbf{D_r}\cdot\nabla_{\mathbf{p}}\ln\Psi$$

$$\dot{\mathbf{p}}_s = \frac{F_G}{8\pi\mu L^2}\frac{A}{2\beta}\sin(2\theta)\hat{\boldsymbol{\theta}}$$

self-rotation

disturbance flow

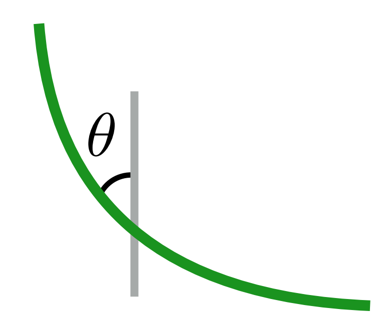

Stokes flow: $$-\mu\nabla_x^2\boldsymbol{u}_d + \boldsymbol{\nabla}_x q_d = \boldsymbol{F}_G\, c(\boldsymbol{x},t), \quad \boldsymbol{\nabla}_x\cdot\boldsymbol{u}_d = 0, \quad c(\boldsymbol{x},t) = \int_\Omega \Psi(\boldsymbol{x},\boldsymbol{p},t)\,\mathrm{d}\boldsymbol{p}.$$

The base orientational distribution depends on the **relative** size between Brownian fluctuations and flexibility

Base state: $n(\mathbf{x}) = \int \Psi(\mathbf{x}, \mathbf{p}, t)\, d\mathbf{p}$ constant (Well-mixed / homogeneous)

$$\Psi_0(\mathbf{x}, \theta, \phi) = \Psi_0(\theta) = \frac{n}{2\pi} \frac{\exp(-2\eta \cos^2 \theta)}{\int_{-1}^{1} \exp(-2\eta u^2) du}$$

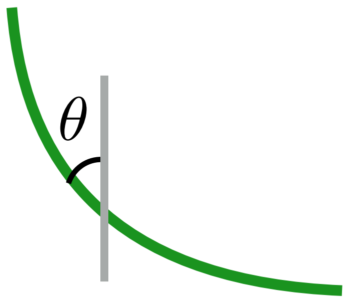

$$\eta = \frac{A\,\mathrm{Pe}}{48\beta \log(1/\epsilon^2)} \qquad \mathrm{Pe} = \frac{F_G L}{k_B T}$$

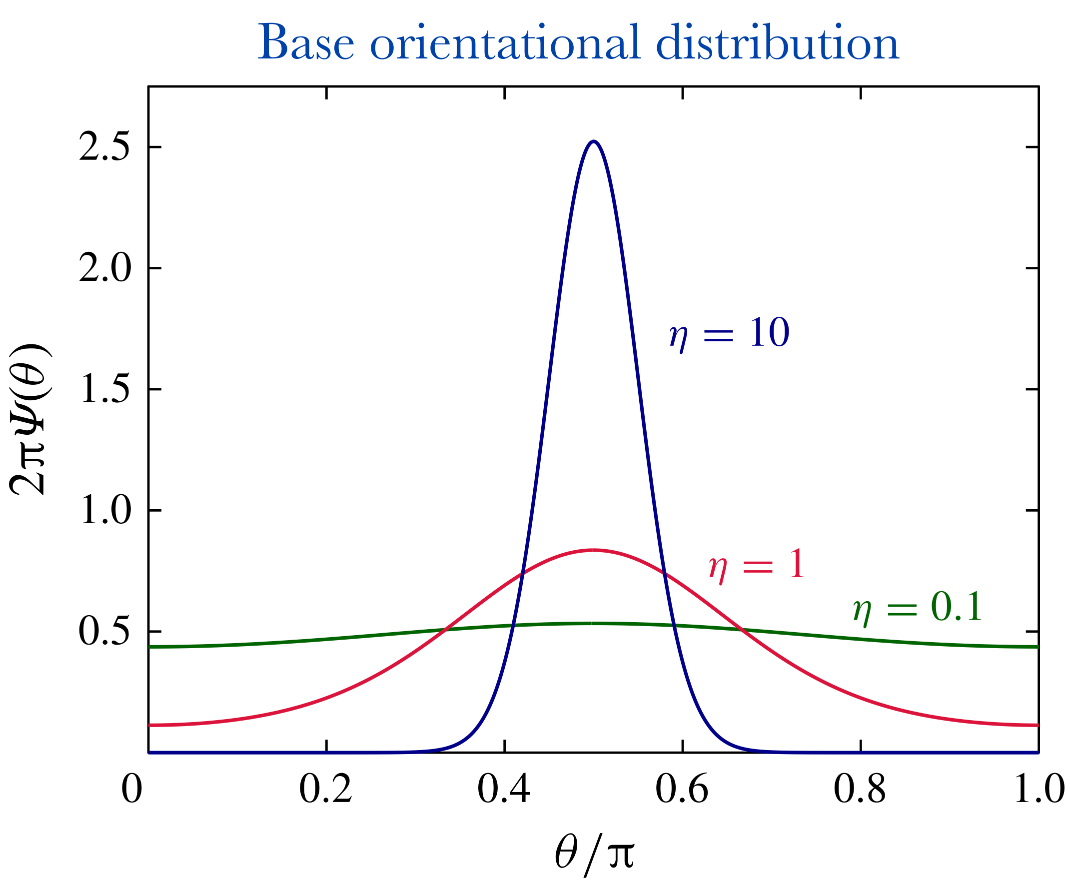

Even for weak Brownian motion and flexibility, their **relative** size affects the base state significantly

Filament compliance leads to a base state which is **more unstable**…

$$\Psi = \Psi_0(\theta) + \varepsilon \hat{\Psi}_1(\mathbf{k}, \mathbf{p}, \omega) e^{i\mathbf{k}\cdot\mathbf{x} - \omega t}$$

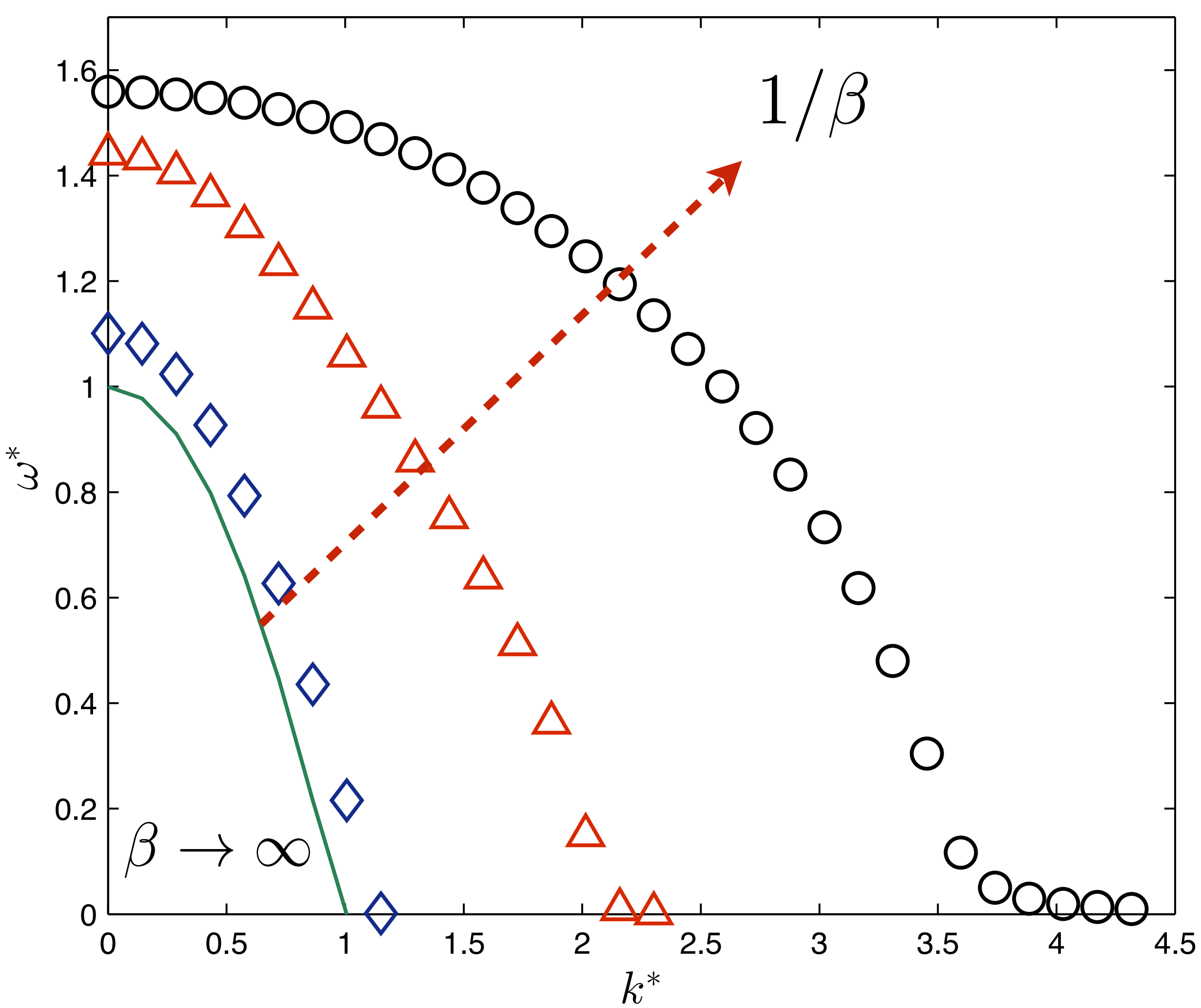

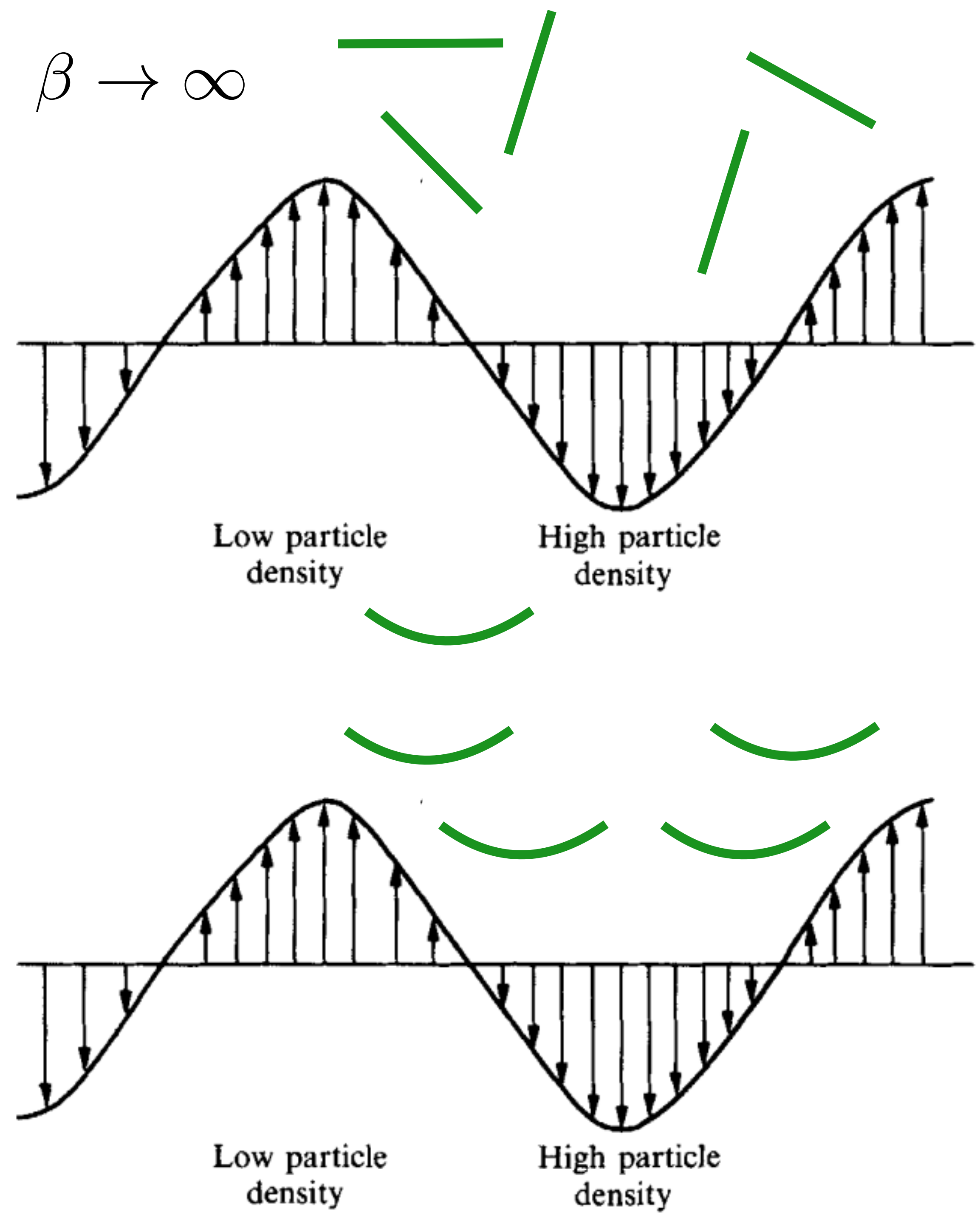

Zeroth wavenumber remains the most unstable

The anisotropic limit leads to a wavelength-independent instability

…but compliance also **suppresses** instability!

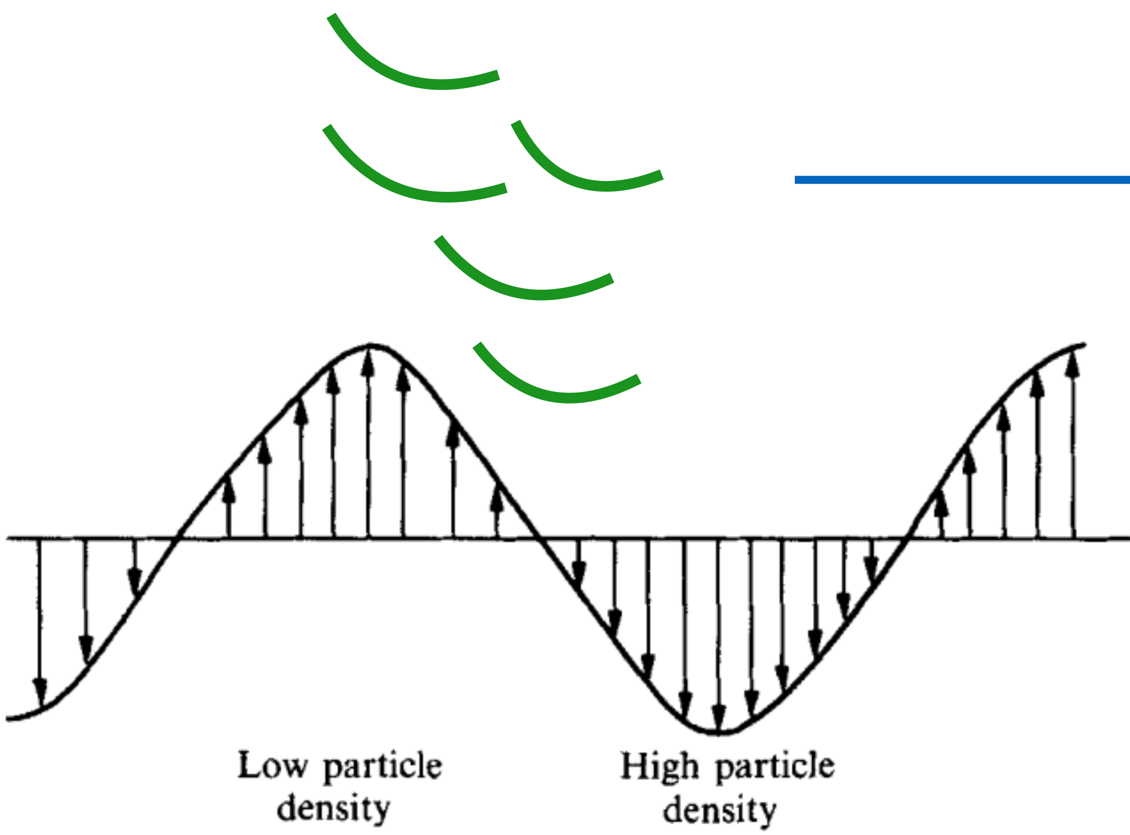

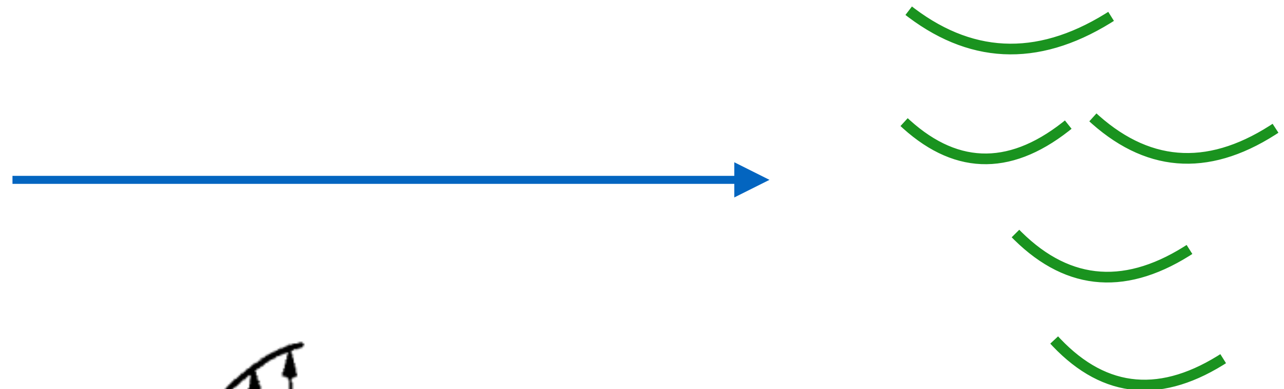

(Particle clustering is inhibited)

Thermal fluctuations also suppress instability $\mathrm{Pe} = \dfrac{F_G L}{k_B T}$

Instability enhancement / suppression is dictated by $\eta \propto \mathrm{Pe}/\beta$:

Instability enhancement / suppression is dictated by $\eta \propto \mathrm{Pe}/\beta$:

$$\mathrm{Pe} = \frac{F_G L}{k_B T}$$

$$\beta = \frac{\pi E a^4}{4 F_G L^2}$$

Zero-wavenumber growth rates:

Anisotropic base state, instability enhanced

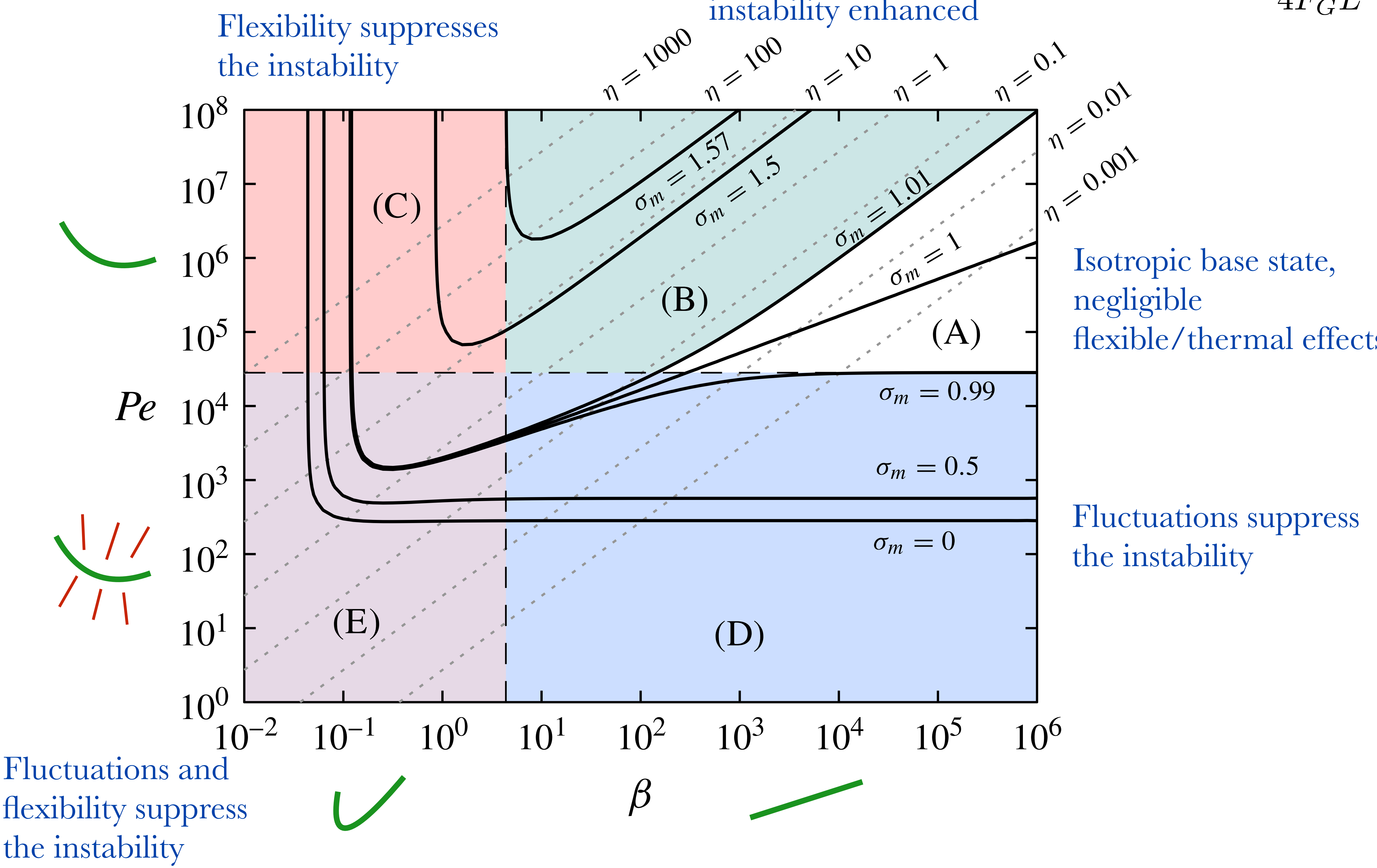

UW-Madison Applied Math Lab

Will Mitchell and Yue Zhao (UW)

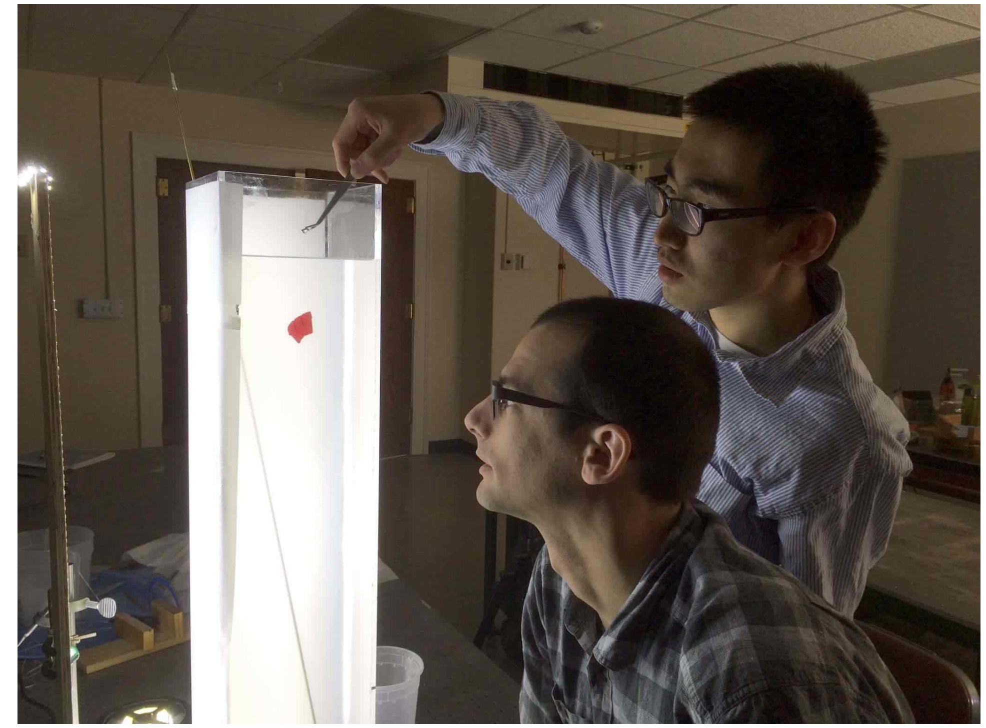

Wall effects: a first look from the UW Applied Math Lab

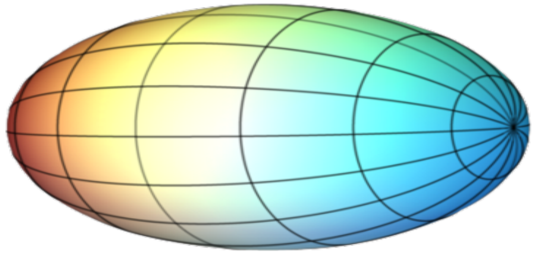

$$\theta \approx -45^\circ, \ \phi \approx 0^\circ$$

(Side wall)

“Reversing”

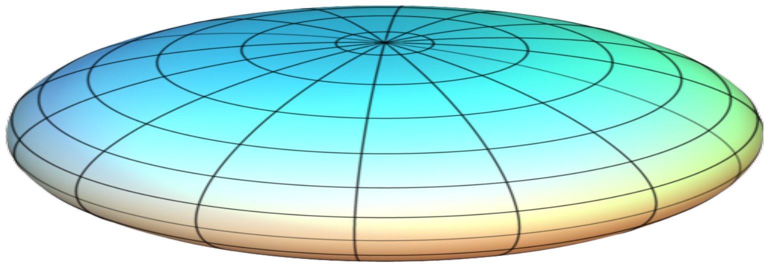

$\theta \approx -45^\circ,\ \phi \approx 45^\circ$ (Front wall)

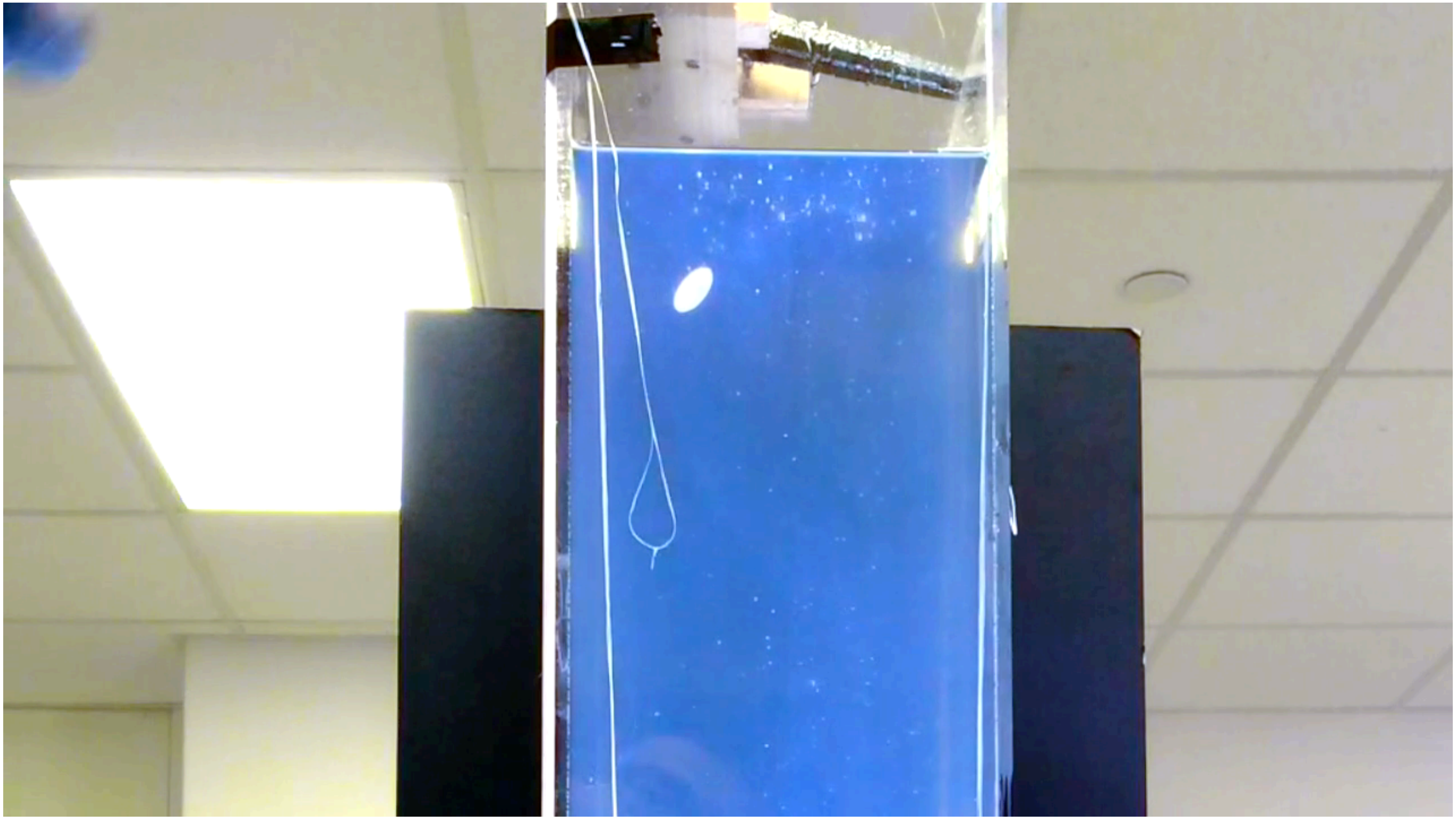

“Glancing”

Consider an arbitrarily oriented prolate or oblate spheroid…

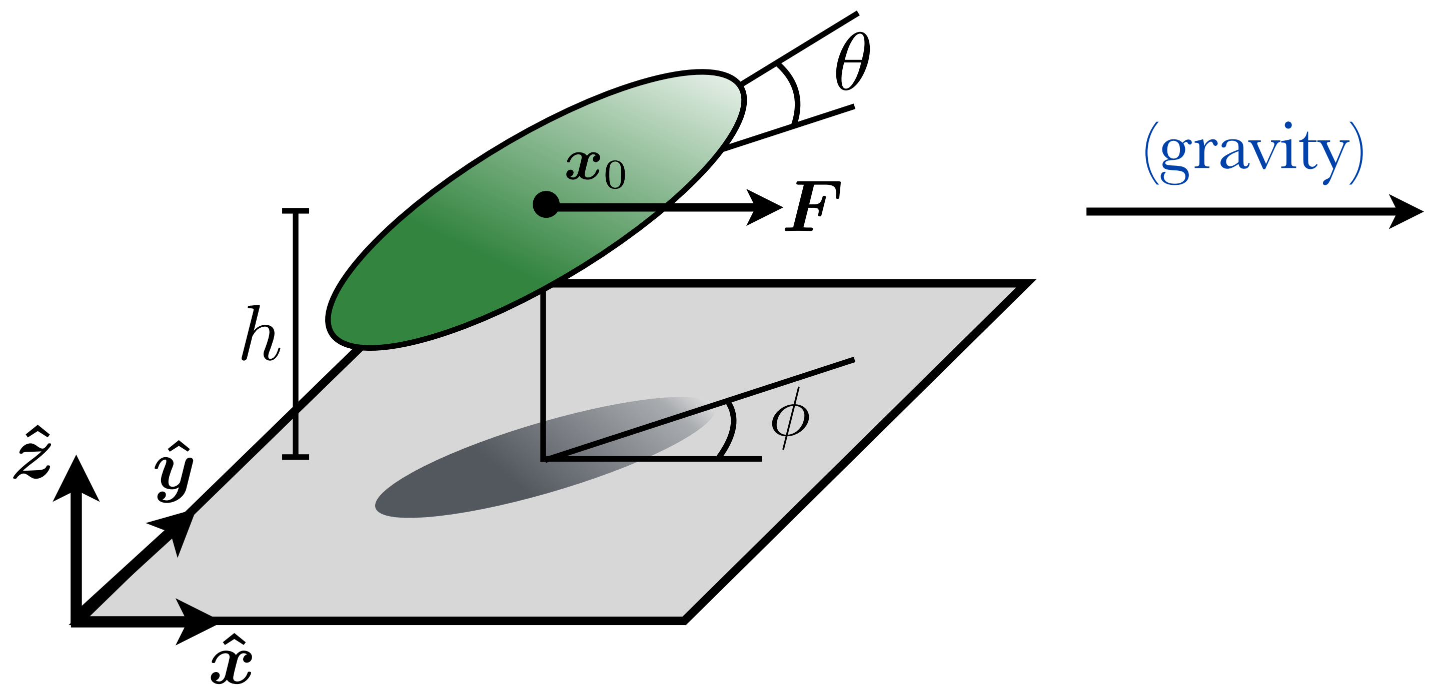

Previous analytical work:

Sphere (exact): Goldman 1967, O'Neill 1964
Spheroid far from wall (2D forces; no dynamics): Wakiya 1959
Slender rod: Russel, Hinch, Leal & Tieffenbruck, 1977

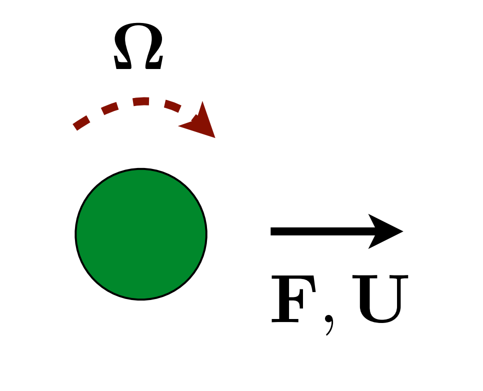

Numerical (3D fluid; dynamics confined to 2D):

First-kind boundary integral method: Hsu + Ganatos 1989, 1994
Regularized Stokeslets with images: Ainley 2008
Ensembles of spheres: Kutteh 2010

Surprisingly, no previously known analytical solutions for general body eccentricity and/or 3D motion

Far-field asymptotic expressions for the body velocity may be derived using the method of reflections

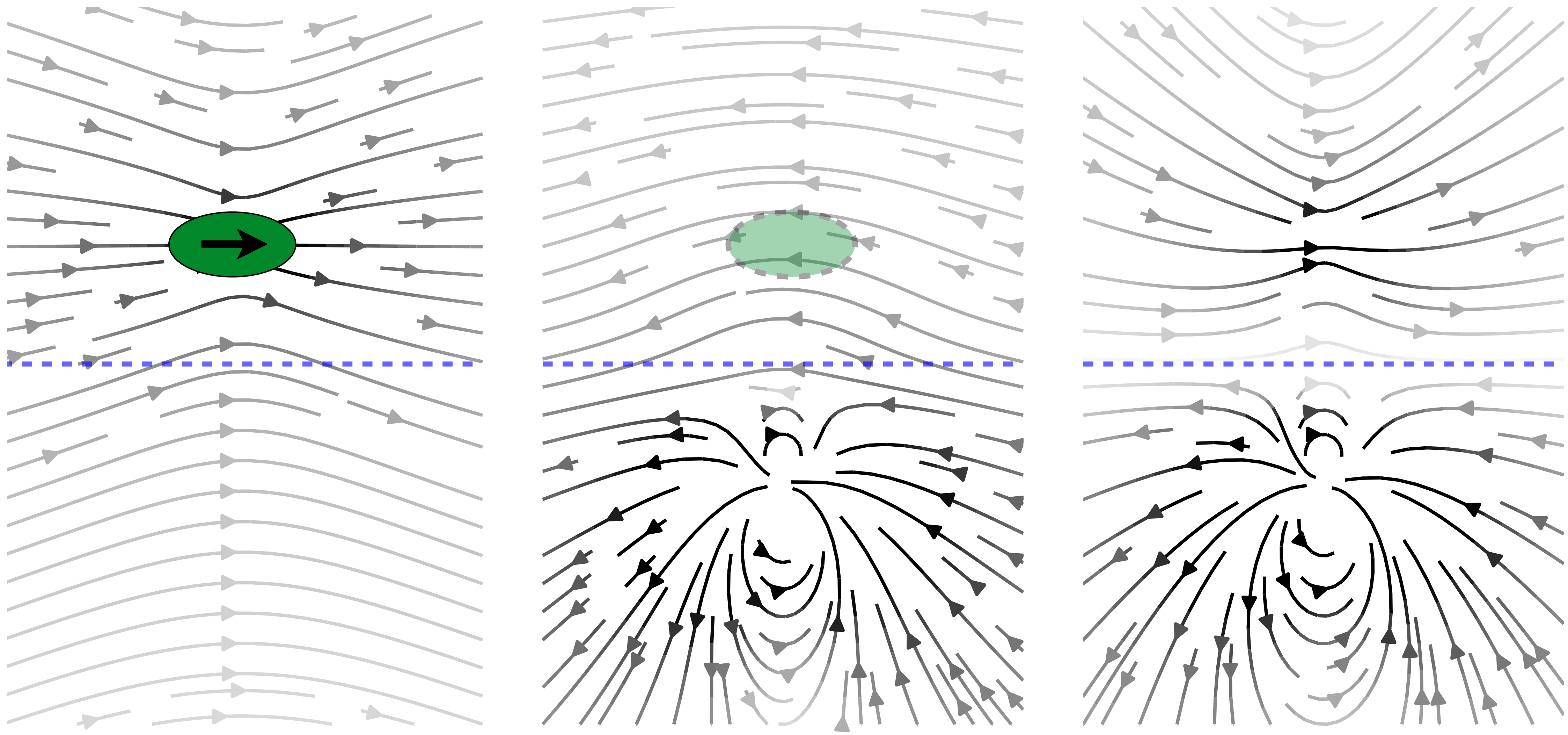

$$G_{ij} f_j \quad + \quad G^*_{ij} f_j \quad = \quad \widetilde{G}_{ij} f_j$$

Stokeslet

Stokeslet image (Blake 1971)

Zero velocity on the wall

Clean ode's were derived for the full 3D dynamics for arbitrary eccentricity (and wall tilt)

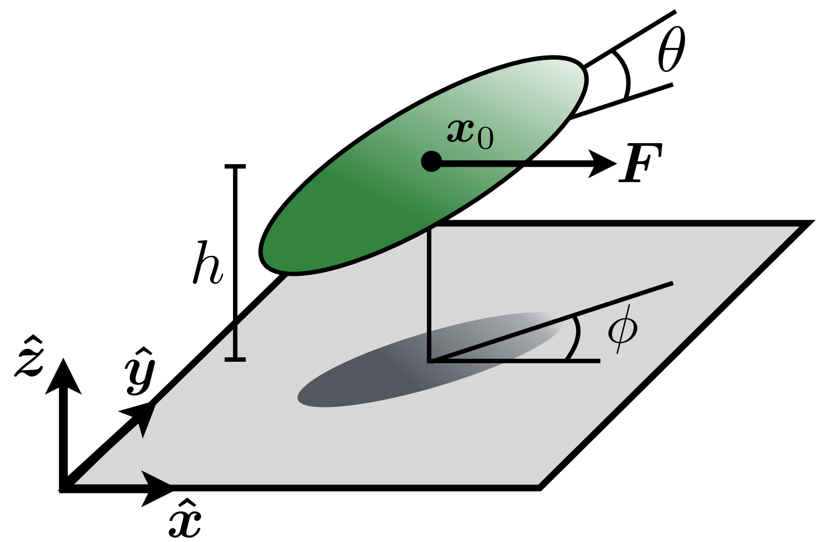

$$\dot{\theta} = \cos\phi \left(\frac{\cos(2\theta)}{h^2} \left[A - \frac{B}{h^2} - C\frac{\cos(2\theta)}{h^2} \right] - \frac{D}{h^4} \right)$$

$$\dot{h} = \cos\phi \sin(2\theta) \left[E - \frac{F}{h^3} \right]$$

$$\dot{\phi} = \frac{3\sin\phi \tan\theta}{64(2-e^2)} \left(\frac{-6e^2}{h^2} + \frac{3e^4\cos^2\theta - 8e^4 + 10e^2 - 4}{h^4} \right)$$

enslaved!

A-F are simple functions of particle eccentricity e

$$\longrightarrow \quad \Psi(h,\theta) = \exp\left(-\frac{2A}{Eh}\right)\left(-\cos(2\theta) + \frac{D}{A}\left(h^{-2} + \frac{E}{Ah} + \frac{E^2}{2A^2}\right)\right)$$

Periodic tumbling, reversing, and glancing…

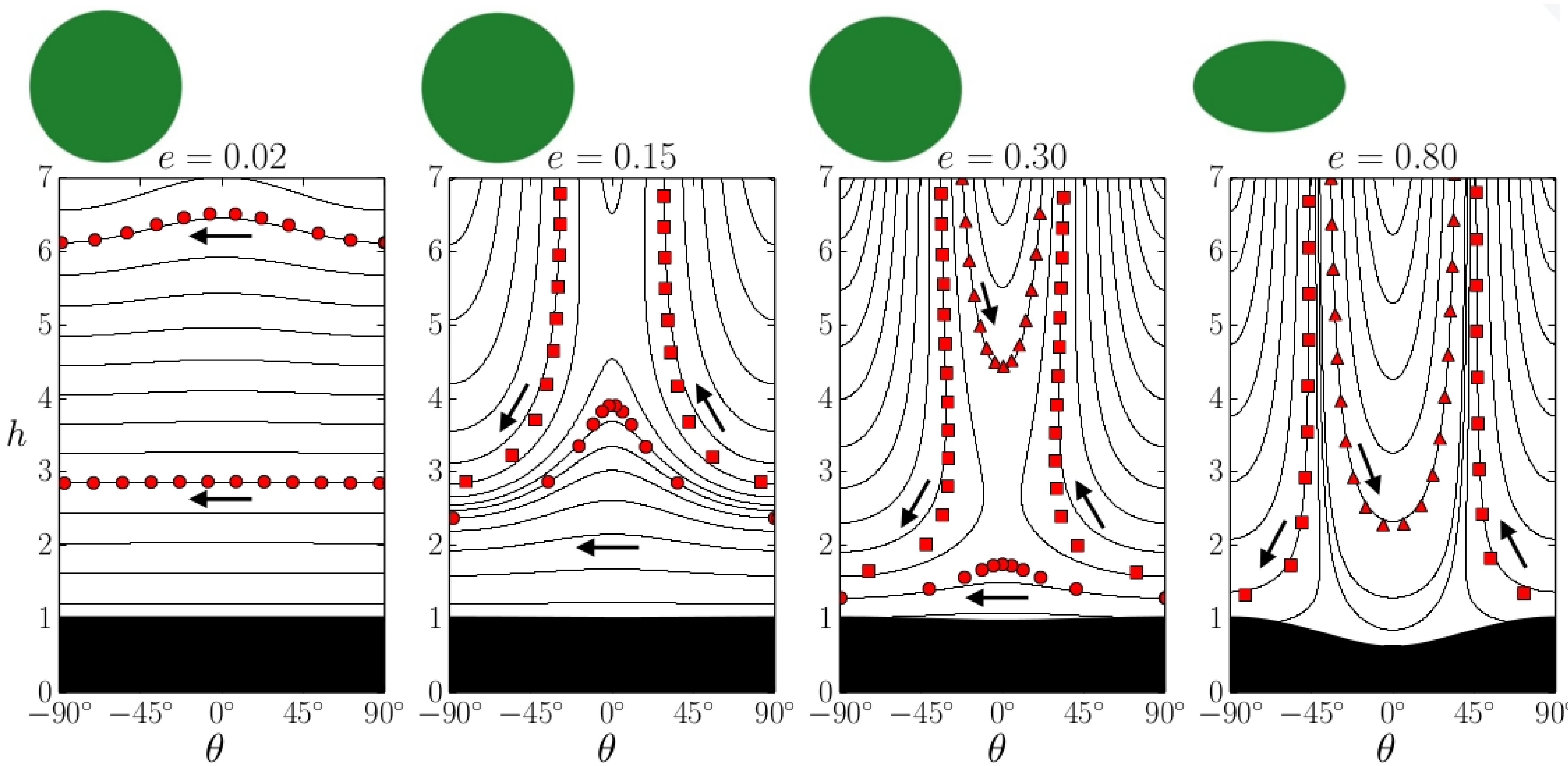

Periodic tumbling (~rolling)

Reversing "appears"

Glancing "appears"

Tumbling vanishes

The trajectory is **very** sensitive to the body shape for nearly spherical bodies!

Natural numerical method: half-space kernels

$$8\pi\mu\,\mathbf{u}(\mathbf{x}) = \int_{S(t)} \mathbf{G}(\mathbf{x},\mathbf{y})\cdot\mathbf{f}(\mathbf{y})\,dS_y + \mu\int_{S(t)} \mathbf{u}(\mathbf{y})\cdot\mathbf{T}(\mathbf{x},\mathbf{y})\cdot\hat{\mathbf{n}}(\mathbf{y})\,dS_y$$

$$+\int_{S^*(t)} \mathbf{G}^*(\mathbf{x},\mathbf{y})\cdot\mathbf{f}(\mathbf{y})\,dS_y + \mu\int_{S^*(t)} \mathbf{u}(\mathbf{y})\cdot\mathbf{T}^*(\mathbf{x},\mathbf{y})\cdot\hat{\mathbf{n}}\,dS_y$$

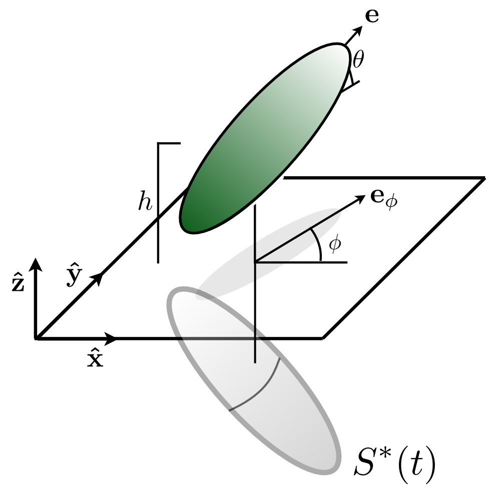

This took some work!

Closure: $\mathbf{x}\in S(t):\ \mathbf{u}(\mathbf{x}) = \mathbf{U} + \mathbf{\Omega}\times\mathbf{x}$ Unknown / specified

$$\int_{S(t)} \mathbf{f}\,dS = \mathbf{F},\quad \int_{S(t)} \mathbf{x}\times\mathbf{f}\,dS = \mathbf{L}$$ Specified / unknown

Either way, results in an integral equation for $\mathbf{f}$

Natural numerical method: half-space kernels

$$8\pi\mu\,\mathbf{u}(\mathbf{x}) = \int_{S(t)} \mathbf{G}(\mathbf{x},\mathbf{y})\cdot\mathbf{f}(\mathbf{y})\,dS_y + \mu\int_{S(t)} \mathbf{u}(\mathbf{y})\cdot\mathbf{T}(\mathbf{x},\mathbf{y})\cdot\hat{\mathbf{n}}(\mathbf{y})\,dS_y$$
$$+\int_{S^*(t)} \mathbf{G}^*(\mathbf{x},\mathbf{y})\cdot\mathbf{f}(\mathbf{y})\,dS_y + \mu\int_{S^*(t)} \mathbf{u}(\mathbf{y})\cdot\mathbf{T}^*(\mathbf{x},\mathbf{y})\cdot\hat{\mathbf{n}}\,dS_y$$

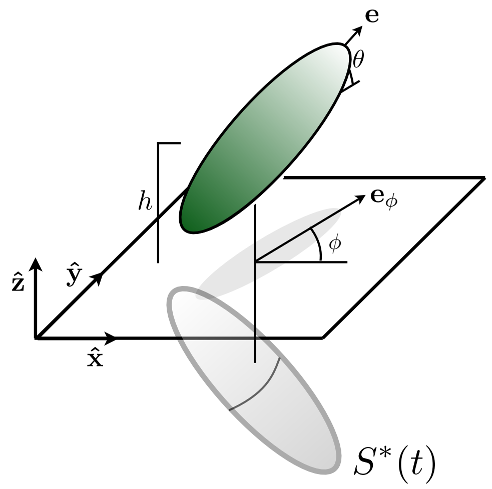

This took some work!

Trouble!

Fredholm integral equation of the first kind for $\mathbf{f}$:

You are *Theoretically Naked*

(Slender body theory: don't use too many gridpoints!)

Going further: a generalized traction integral equation **(with walls / background flows)**

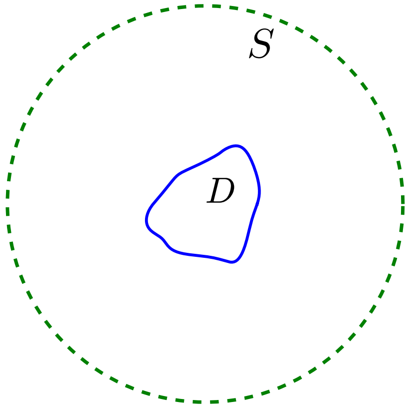

Lorentz reciprocal identity (~ Green's identity)

$$\langle \boldsymbol{u}', \boldsymbol{f} \rangle_D + \langle \boldsymbol{u}', \boldsymbol{f} \rangle_S = \langle \boldsymbol{u}, \boldsymbol{f}' \rangle_D + \langle \boldsymbol{u}, \boldsymbol{f}' \rangle_S$$

$$u_i'(\boldsymbol{x}) = \frac{1}{8\pi} \int_D T_{ijk}(\boldsymbol{x}, \boldsymbol{y}) n_k(\boldsymbol{y}) \psi_j(\boldsymbol{y}) \, dS_{\boldsymbol{y}} + \frac{c}{8\pi} \int_D C_{ij}(\boldsymbol{x}, \boldsymbol{y}) \psi_j(\boldsymbol{y}) \, dS_{\boldsymbol{y}}$$

Distribution of stresslets (rank deficient) → Completion flow (e.g. internal singularities)

Going further: a generalized traction integral equation **(with walls / background flows)**

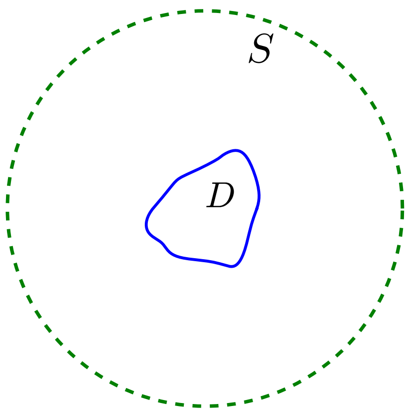

Lorentz reciprocal identity (~ Green's identity)

$$\langle \boldsymbol{u}', \boldsymbol{f} \rangle_D + \langle \boldsymbol{u}', \boldsymbol{f} \rangle_S = \langle \boldsymbol{u}, \boldsymbol{f}' \rangle_D + \langle \boldsymbol{u}, \boldsymbol{f}' \rangle_S$$

$$u_i'(\boldsymbol{x}) = \frac{1}{8\pi} \int_D T_{ijk}(\boldsymbol{x}, \boldsymbol{y}) n_k(\boldsymbol{y}) \psi_j(\boldsymbol{y}) \, dS_{\boldsymbol{y}} + \frac{c}{8\pi} \int_D C_{ij}(\boldsymbol{x}, \boldsymbol{y}) \psi_j(\boldsymbol{y}) \, dS_{\boldsymbol{y}}$$

Distribution of stresslets (rank deficient) → Completion flow (e.g. internal singularities)

Resulting integral equation, e.g. near a wall, with a background shear flow (rate $\dot{\gamma}$)

$$\frac{1}{2} f_j(\boldsymbol{y}) + \frac{1}{8\pi} n_k(\boldsymbol{y}) \int_D T_{ijk}^{\text{half}}(\boldsymbol{y}', \boldsymbol{y}) f_i(\boldsymbol{y}') dS_{\boldsymbol{y}'} + \int_D C_{ij}^{\text{half}}(\boldsymbol{y}', \boldsymbol{y}) f_i(\boldsymbol{y}') dS_{\boldsymbol{y}'}$$
$$= c_0 \left(U_j + \epsilon_{jk\ell} \Omega_k (y_\ell - Y_\ell) \right) - \mu \dot{\gamma} \left(\delta_{1j} n_3(\boldsymbol{y}) + \delta_{3j} n_1(\boldsymbol{y}) \right) + \frac{c_1 \dot{\gamma}}{2} \left(\delta_{1j} y_3 - \delta_{3j} y_1 \right) + \frac{c_1 \dot{\gamma}}{2} \left(\delta_{1j} z_3(\boldsymbol{y}) + \delta_{3j} z_1(\boldsymbol{y}) \right)$$

Second-kind boundary integral equation for **f**

(See also: Liron & Barta '92, Kim & Power '93, Ingber & Mondy '93, Keaveny & Shelley '11)

The analytical predictions are confirmed for all but the closest of wall-interactions

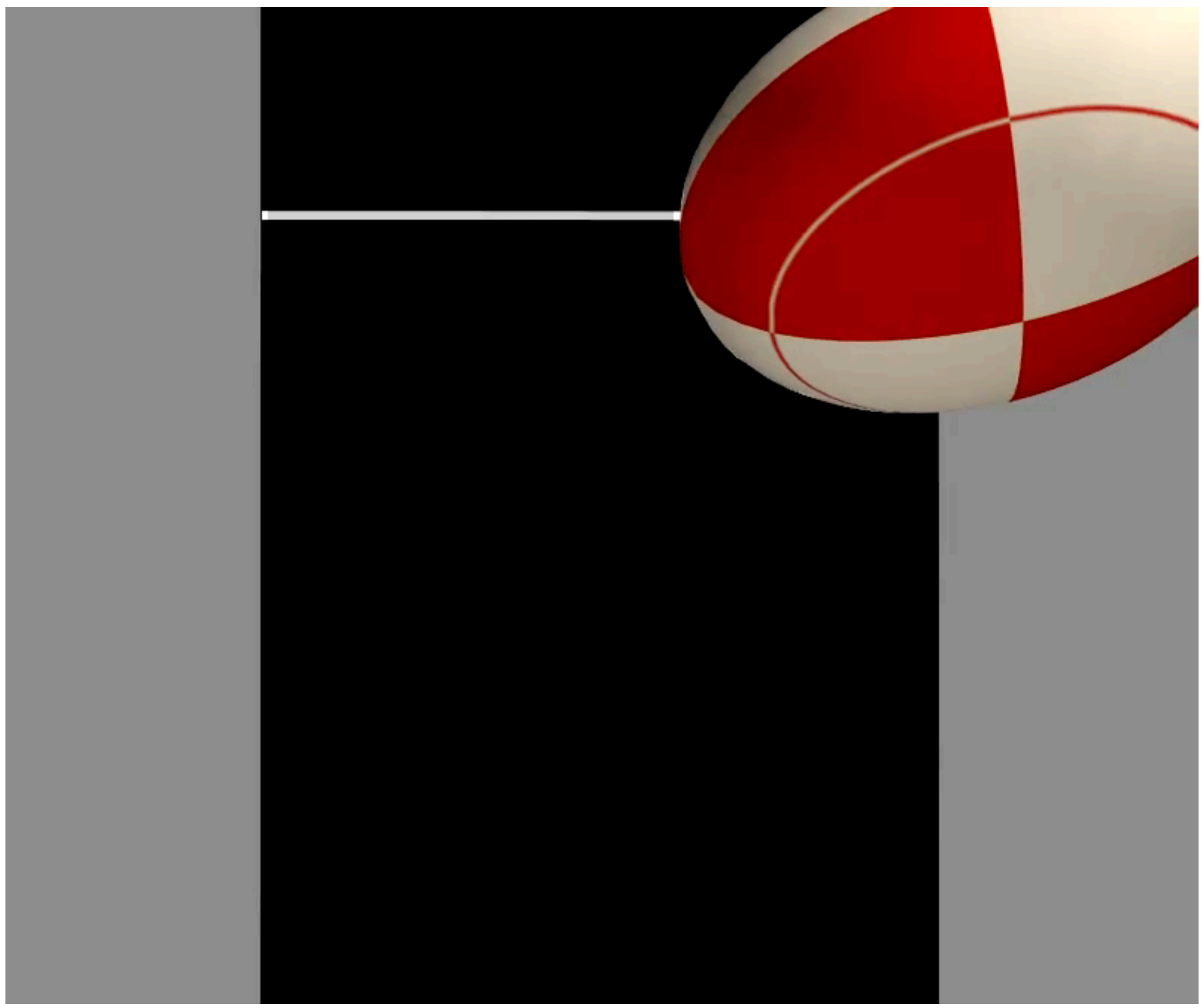

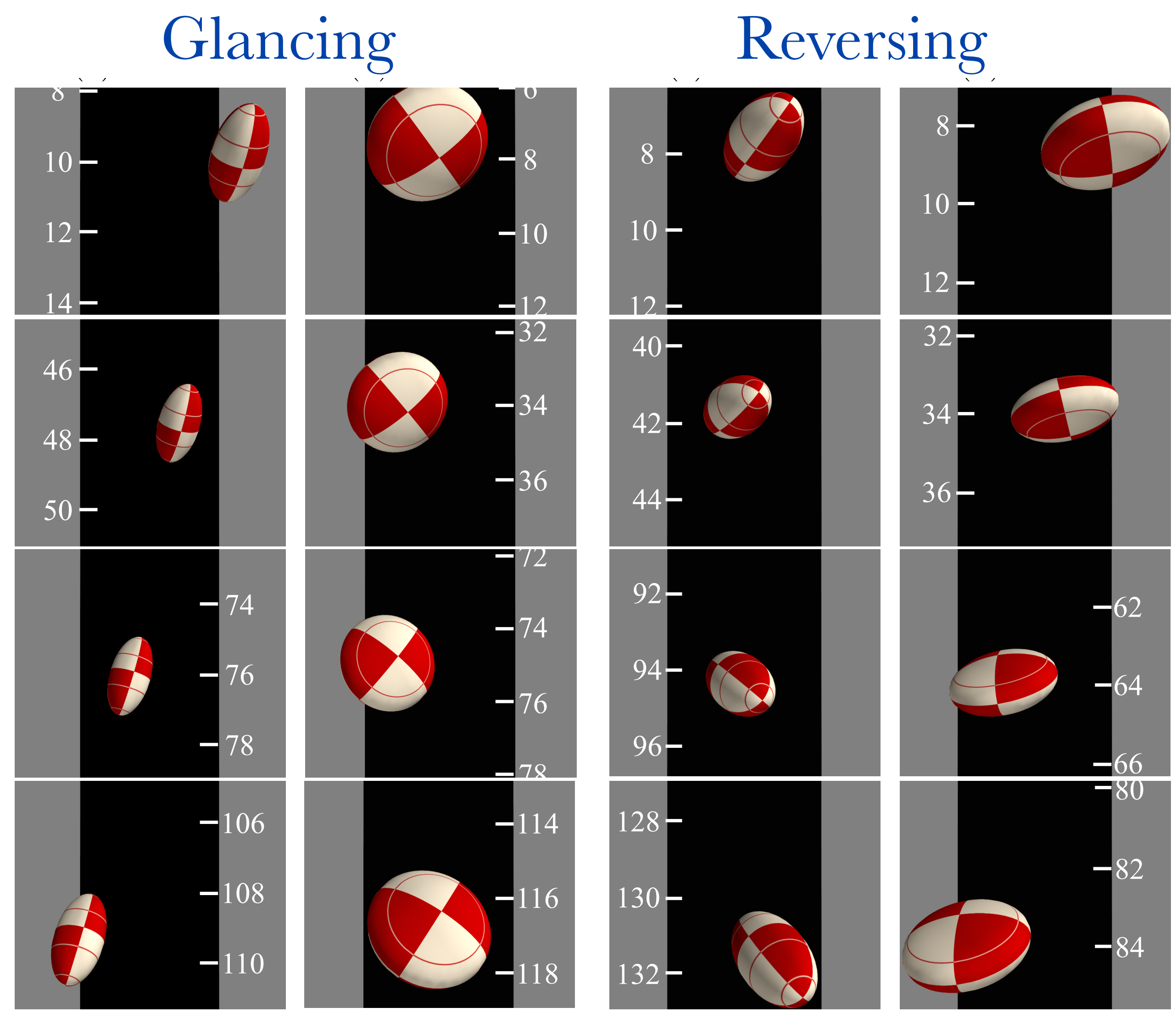

But now we can say more! Pointwise traction on a sedimenting spheroid

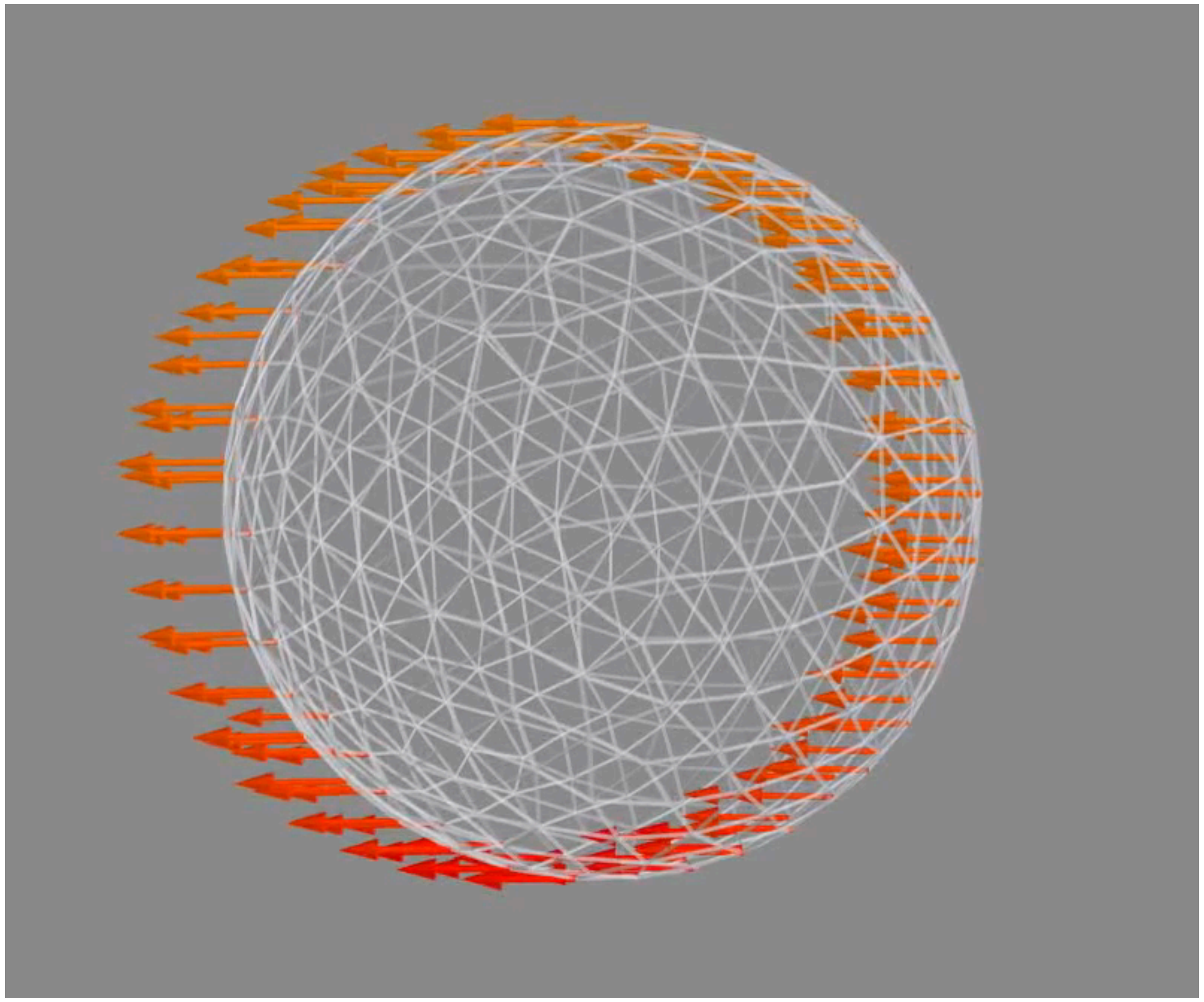

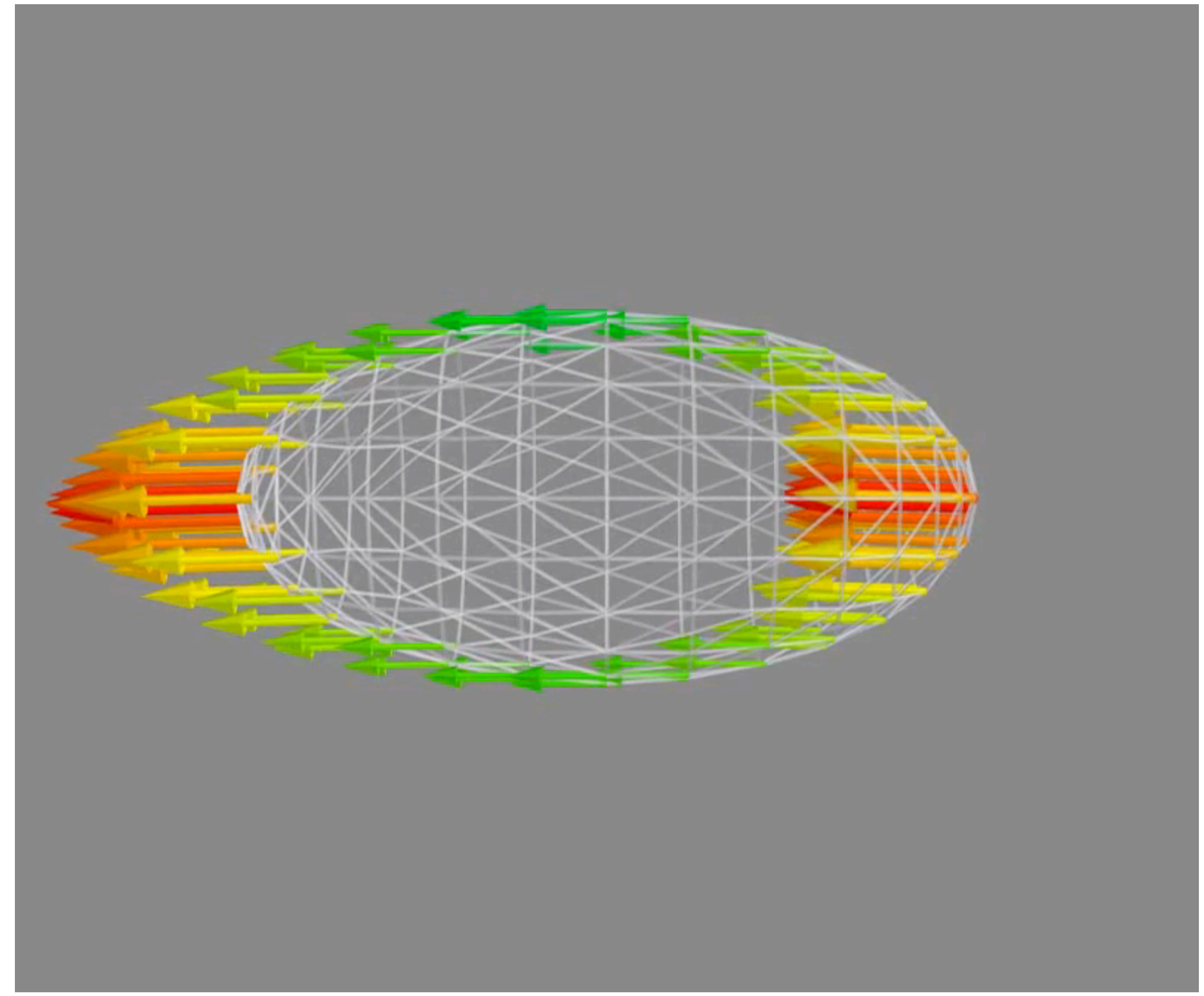

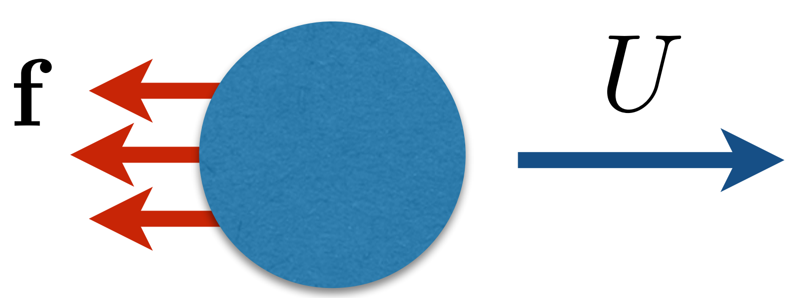

Application: hydrodynamics of self-propulsion near surfaces

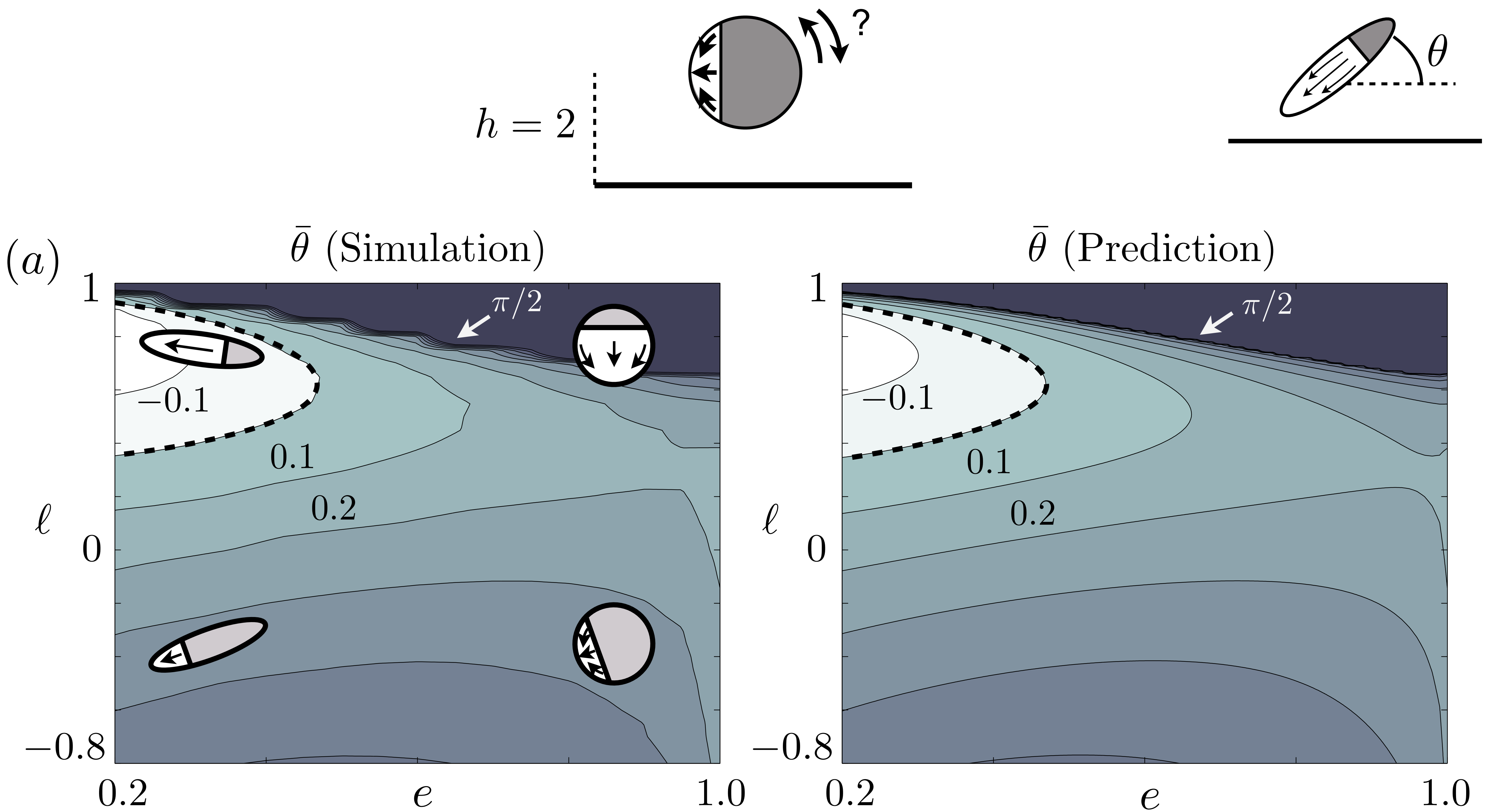

Spagnolie & Lauga, *J. Fluid* Mech., (2012).

Other directions: viscous erosion

$$\frac{\partial}{\partial t}\mathbf{x}(\mathbf{s},t) = -\alpha|(\mathbf{I}-\hat{\mathbf{n}}\hat{\mathbf{n}})\cdot\mathbf{f}(\mathbf{s},t)|$$

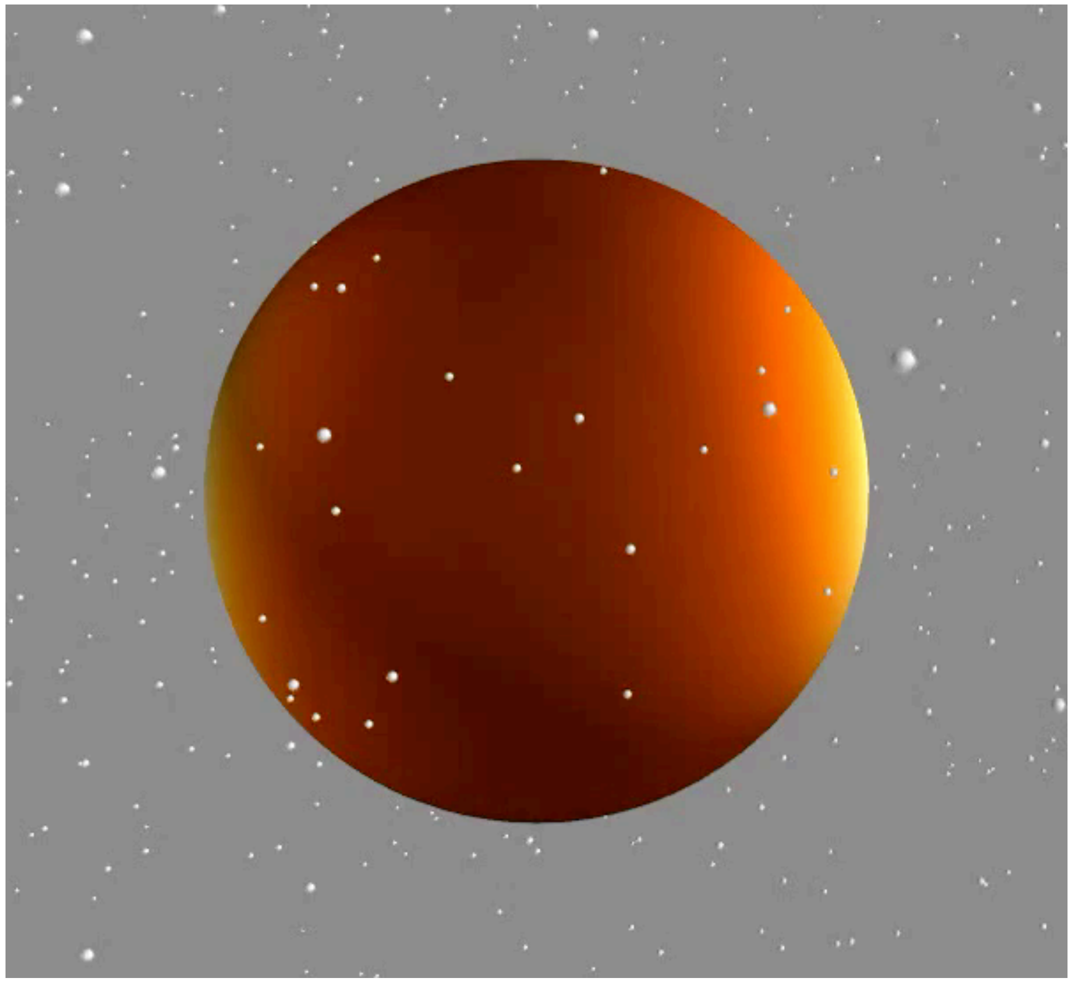

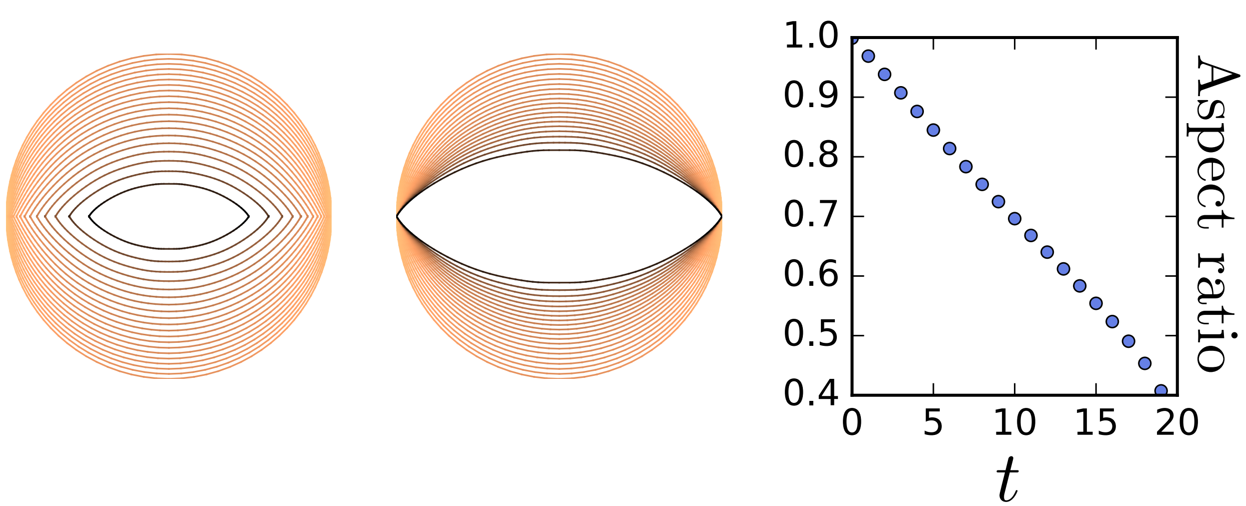

(**Not** Pironneau's drag minimizing shape)

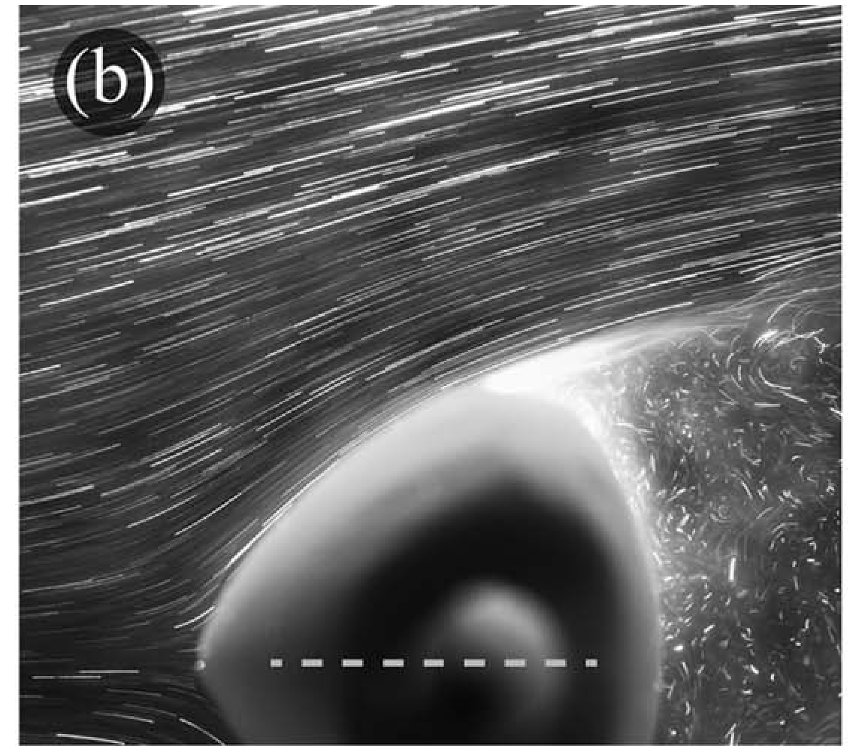

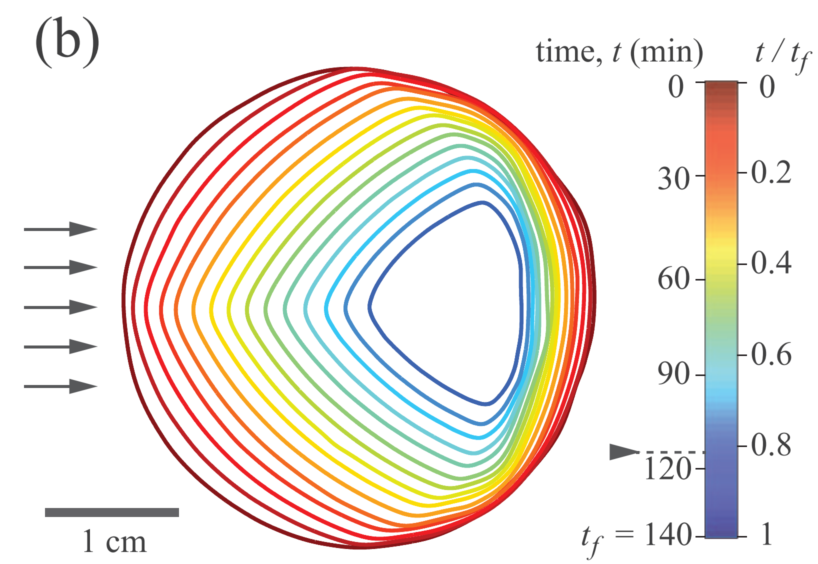

Moore et al. PNAS '13

In a shear flow without/with a wall…

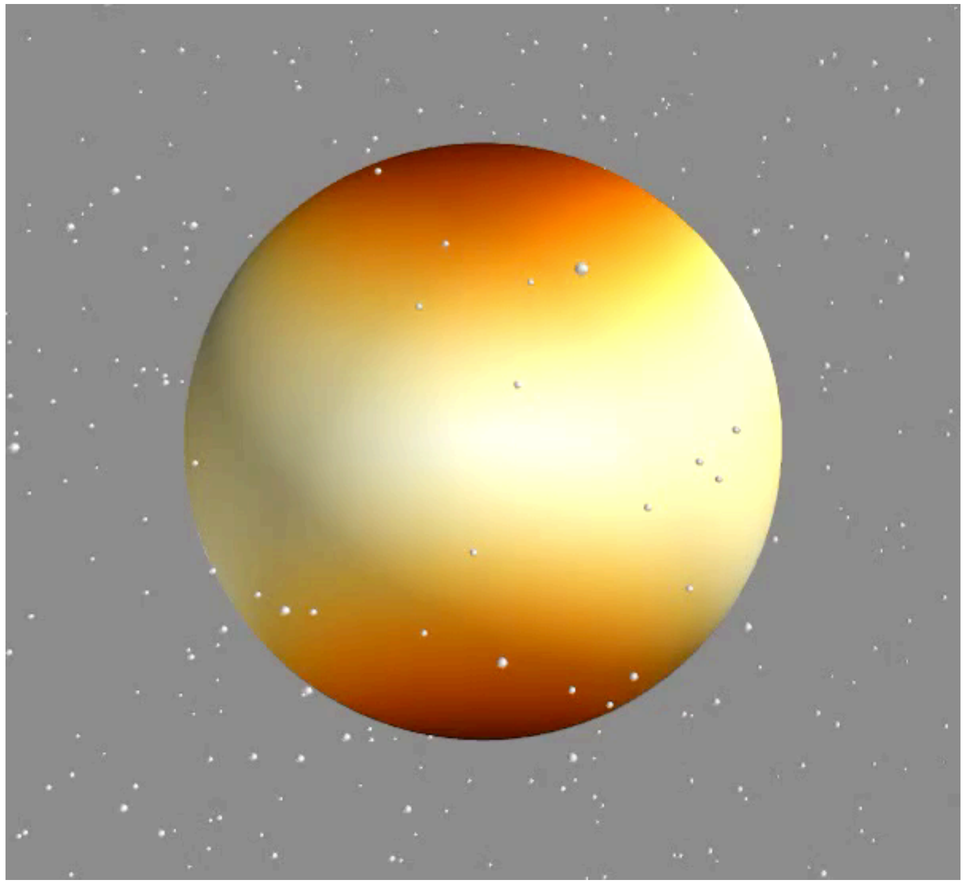

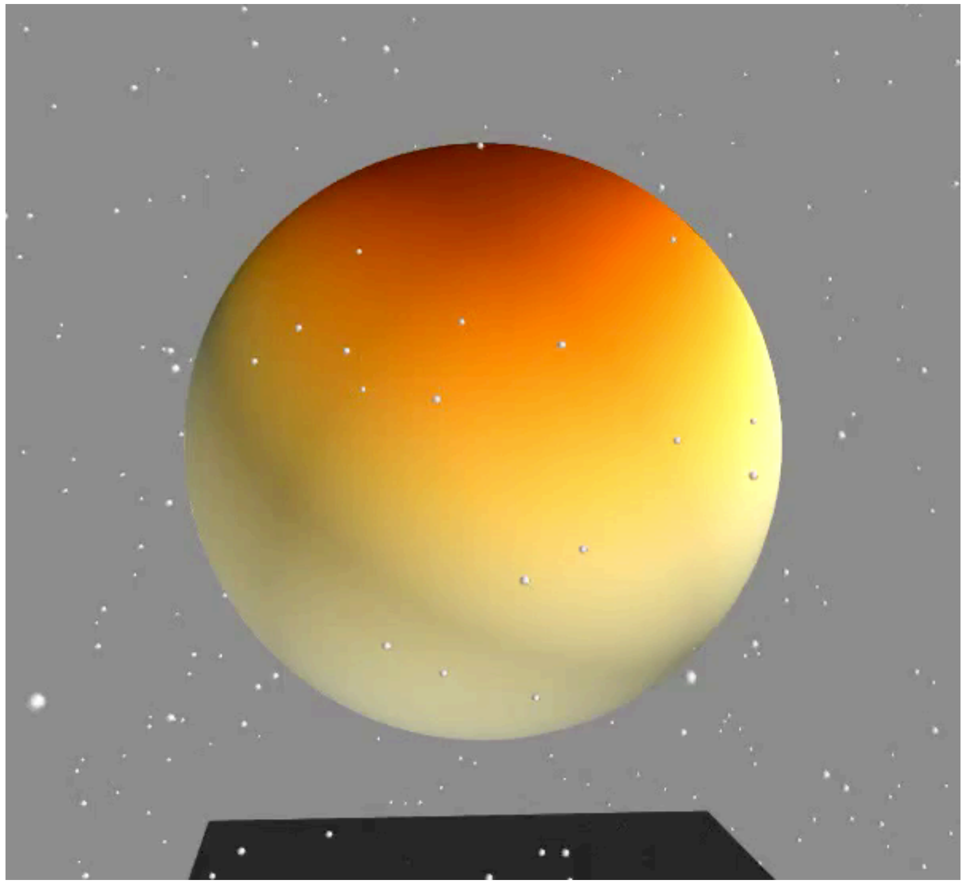

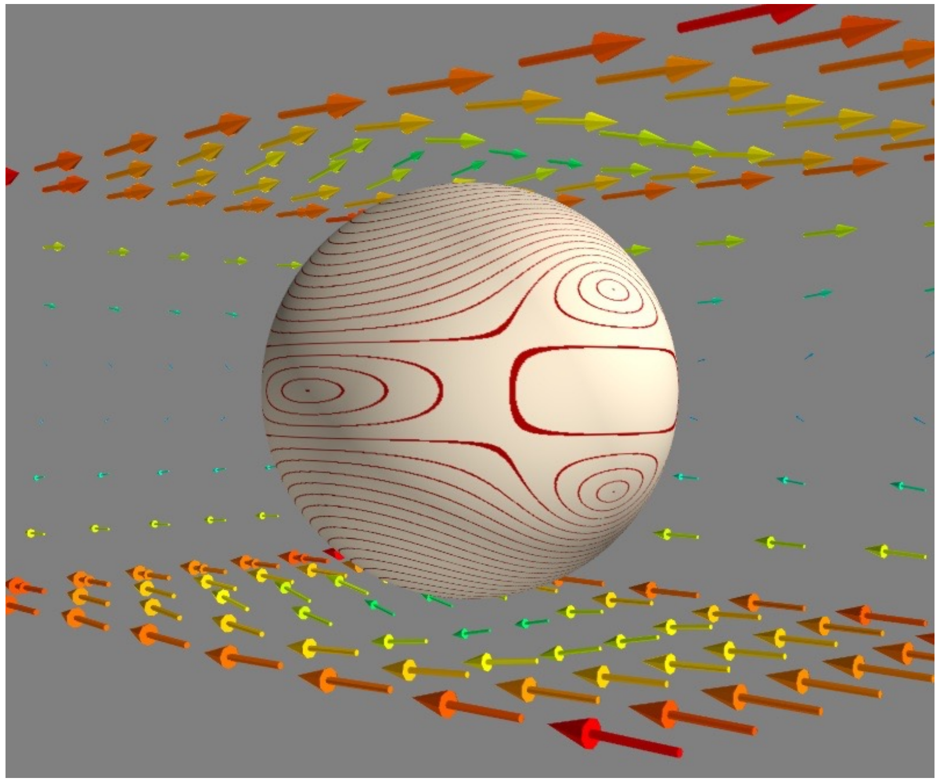

Thanks to collaborators:

Lei Li
UW-Madison

Harishankar Manikantan
UCSB

David Saintillan
UCSD

Will Mitchell
UW-Madison

The sedimentation of flexible filaments,
L. Li, H. Manikantan, D. Saintillan, and S.E. Spagnolie, *J. Fluid Mech.*, (2013).

The instability of a sedimenting suspension of weakly flexible fibres,
H. Manikantan, L. Li, S.E. Spagnolie, and D. Saintillan, *J. Fluid Mech.*, (2014).

Sedimentation of spheroidal particles near walls in viscous fluids:
glancing, reversing, tumbling, and sliding,
W.H. Mitchell and S.E. Spagnolie, *J. Fluid Mech.*, (2015).

Generalized traction integral equations for viscous flows with an application to erosion problems,
W.H. Mitchell and S.E. Spagnolie, (preprint).

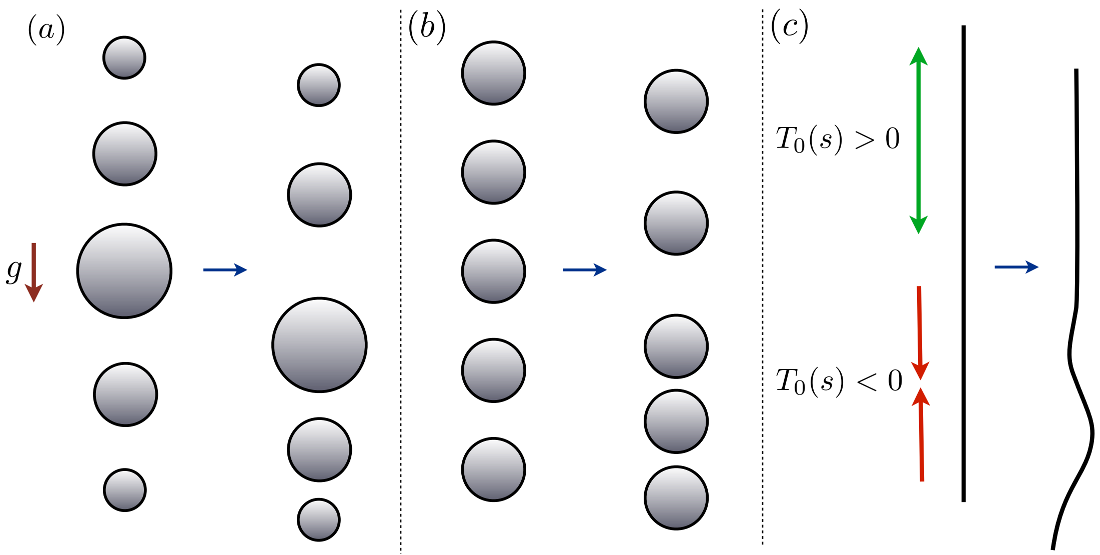

Thank you!
Q&A

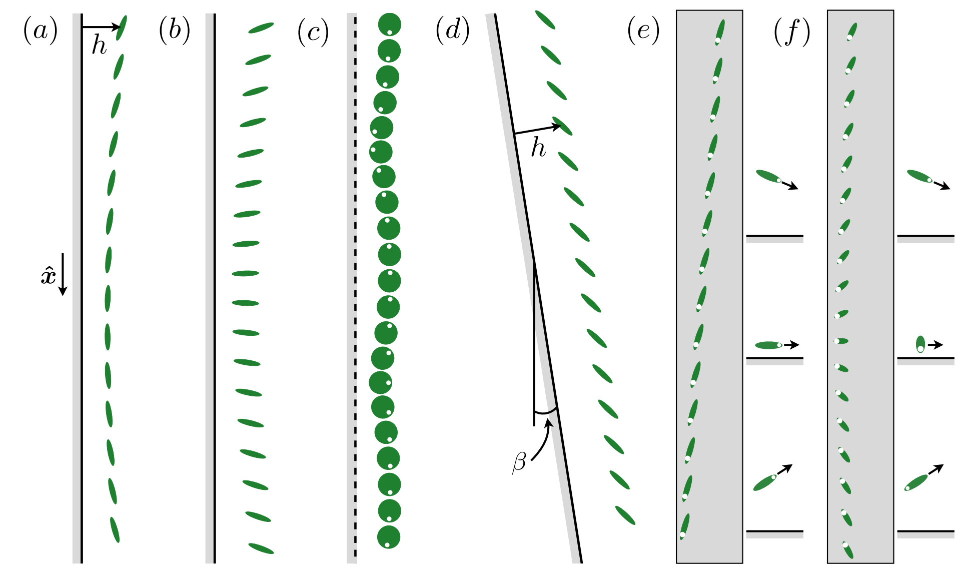

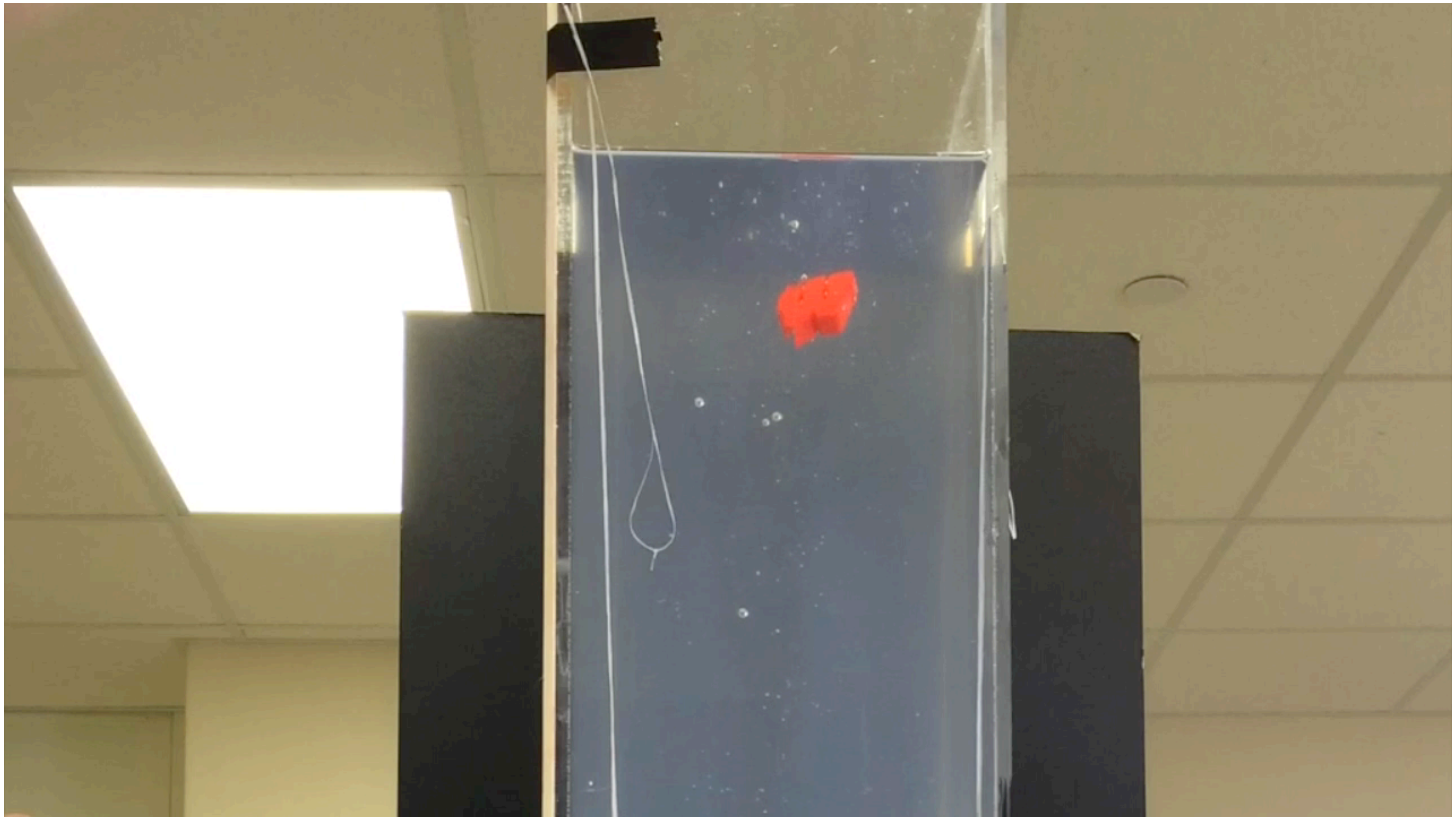


LOONEY TUNES
"That's all Folks!"